Fall 12-18-2015

Response of Fishes to Restoration Projects in Bayou St. John located within the City of New Orleans, Louisiana, including Hydrological Characterization and Hydrodynamic Modelling

Patrick W. Smith
University of New Orleans, patricksmith111@gmail.com

Response of Fishes to Restoration Projects in Bayou St. John located within the City of New
Orleans, Louisiana, including Hydrological Characterization and Hydrodynamic Modelling

A Dissertation

Submitted to the Graduate Faculty of the
University of New Orleans
in partial fulfillment of the
requirements for the degree of

Doctor of Philosophy
In
Engineering and Applied Science
Earth and Environmental Sciences

by

Patrick W. Smith

B.Sc. Georgia Regents University, 2008
M.Sc. University of New Orleans, 2012
December, 2015

Dedication

I dedicate this manuscript to my son, Henry Holden Smith. I look forward to raising him and hope there are many great urban ecosystems for his and future generations to enjoy.

provided me with a great deal of support and understanding. Both he and my father instilled a

great respect for nature that certainly shaped who I am as a scientist. Last, but not least, I would

like to thank my wife, Greer, who very understanding and supportive throughout this arduous

process. Without her, it's quite possible that I would have never considered graduate school.

Table of Contents

List of Figures

List of Tables

Abstract

Quantifying the impacts of restoration on coastal waterways is crucial to understanding their effectiveness. Here, I look at the impacts of multiple restoration projects on urban waterways within the city limits of New Orleans, LA, with an emphasis on the response of fishes. First I report the effects of two projects designed to improve exchange down estuary on the hydrologic characteristics of Bayou St. John (BSJ). Within BSJ, flow is dominated by subtidal wind driven processes. Removal of an outdated flood control structure did not appear to alter exchange in BSJ, but removal combined with sector gate openings did. I also refined a three dimensional hydrodynamic model of this system to have accurate predictions of velocity and elevation. Temperature and salinity were difficult to constrain with this model. Solutions of this model were used to compare flow metrics, along with linearly interpolated temperature, and other variables to Red Drum (*Sciaenops ocellatus*) activity and movement patterns. Relationships between Red Drum activity and velocity suggested a response to subtidal, wind driven flow. Overall, high Sedentariness, a measure of inactivity, was found suggesting high levels of site fidelity. Higher mean Sedentariness during the night was also found. I also used a pseudo-BACI design to analyze the fish assemblage response to removal of an outdated flood control structure and the impacts of sector gate openings on fish guild species richness in BSJ. Limited differences were found when comparing fish assemblages before and after removal, but these differences were likely due to a decrease in salinity not restoration efforts. No significant differences in Freshwater or Estuarine fish guild species richness was observed for any of the control or impact sites. Marine fish species richness was found to be higher immediately following sector gate openings at the site closest to the structure, suggesting an initial pulse of young marine organisms is provided via these events. The findings here can be used to optimize management of exchange flow in coastal impounded waterways.

Chapter 1

Characterization of Exchange Flows in Bayou St. John, an Urban Waterway in New Orleans, Louisiana: Response Following Restoration and Floodgate Mediated Water Pulses

Introduction

The use of flood control structures, such as floodgates, is common in coastal areas around the world (Dick and Osunkoya, 2000; Coops and Hosper, 2002; Warren et al., 2002; CPRA, 2012). Their use for flood protection implicitly alters hydrology, connectivity, and tidal exchange. Complete or partial restoration of exchange in partially disconnected, degraded systems estuaries can improve ecosystem function (Llanso et al., 1998; Warren et al., 2002; Layman et al., 2005).   Evidence of this includes increases in salt marsh plant species and diversity (Sinicrope et al., 1990) and fish diversity (Chapter 3 of this document). In particular, many economically important fishes and invertebrates are associated with increased connectivity (e.g., estuarine dependent species; Lellis-Dibble 2008). As such, connectivity and tidal exchange have been suggested as primary determinants of estuarine community structure and improvements are often major components of estuarine restoration (Warren et al., 2002).

Many anthropogenic impacts have affected Bayou St. John (BSJ) in the 300 years since the founding of New Orleans (Ward, 1982). Exchange with Lake Pontchartrain, a brackish oval shaped semi-enclosed waterbody, is currently restricted by a sector gate with sluice valves. The main purpose of this structure is for flood protection, as much of the surrounding area is below sea level. While sluice valves have been shown to allow for some tidal exchange (Schroeder, 2011), opening the sector gates may better serve restoration efforts (BKI, 2011).

Collaboration among the Orleans Levee District, the University of New Orleans (UNO), the Lake Pontchartrain Basin Foundation, the Louisiana Department of Wildlife and Fisheries, and Burk-Kleinpeter, Inc. (BKI) generated a new water management plan for BSJ (BKI, 2011). This plan includes an adaptive management approach, with a major goal being increased recreational fishery productivity by increasing exchange with Lake Pontchartrain. In order for this to be successful, an outdated flood control structure that impeded flow in BSJ (Schroeder, 2011) was removed on 30 April 2013. A channel was dredged through a sand bar on the Lake Pontchartrain side of BSJ to allow more exchange between the Lake and BSJ and approximately 2000 m^2 of emergent vegetation was planted around the newly created channel. Experimental openings of the sector gates have also occurred with the goal of recruiting juvenile marine organisms. Specifically, a head differential between BSJ and Lake Pontchartrain is created. This differential is created by a combination of closing sluice valves on a sector gate that separates Lake Pontchartrain and BSJ and pumping or draining water into the nearby City Park Lagoons. Then, a partial or complete opening of the sector gates allows a pulse of water and aquatic organisms to enter BSJ from Lake Pontchartrain. Two openings, on 19 August 2013 and 19 February 2014 occurred during this study. Both openings lasted approximately four hours, starting around 0800 local time. Both openings occurred near low tide in Lake Pontchartrain. Outside of experimental gate openings, water elevations are maintained by the Orleans Levee District at approximately -0.24 m NAVD88 via sluice valves on the sector gate.

Here, I reported results of initial water pulses from data collected in the field and model simulations. I described the hydrological conditions in the Bayou during two flood gate openings and refined a three dimensional model to better understand water exchange during openings and compared the results with normal conditions. Using four historical transects, I

evaluated water fluxes for both periods, and for each scenario varied atmospheric forcing to test

model sensitivity to wind stress and cloud cover. Specifically, I aimed to answer the following

questions:

1.   What were the general hydrological characteristics during normal low energy,

    medium energy cold front events, and high energy sector gate opening conditions?

    How were current velocities and discharges distributed throughout BSJ during these

    three conditions? How did these findings compare to a study conducted prior to any

    restoration efforts?

2.   Were temperature, elevation, current velocity, and salinity well constrained using

    three dimensional ECOMSED model simulations? How did altering atmospheric

    inputs affect model results? How sensitive was this model to wind stress and cloud

    cover?

Materials and Methods

Study Area

    Bayou St. John is an urban waterway located in the north-central portion of the City of

New Orleans, Louisiana (Fig. 1.1). Much of its banks have been stabilized by concrete, and it is

surrounded by houses and roadways with 16 bridges crossing it. It is approximately 6.5 km long

and for most of its length has a north-south orientation. The width of the Bayou varies from 45

m to 200 m. Average depth of the Bayou is approximately 2.5 m, with the northern section

(north of I610) being significantly deeper and wider than the southern section (Martinez et al.,

2008; Brogan, 2010). The northern extremity is partially connected to Lake Pontchartrain via a

sector gate (30 1' 27.32" N, -90 4' 58.33" E). It contains three sluice valves, two measuring

91.44 cm in diameter and one at 60.96 cm used to manage BSJ's water elevation. The most

southern point ends at the corner of Jefferson Davis Parkway and Lafitte Street (29 58' 23.9" N, -90 5' 28.53" E), where a 60.96 cm differential valve is located. This valve, a 76.2 cm culvert at Interstate 610 (29 59' 30.8" N, -90 05' 10.7" W) and several weirs are used for drainage. Its connection with Lake Pontchartrain provides BSJ with brackish water (salinity range ~ 1.5 to 8).
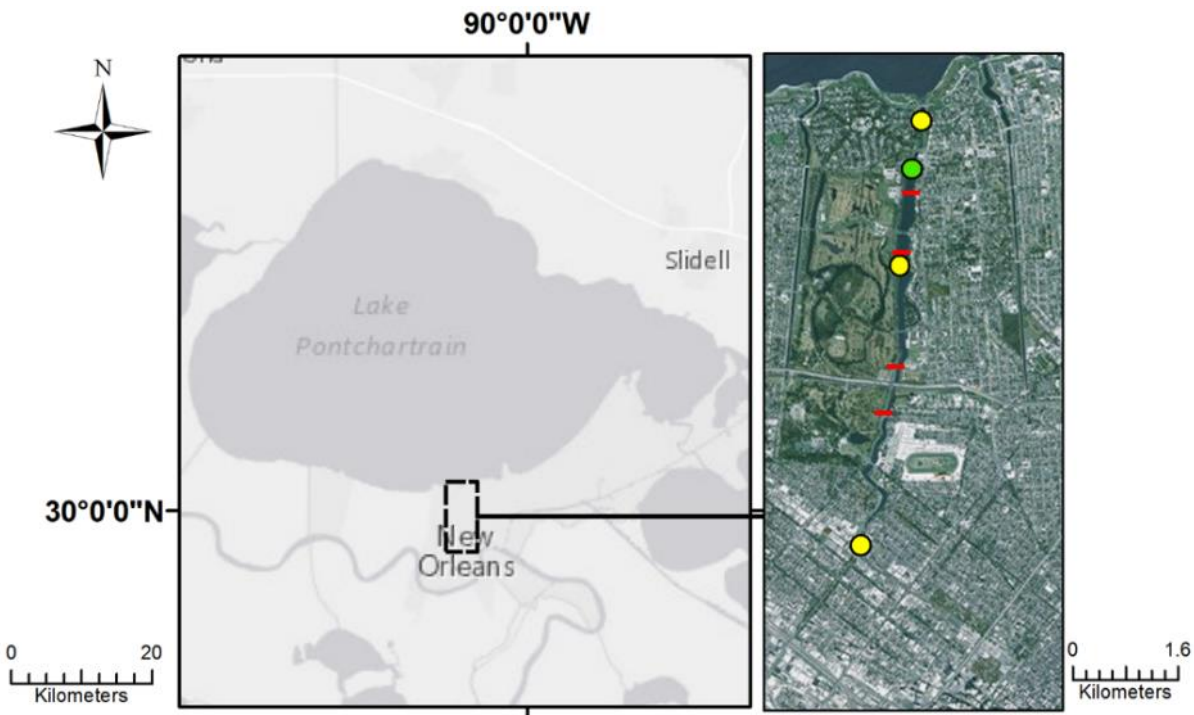
Figure 1.1. Map showing the study area, its location in Southeastern Louisiana, and observed data sites.   As can be seen in the larger map, Bayou St. John is located within the New Orleans, LA City Limits. Yellow points indicate USGS stations where salinity, temperature, and elevation data were used, each point indicating one station, except one. A sector gate restricting exchange between Lake Pontchartrain and the Bayou exists at the northern most yellow point. Two USGS stations are located on this structure, one in Lake Pontchartrain and one in Bayou St. John. The green point shows the location of the Nortek Vector Field Acoustic Doppler Velocimeter (Vector ADV) that was deployed from 3 February 2014 at 1350 until 28 February 2014 at 1030. The red lines show transect locations where discharges were calculated. Note Bayou St. John's connection with Lake Pontchartrain to the north and its abrupt ending to the south. This figure was created using ArcMap 10.1.

Observational Data

Five *in situ* datasets were used to evaluate BSJ's hydrology and assess model performance. Four United States Geological Survey (USGS) water quality stations, three of which are within the study area and one in Lake Pontchartrain on the sector gate were used to

4

test the model sensitivity to temperature, salinity, and elevation (Fig 1.1). Upon inspection, the elevations reported at the southern station appeared to be incorrect. They were all higher in elevation than any other location within BSJ, but behaved similarly. This suggested that these values represented actual changes in elevation, but were shifted up. To correct for this 0.11 m was subtracted from the each observation, creating a new parameter called corrected elevation. A Nortek Vector Field Acoustic Doppler Velocimeter (Vector ADV) was deployed 925 mm from the bed at the northern end of the Bayou from 3 February 2014 at 1350 until 28 February 2014 at 10:30 (30° 1' 8.5398" N, -90° 5' 2.3922" E; Fig. 1.1). The Vector ADV recorded velocity in the X, Y, and Z direction and water depth at a frequency of 2 Hz, with a burst interval of 1,500 seconds, and 600 samples per burst. This yielded average values every 25 minutes. A maximum velocity setting of 0.3 m/s was used as this was much larger than what was measured in a previous study (Schroeder, 2011). Resultant vector magnitudes from each burst sample were calculated using X and Y velocity measurements and compared to simulated values.

Simulations

Two time periods, summer and winter, were simulated and compared to measurements. The summer simulation began on 1 August 2013 at 0000, and lasted 480 hours, ending on 21 August at 0000. The winter simulation began on 3 February 2014 at 1400 and lasted 418 hours ending on 21 February at 1400. A sector gate opening occurred during each period, beginning on 19 August 19 2013 at 800 and 19 February 2014 at 800 and lasting for approximately four hours each.

The Estuarine, Coastal and Ocean Modeling System with Sediments (ECOMSED) model developed by Blumberg and Mellor (1987) within Hydroqual Inc. was used to simulate hydrologic parameters for both time periods. This is a three dimensional model that uses the

finite control volume principle. It is composed of many different modules that can be activated or deactivated. For this study, a slightly modified three dimensional model, configured by Schroeder (2011) was used. Boundary condition inputs were altered to correct for an error in the way these were implemented.

Initial conditions included in the model were bathymetry, water depth, temperature, and salinity (Fig. 1.2). An orthogonal square Cartesian mesh (70 x 300 cells with 20 UTM meters) with depth discretized into six sigma levels was used (Schroeder, 2011). Areas around some bridges were artificially widened to increase the number of nodes within the model. To eliminate problems associated with ramping the starting depths and elevations were corrected. Each simulation was started arbitrarily at 0 m elevation and starting elevations were subtracted from each input depth and added to each input elevation in the boundary conditions to lessen the amount of inertia during ramping. In other words, I corrected each depth and elevation to the initial starting elevation of 0 m to remove a decrease in elevation that would have occurred during the ramping period. A minimum depth of 2 m was used to prevent any cell drying. Initial water temperature and salinity values were assigned based on USGS maintained continuous water quality station at the mouth of the Bayou. The same salinity and temperature was assigned to each node and sigma level.
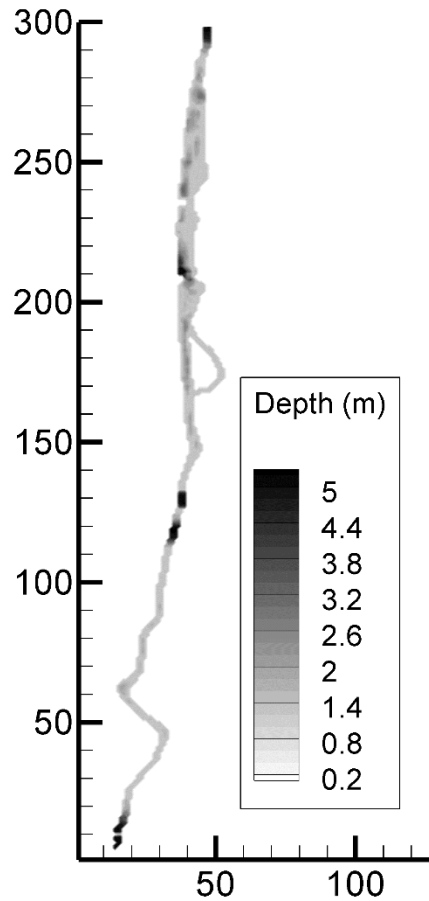
Figure 1.2. Bathymetry of Bayou St. John. The data shown were derived from bathymetry taken in 2008, with a minimum depth of 2m (Martinez et al., 2008) and are the bathymetry of the Bayou as used in the ECOMSED 3D model.

For each simulation, the same open boundary in the north with temperature, salinity, and water elevation was used. Parameter values were obtained from a USGS maintained continuous water quality station. Five parameters were used to estimate the meteorological forcings (monthly precipitation, monthly evaporation, wind speed, wind direction, and heatflux). Standardized values from Fontenot (2004) were used for precipitation per month (m) and evaporation per month (m). Meteorological values used to determine wind speed, wind direction, and heatflux were downloaded from the National Oceanic and Atmospheric Association maintained National Climate Data Center's Quality Controlled Local Climatological

Data for New Orleans Lakefront Airport (cdo.ncdc.noaa.gov). I used the variables Sky

Condition, Dry Bulb Celsius, Wind Speed, and Wind Direction. A sensible heat flux A&BFLX

method was used because it has been demonstrated to be the most successful in estuarine

systems (Blumberg and Mellor, 1987):

$$H_c = C * f(w) * (Ta - Ts)$$ **(1.1)**

,where H_c is sensible Heatflux, C is cloud cover correction, f(w) is Wind speed function, Ta is

the atmospheric temperature (K) and Ts is the water surface temperature (K). Wind speed

function was calculated using the following equation (Blumberg and Mellor, 1987):

$$f(w) = 6.9 + 0.34 * W^2$$ **(1.2)**

, where f(w) is wind speed function and W is wind speed (m/s).

Meteorological forcings were varied to determine the most accurate simulations. For

each season, six different simulations were performed (Table 1.1). Three different reductions in

wind speed were used (50%, 75%, and 100%). All simulations were reduced by at least 50%

because local topography likely dampens wind speed. Percent cloud cover is an influential

parameter and its effect was removed in some simulations. Mean f(w) was also used in place of

calculated f(w) for some simulations to test for model sensitivity.

Table 1.1. Summary of the different simulations of Bayou St, John (BSJ) hydrology performed and analyzed. Two different time periods, denoted as Seasons with different combinations of three different wind speed corrections, denoted in percent of measured speed, three different wind speed functions f(w), and simulations with and without cloud cover corrections were simulated.

| | Simulation Trials | | |
Season	Wind speed correction (%)	*f(w)*	Cloud Cover
Winter	0	None	Removed
Winter	25	Calculated	On
Winter	25	Calculated	Removed
Winter	25	Mean	Removed
Winter	50	Calculated	On
Winter	50	Calculated	Removed
Summer	0	None	Removed
Summer	25	Calculated	On
Summer	25	Calculated	Removed
Summer	25	Mean	Removed
Summer	50	Calculated	On
Summer	50	Calculated	Removed

Discharge was calculated at simulation latitudes 107, 146, 214, and 258 within the Bayou (Fig. 1.1). From lowest to highest latitude, they are referred to here as the far south, south, mid, and north transects. Discharges were calculated by integrating simulated resultant vector velocities across each transect for each time step. Velocity measurements from the best performing simulation from the winter simulation were used. For the summer simulations, the best performing model with respect to elevation was used. This is because change in elevation is the most closely associated measurement to velocity during the summer time period.

A combination of quantitative and qualitative tools was used to determine model performance (Bennett et al., 2013). The best model for each parameter (salinity, temperature, elevation, and when available velocity) for three locations for both seasons was judged using a reformed Willmott's index of agreement (d_m; Legates and McCabe, 1999) using the R package hydroGOF (Zambrano-Bigiarini, 2014):

$$d_m = 1 - \frac{\sum_{i=1}^{N} |O_i - S_i|^j}{\sum_{i=1}^{N} |S_i - \bar{O}| + |O_i - \bar{O}|^j} \tag{1.3}$$

,where O is an observation, S is a simulation and is an observation. This index was designed for

comparison of hydrological models and has been suggested as being better than correlation-

based measures. To better detect additive and proportional differences between observations and

simulations and lessen the effects of outliers, a value of j=1 was used (Legates and McCabe,

1999). Values range from 0 to 1, with higher values indicating higher agreement. A value of 1

indicates perfect agreement. After the best model-parameter-location was determined, the mean

value across stations for each parameter was used to select the best model-parameter

combination. Selection of the best model for each season was based upon model-parameter

averages. Agreement of elevation and velocity were prioritized over temperature and salinity,

because of the cell size and study area size. It is likely that these two parameters vary more

across time and space at a 20m x 20m resolution within a 57 hectare waterbody than temperature

or salinity. Model phasing and trending will be graphically displayed and visually assessed for

all models-parameter-location combinations.

Results

Observations

During the summer time period, at the northern USGS gage, elevation ranged from -1.11

m to -0.62 m with a mean of -0.98 m (Fig. 1.3), temperature ranged from 27.9 ℃ to 33.8 ℃ with

a mean of 31.4 ℃ (Fig. 1.4), and salinity ranged from 2.0 to 3.1 with a mean of 2.5 (Fig. 1.5;

Table 1.2). At the middle USGS gage, elevation ranged from -1.10 m to -0.72 m with a mean of

-0.97 m (Fig. 1.3), temperature ranged from 28.8 ℃ to 35.3 ℃ with a mean of 32.2 ℃ (Fig. 1.4),

and salinity ranged from 2.0 to 2.1 with a mean of 2.1 (Fig. 1.5). At the southern USGS gage,

elevation ranged from   -1.00 m to -0.62 m with a mean of -0.87 m, temperature ranged from

28.3 ℃ to 35.1 ℃ with a mean of 31.8 ℃ (Fig. 1.4), and from salinity ranged from 2.3 to 2.8

with a mean of 2.6 (Fig. 1.5). Corrected elevation at the southern USGS gage had a range of -

0.73 m to -1.10 m with a mean of -0.98 m (Fig. 1.3). Elevation at the Lake Pontchartrain USGS

station ranged from -0.31 m to 0.26 m with a mean of -0.04 m (Fig. 1.3). Little tidal variation is

observed during this time period at any of the USGS locations inside of BSJ, especially when

compared to the Lake. All elevations from simulation time 0 to 370 were mean centered and

plotted to isolate tidal dynamics to better visualize the lack of variation (Fig. 1.6).
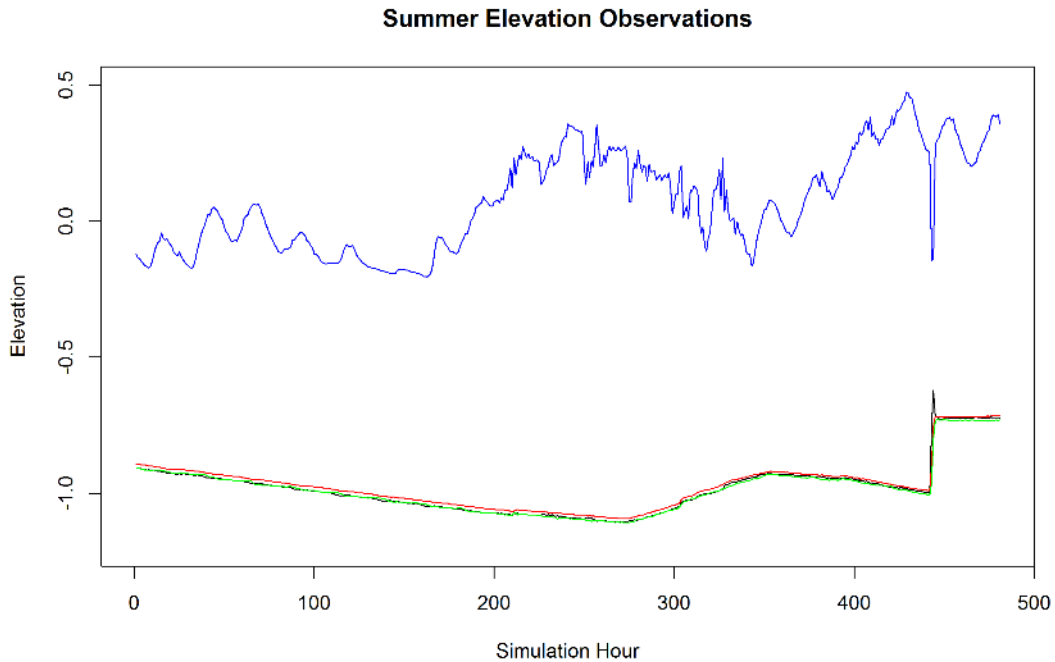
Figure 1.3. Elevation (m) from three USGS Stations within BSJ (northern is black, mid is red, and southern is green) and one from Lake Pontchartrain (blue) on the BSJ sector gate in BSJ during the summer simulation period. A sector gate opening was observed here and can be seen with the sharp increase in BSJ elevations and sharp decrease in Lake Pontchartrain elevations. Note the higher variability observed in Lake Pontchartrain.

11

Summer Temperature Observations
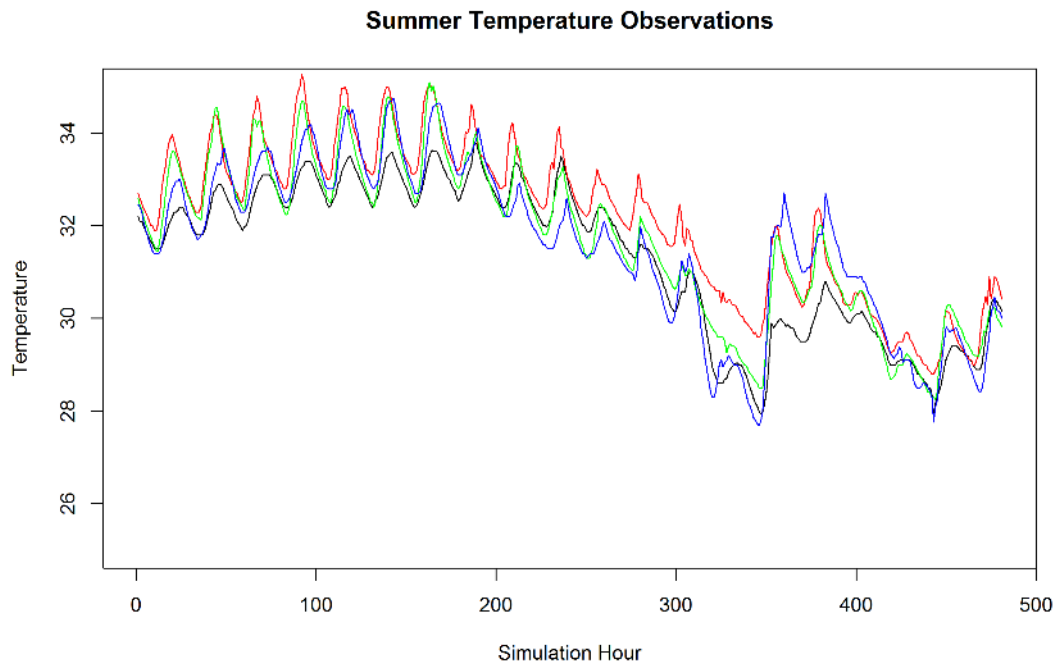
Figure 1.4. Temperature (ºC) from three USGS Stations within Bayou St. John and one from Lake Pontchartrain on the BSJ sector gate (Lake Pontchartrain is blue, northern is black, mid is red, southern is green) in Bayou St. John during the summer period. Temperatures from within BSJ and Lake Pontchartrain tend to trend more closely than for elevation.

Summer Salinity Observations
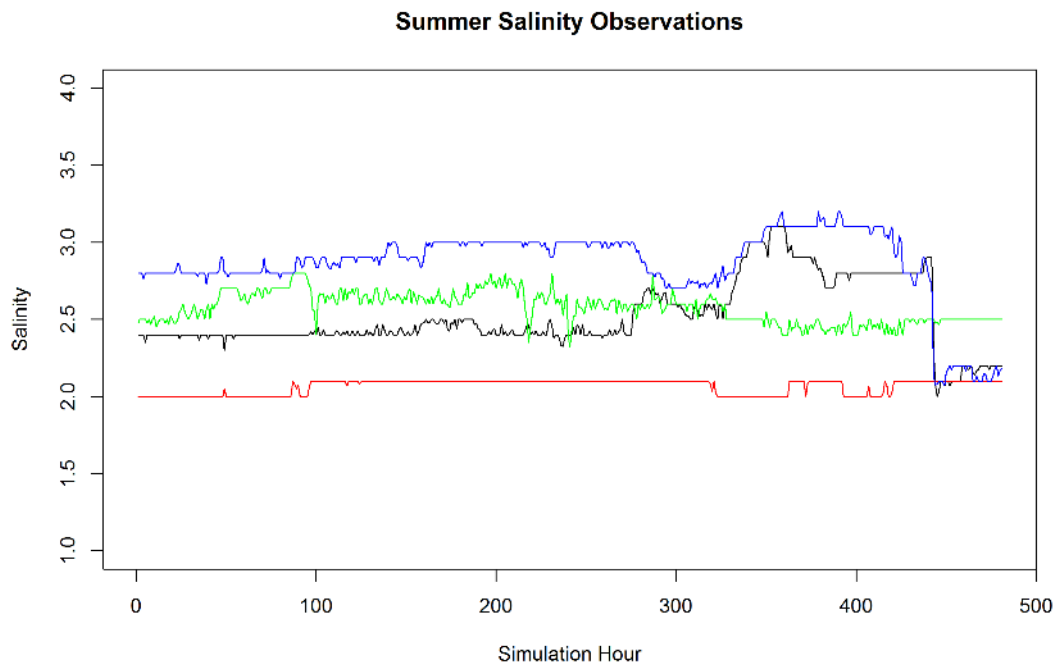
Figure 1.5. Salinity from three USGS Stations within Bayou St. John (BSJ) and one from Lake Pontchartrain on the BSJ sector gate (Lake Pontchartrain is blue, northern is black, mid is red, southern is green) in BSJ during the summer period. Notice the small variation in salinity across all stations measured.

12

Table 1.2. Summary statistics (μ± sd) for each parameter and station combination for both seasons. Three USGS maintained stations are shown. Elevation is measured in meters and temperature in °C. Note that for the southern station, elevation was corrected by adding 0.11 m to each observation due to a presumed measurement error.

	Summer		
	North	Mid	South
Elevation	-0.98 + 0.10	-0.97 + 0.10	-0.98 + 0.10
Temperature	31.4 + 1.6	32.2 + 1.6	31.8 + 2.3
Salinity	2.5 + 0.22	2.1 + 0.22	2.6 + 0.06
	Winter		
	North	Mid	South
Elevation	-0.76 + 0.14	-0.76 + 0.14	-0.77 + 0.14
Temperature	11.9 + 2.1	12.4 + 2.0	12.4 + 2.3
Salinity	2.6 + 0.10	2.5 + 0.03	2.2 + 0.06

Mean Centered Summer Elevation
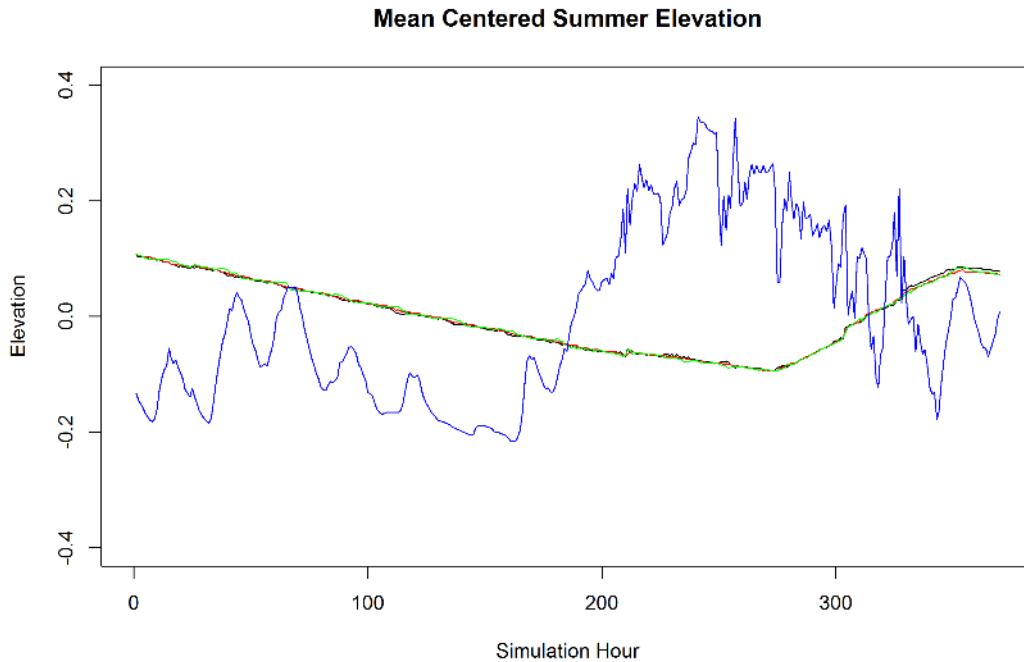
Figure 1.6. Mean centered elevations (m) from four USGS stations. Three are from in Bayou St. John (BSJ; northern is black, mid is red, southern is green) and one is from Lake Pontchartrain (blue) from simulation hour 0 to 370. This is representative of the overall change in elevation before the sector gate opening during the summer simulation period. Higher overall variation was observed in Lake Pontchartrain than BSJ.

During the winter time period, at the northern USGS gage, elevation ranged from -0.82 m to -0.18 m with a mean of -0.76 m (Fig. 1.7), temperature ranged from 8.9 °C to 18.3 °C with a mean of 11.9 °C (Fig. 1.8; Table 1.2), and salinity ranged from 2.4 to 2.8 with a mean of 2.6 (Fig.

13

1.9). At the middle USGS gage, elevation ranged from -0.20 m to -0.82 m with a mean of -0.76

m (Fig. 1.7), temperature ranged from 9.5 ℃ to 17.5 ℃ with a mean of 12.4 ℃ (Fig. 1.8), and

salinity ranged from 2.4 to 2.6 with a mean of 2.5 (Fig. 1.9). At the southern USGS gage,

elevation ranged from -0.73 m to -0.10 m with a mean of -0.66 m (Fig. 1.7), temperature ranged

from 8.5 ℃ to 18.7 ℃ with a mean of 12.4 ℃ (Fig. 1.8), and from salinity ranged from 2.1 to 2.3

with a mean of 2.2 (Fig. 1.9). Corrected elevation at the southern USGS gage had a range of

-0.84 m to -0.21 m with a mean of -0.77 m (Fig. 1.7). Elevation at the Lake Pontchartrain USGS

station ranged from -0.20 m to 0.47 m with a mean of 0.07 m (Fig. 1.7). Unlike the summer

period, equilibrium with the Lake during the flood gate opening occurred, and some tidal

variation was observed inside BSJ during the winter period (Figs. 1.7 and 1.10). A dampened

signal with a similar slope is apparent at the northern BSJ gage after simulation hour 200 (Fig.

1.10).

Winter Elevation Observations
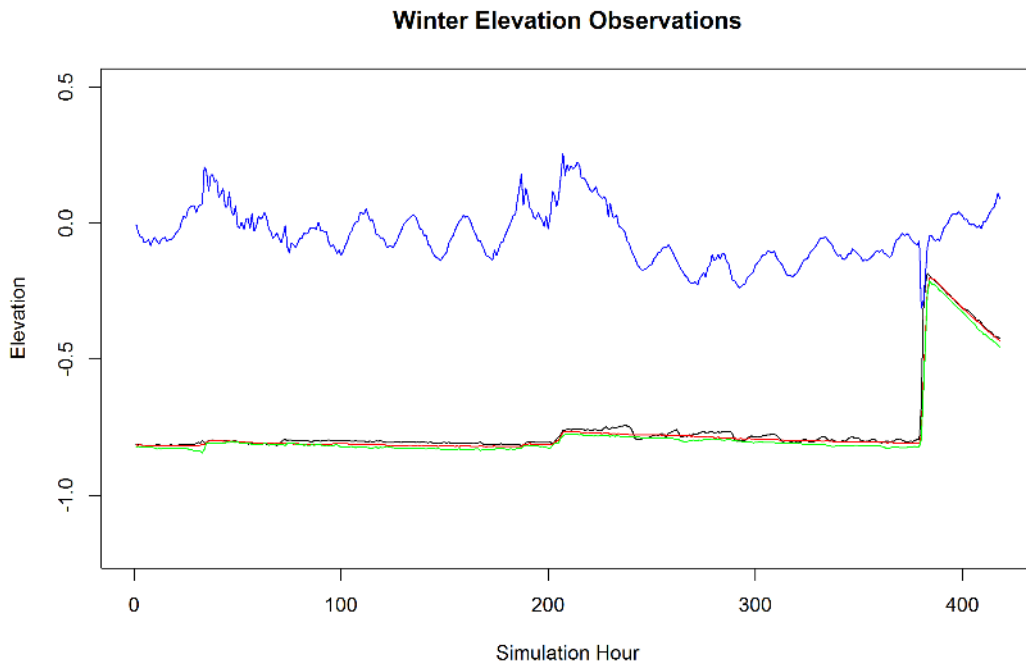
Figure 1.7. Elevation (m) from three USGS Stations within BSJ (northern is black, mid is red, and southern is green) and one from Lake Pontchartrain (blue) on the BSJ sector gate during the winter simulation period. A sector gate opening was observed here and can be seen with the sharp increase in BSJ elevations and sharp decrease in Lake Pontchartrain elevations. Note the higher variability observed in Lake Pontchartrain. A dampened tidal signal that is similar in slope to Lake Pontchartrain may exist in the northern BSJ station after simulation hour 225.

Winter Temperature Observations
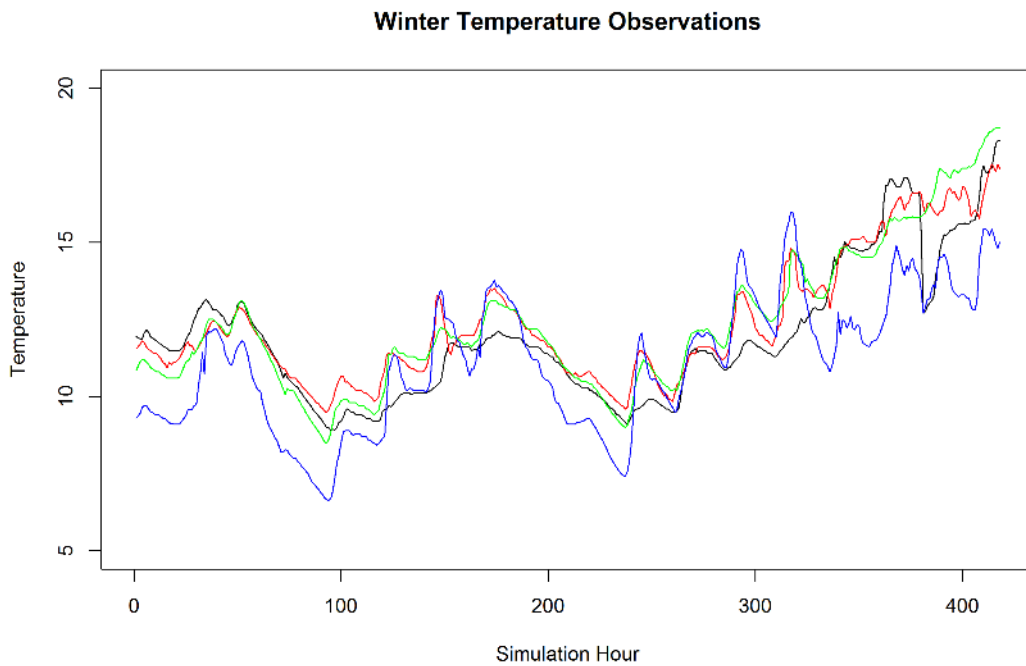
Figure 1.8. Temperature (°C) from three USGS Stations within Bayou St. John and one from Lake Pontchartrain on the BSJ sector gate (Lake Pontchartrain is blue, northern is black, mid is red, southern is green) in Bayou St. John during the winter period. Similar trends in temperature signals can be seen for all four sites.

15

Winter Salinity Observations
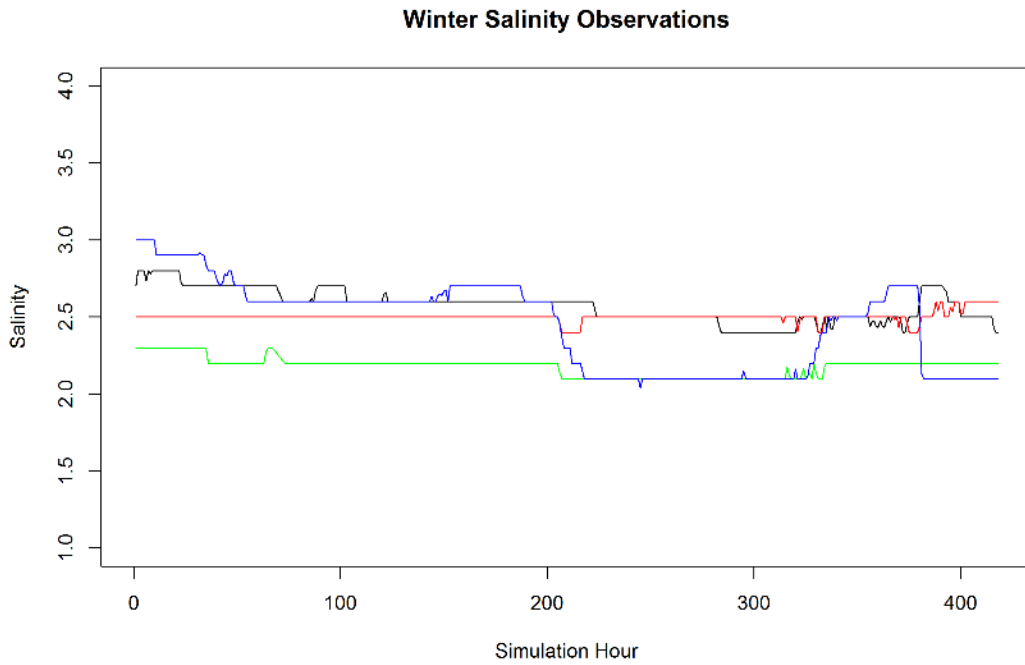
Figure 1.9. Salinity from three USGS Stations within BSJ and one from Lake Pontchartrain on the BSJ sector gate (Lake Pontchartrain is blue, northern is black, mid is red, southern is green) during the winter simulation period. Little variation in salinity across all sites for this time period.

Mean Centered Winter Elevation
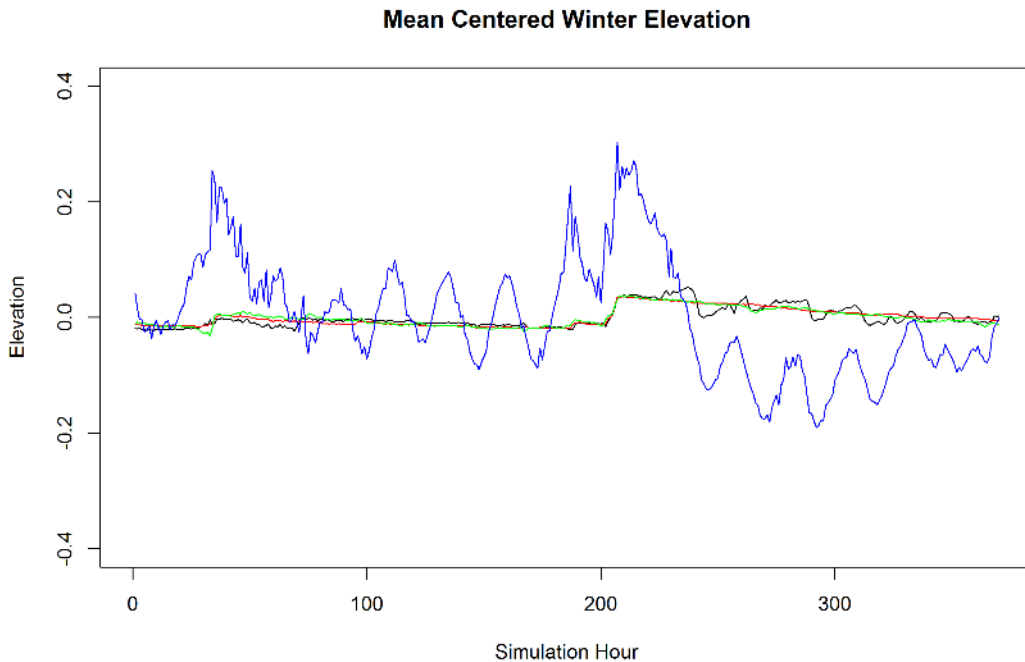
Figure 1.10. Mean centered elevations (m) from four USGS stations. Three are from in BSJ (northern is black, mid is red, southern is green) and one is from Lake Pontchartrain (blue) from simulation hour 0 to 370. This shows the overall change in elevation before the sector gate opening during the winter simulation period. Note similarity in slopes between the northern BSJ station and Lake Pontchartrain after simulation hour 225.

16

Summer Simulations

Across simulations, Elevation predictions were similar to observations. Values for d_m ranged from 0.983 to 0.988 for the northern station, 0.921 and 0.924 for the middle station, and 0.956 to 0.964 for the southern station (Table 1.3). Corrected elevations were used for the southern station as per the materials and methods. The model without cloud cover correction, a 50% reduction in wind speed, and calculated f(w) yielded the best overall elevation predictions (Figs. 1.11-1.13). This model produced the highest agreement for both the north and south stations. It should be noted that this simulation had the lowest agreement for the middle station. There was little variation among simulations for this station (d_m range 0.03) and the simulation with a 50% reduction in wind speed, cloud cover correction, and calculated f(w) performed best (Fig. 1.12).

Table 1.3. Results of the summer period simulations for BSJ hydrology in response to a floodgate opening. The indices of agreement (d_m) of all simulations for elevation, temperature and salinity for each USGS field location are shown here. The best performing simulation for a given site and parameter are indicated by bold and italicized text.

Model	Location	Parameter	d_m	Model	Location	Parameter	d_m
25% Wind speed, Cloud Cover Off, Mean f(w)	North	Elevation	0.984	25% Wind speed, Cloud Cover Off, Calculated f(w)	North	Elevation	0.983
		Temperature	0.820			Temperature	0.792
		Salinity	0.110			Salinity	0.145
	Middle	Elevation	0.921		Middle	Elevation	0.922
		Temperature	0.231			Temperature	0.320
		Salinity	*0.075*			Salinity	0.065
	South	Elevation*	0.960		South	Elevation*	0.956
		Temperature	0.295			Temperature	0.401
		Salinity	*0.324*			*Salinity*	*0.324*
No Meteorology	North	Elevation	0.983	50% Wind speed, Cloud Cover Off, Calculated f(w)	North	*Elevation*	*0.988*
		Temperature	0.822			Temperature	0.811
		Salinity	*0.179*			Salinity	0.096
	Middle	Elevation	0.923		Middle	Elevation	0.921
		Temperature	0.241			Temperature	0.314
		Salinity	0.060			Salinity	0.062
	South	Elevation*	0.957		South	*Elevation**	*0.964*
		Temperature	0.199			*Temperature*	*0.409*
		Salinity	*0.324*			*Salinity*	*0.324*
25% Wind speed, Cloud Cover On, Calculated f(w)	North	Elevation	0.984	50% Wind speed, Cloud Cover On, Calculated f(w)	North	Elevation	0.984
		Temperature	0.862			*Temperature*	*0.877*
		Salinity	0.166			Salinity	0.139
	Middle	Elevation	0.923		Middle	*Elevation*	*0.924*
		Temperature	0.490			*Temperature*	*0.493*
		Salinity	0.059			Salinity	0.058
	South	Elevation*	0.958		South	Elevation*	0.959
		Temperature	0.400			Temperature	0.382
		Salinity	*0.324*			*Salinity*	*0.324*

*indicates that corrected elevation was used, see Materials and Methods for details
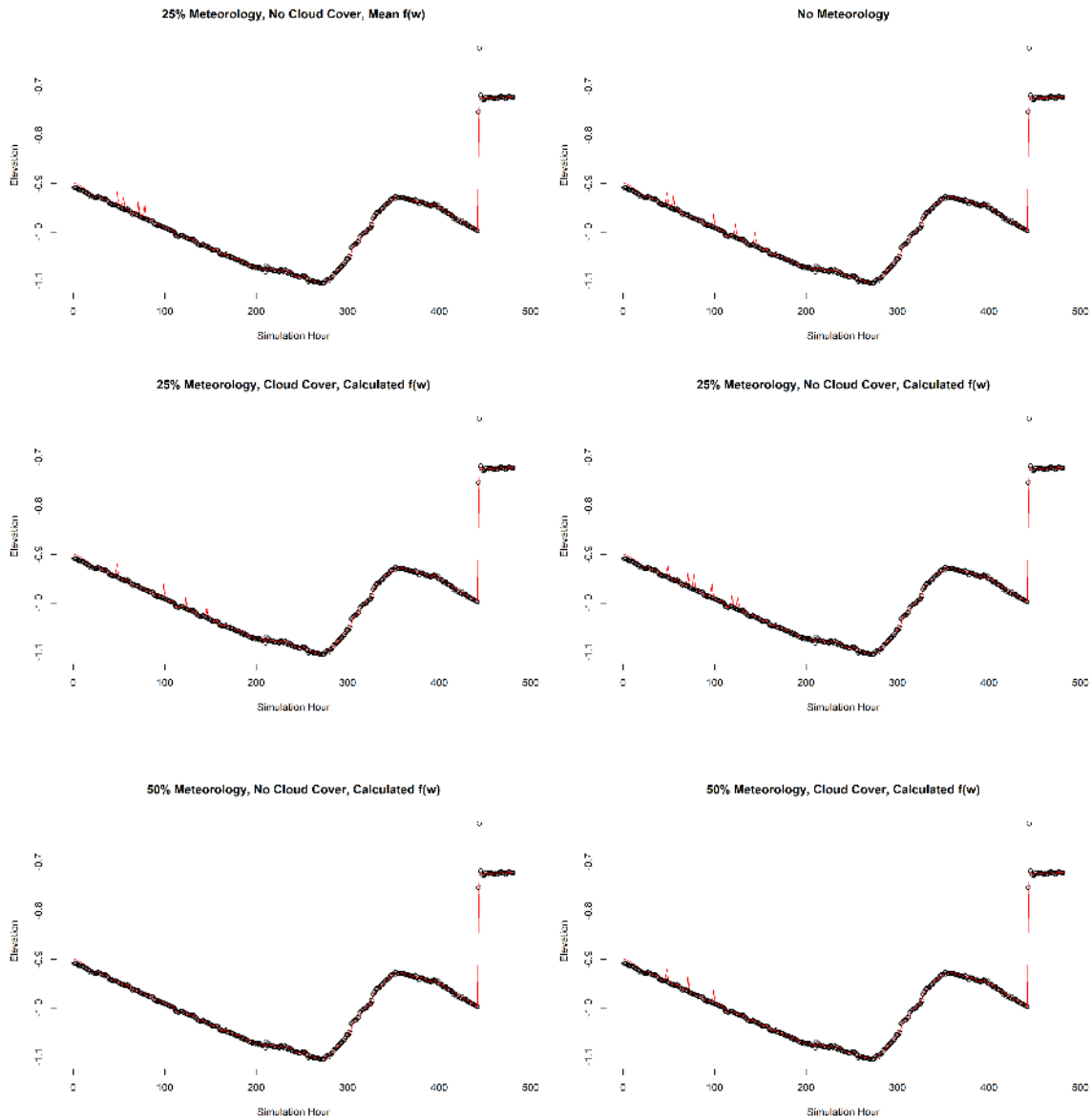
Figure 1.11. Predicted versus observed elevations (m) for 6 simulations during the summer time period for the northern USGS station. Observations are represented as points and predictions are represented as red lines. From left to right top to bottom: 1. 25% Wind speed, cloud cover off, mean f(w); 2. No Meteorology; 3. 25% Wind speed, cloud cover on, calculated f(w); 4. 25% Wind speed cloud cover off, calculated f(w); 5. 50% Wind speed, cloud cover off, calculated f(w); 6. 50% Wind speed, cloud cover on, calculated f(w).
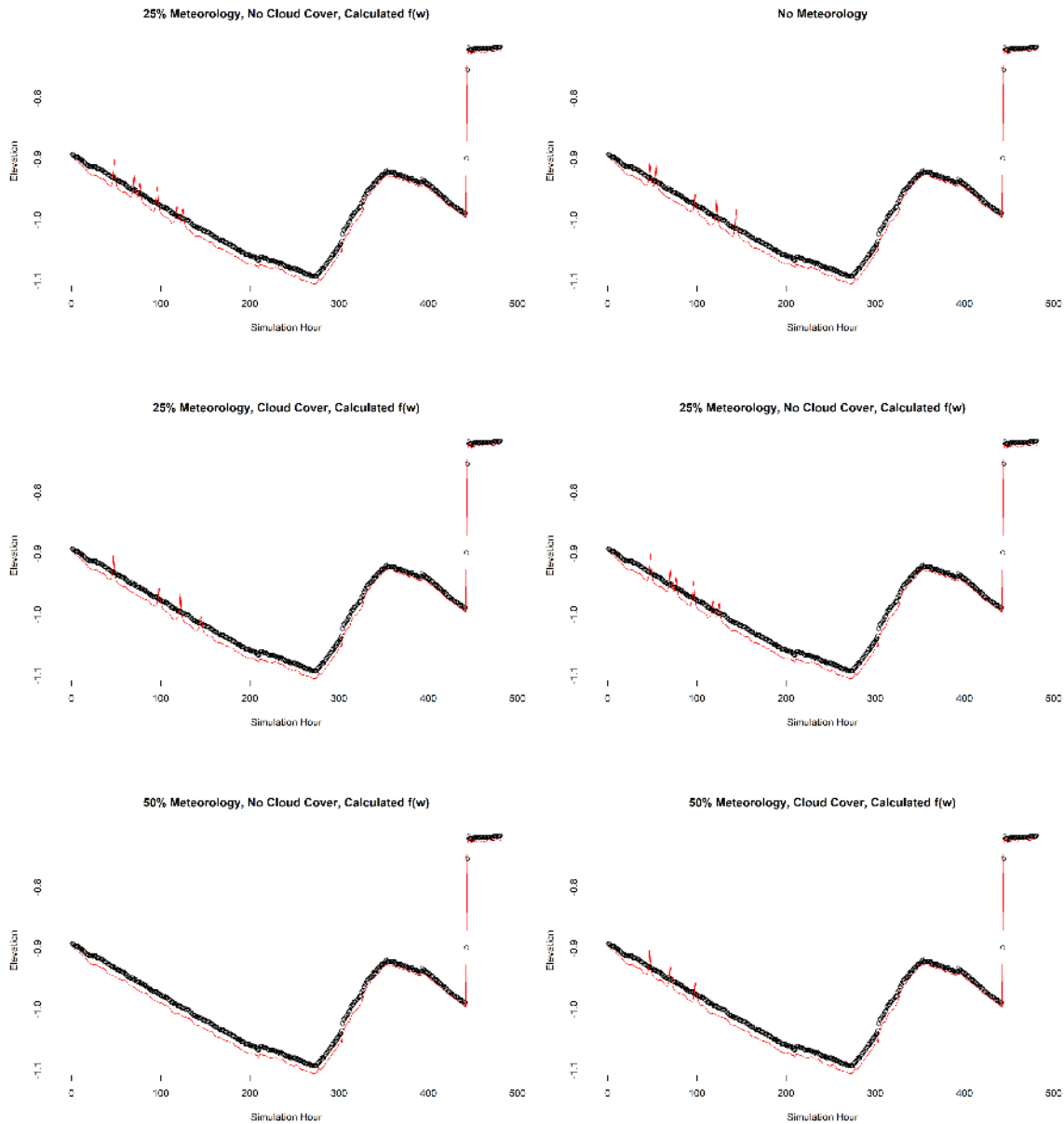
Figure 1.12. Predicted versus observed elevations (m) for 6 simulations during the summer time period for the mid USGS station. Observations are represented as points and predictions are represented as red lines. From left to right top to bottom: 1. 25% Wind speed, cloud cover off, mean f(w); 2. No Meteorology; 3. 25% Wind speed, cloud cover on, calculated f(w); 4. 25% Wind speed cloud cover off, calculated f(w); 5. 50% Wind speed, cloud cover off, calculated f(w); 6. 50% Wind speed, cloud cover on, calculated f(w).
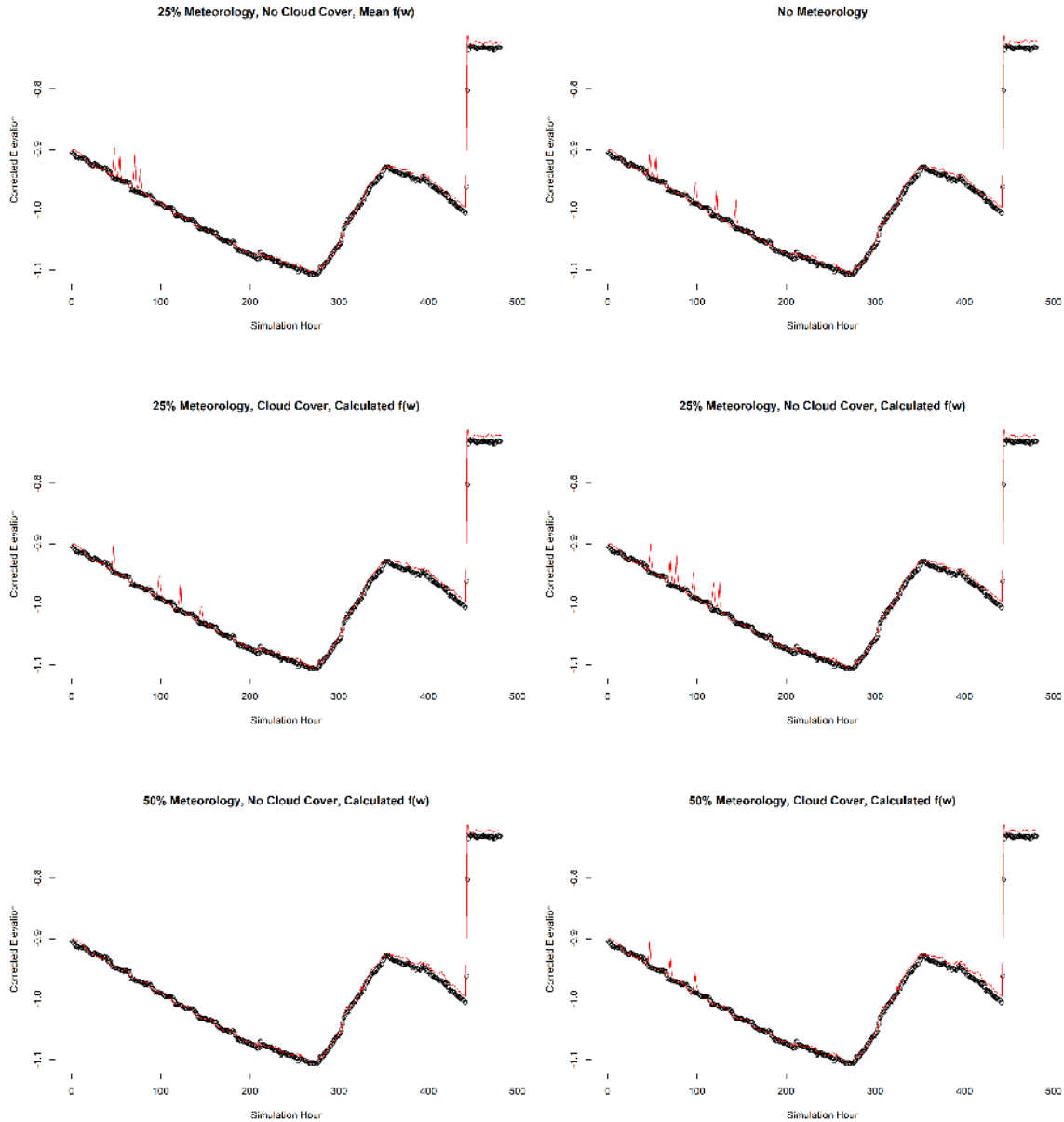
Figure 1.13. Predicted versus corrected observed elevations (m) for 6 simulations during the summer time period for the south USGS station. Observations are represented as points and predictions are represented as red lines. From left to right top to bottom: 1. 25% Wind speed, cloud cover off, mean f(w); 2. No Meteorology; 3. 25% Wind speed, cloud cover on, calculated f(w); 4. 25% Wind speed cloud cover off, calculated f(w); 5. 50% Wind speed, cloud cover off, calculated f(w); 6. 50% Wind speed, cloud cover on, calculated f(w).

Temperature predictions were better than salinity, but produced low agreement overall (Table 1.3). Values for d_m ranged from 0.792 to 0.877 for the northern station, 0.490 and 0.493 for the middle station, and 0.295 to 0.409 for the southern station. The model with 50% wind

speed, cloud cover on, and a calculated f(w) had the highest overall agreement with temperature

($d_m = 0.877$, 0.493, and 0.382, for north, middle, and south, respectively; Figs. 1.14-1.16). It is

also apparent that the overall trends in temperature were relatively well captured for the northern

station, including diurnal oscillations (Fig. 1.14). Predicted temperature values for the two sites

further from the boundary do not capture diurnal oscillations and only those with cloud cover

corrections show similar trends with the observed data. Simulations without cloud cover

corrections lost heat at the middle and southern stations (Figs. 1.15 and 1.16).
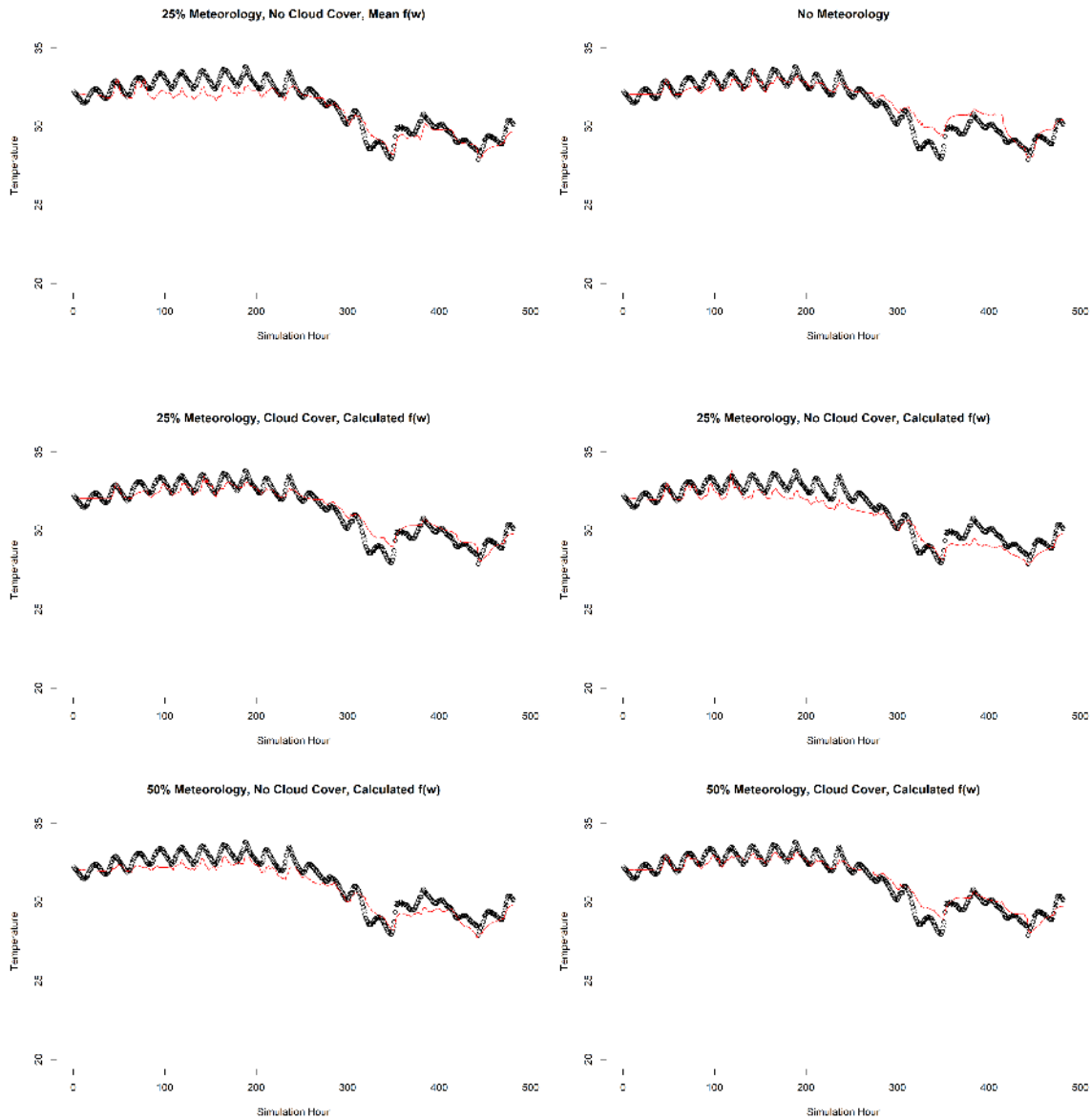
Figure 1.14. Predicted versus observed temperature (ºC) for 6 simulations during the summer time period for the northern USGS station. Observations are represented as points and predictions are represented as red lines. From left to right top to bottom: 1. 25% Wind speed, cloud cover off, mean f(w); 2. No Meteorology; 3. 25% Wind speed, cloud cover on, calculated f(w); 4. 25% Wind speed cloud cover off, calculated f(w); 5. 50% Wind speed, cloud cover off, calculated f(w); 6. 50% Wind speed, cloud cover on, calculated f(w).

23
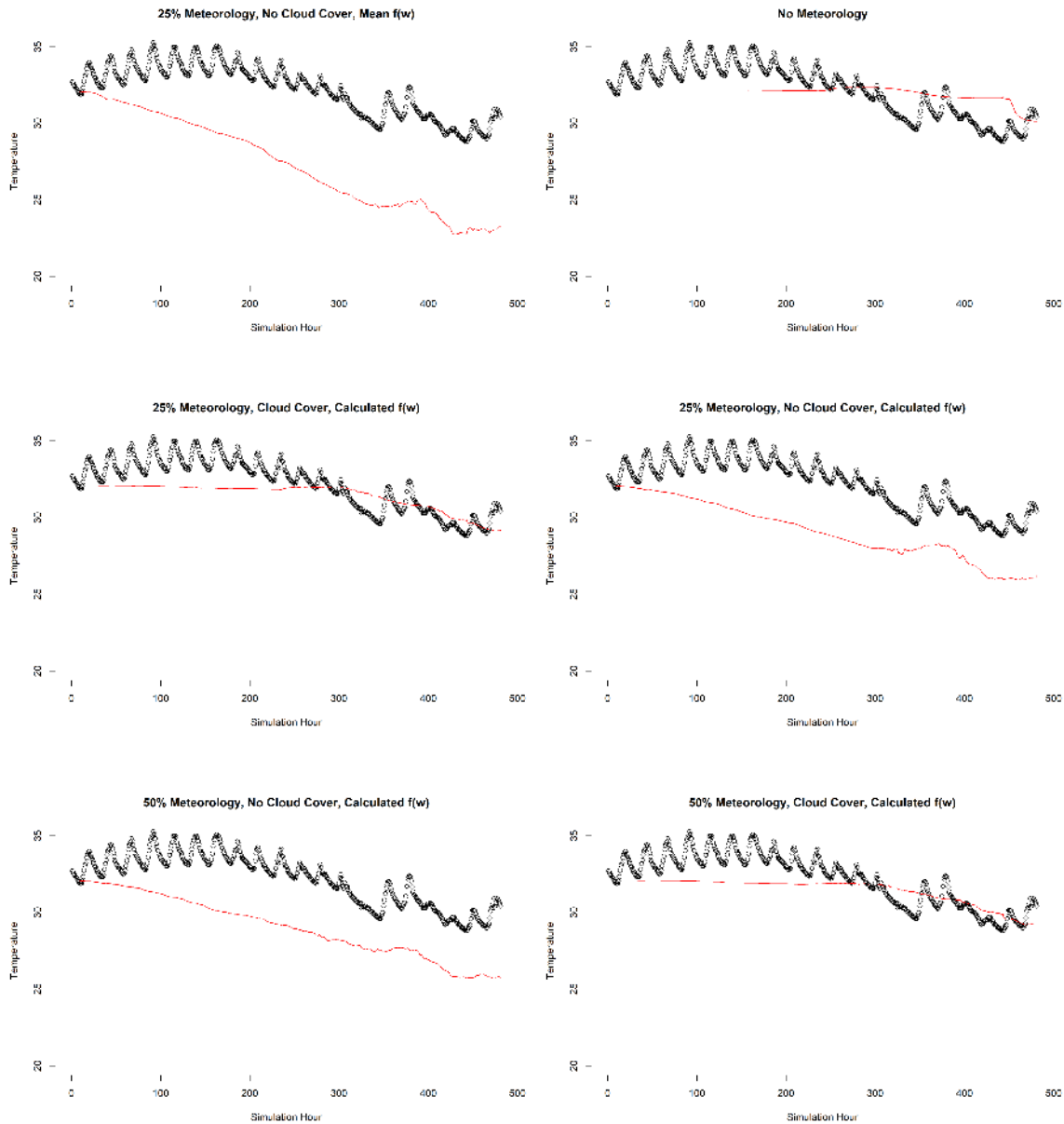
Figure 1.15. Predicted versus observed temperature (℃) for 6 simulations during the summer time period for the mid USGS station. Observations are represented as points and predictions are represented as red lines. From left to right top to bottom: 1. 25% Wind speed, cloud cover off, mean f(w); 2. No Meteorology; 3. 25% Wind speed, cloud cover on, calculated f(w); 4. 25% Wind speed cloud cover off, calculated f(w); 5. 50% Wind speed, cloud cover off, calculated f(w); 6. 50% Wind speed, cloud cover on, calculated f(w).
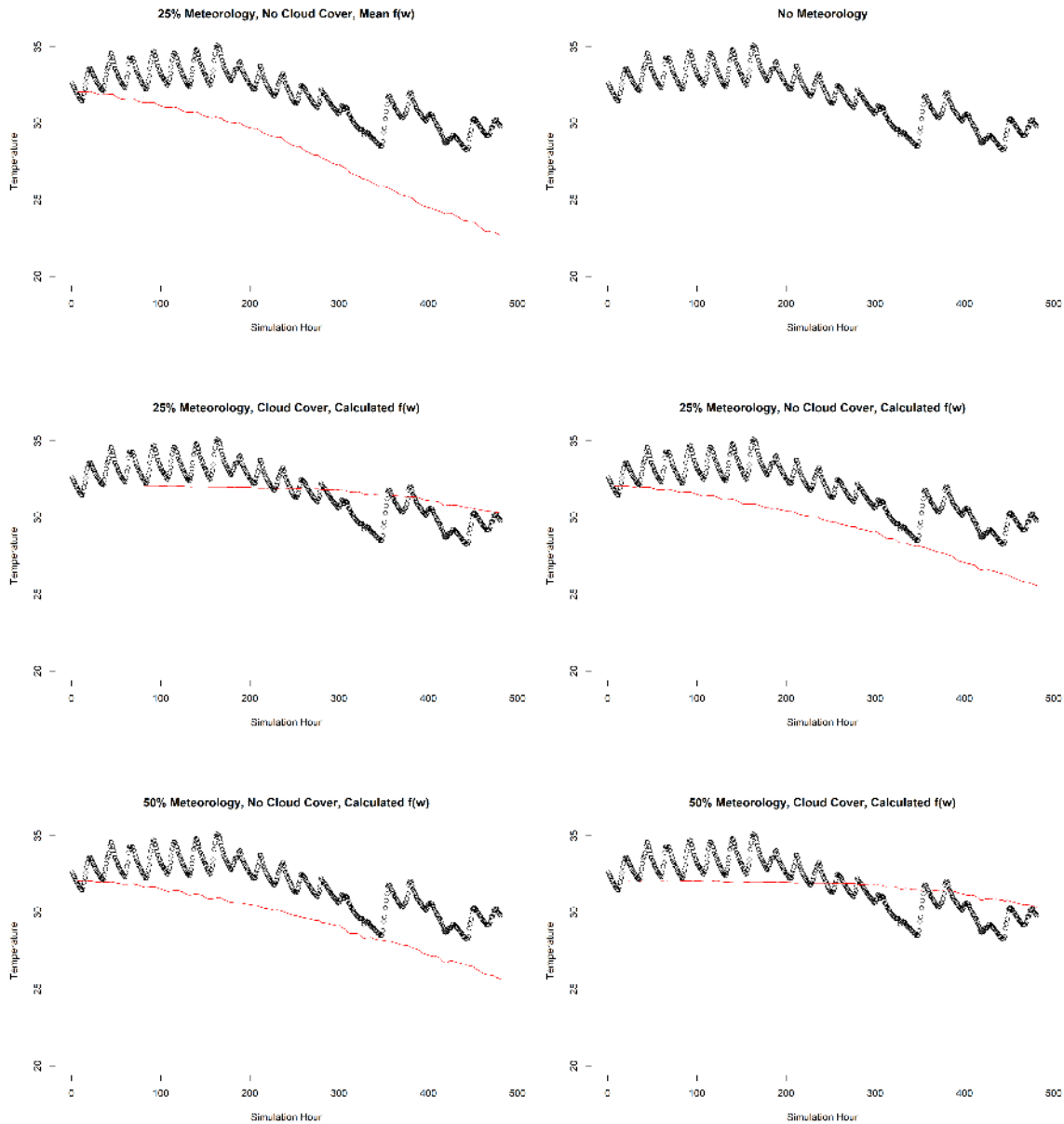
Figure 1.16. Predicted versus observed temperature (ºC) for 6 simulations during the summer time period for the south USGS station. Observations are represented as points and predictions are represented as red lines. From left to right top to bottom: 1. 25% Wind speed, cloud cover off, mean f(w); 2. No Meteorology; 3. 25% Wind speed, cloud cover on, calculated f(w); 4. 25% Wind speed cloud cover off, calculated f(w); 5. 50% Wind speed, cloud cover off, calculated f(w); 6. 50% Wind speed, cloud cover on, calculated f(w).

Across simulations, salinity had the lowest index of agreement (Table 1.3). Values for d_m ranged from 0.096 to 0.179 for the northern station, 0.058 and 0.075 for the middle station, and all simulations had values of 0.324 for the southern station (Figs. 1.17-1.19). Two simulations

25

seemed to more accurately predict salinity than the others. The simulation with no

meteorological forcings predicted the northern section the best and the simulation with 25%

wind speed, no cloud cover, and a mean f(w) value predicted the middle satiation's salinity the

best. All six simulations predicted the southern site's salinity to not change during the entire

simulation and thus produced the same d_m value.
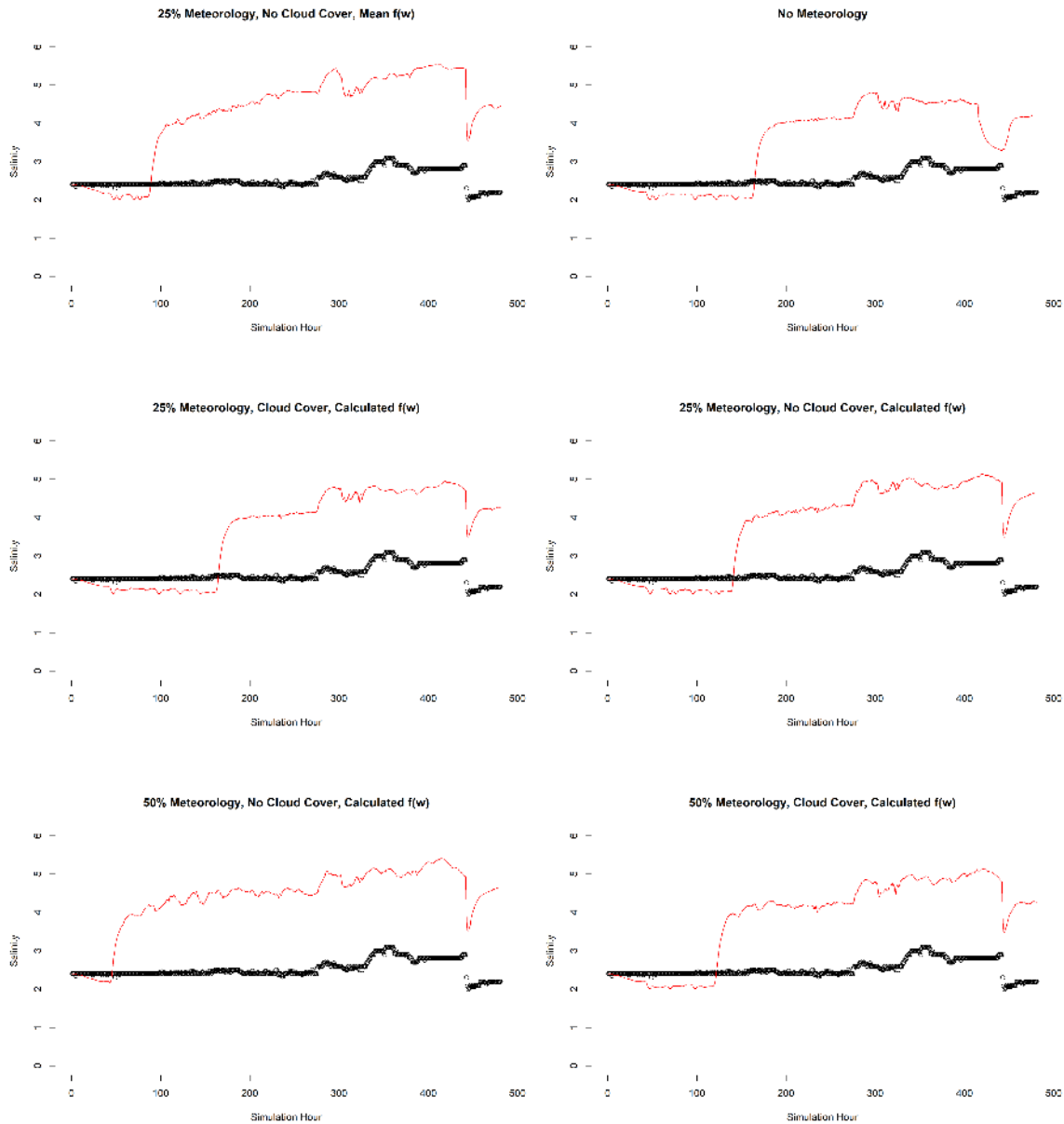
Figure 1.17. Predicted versus observed salinity for 6 simulations during the summer time period for the northern USGS station. Observations are represented as points and predictions are represented as red lines. From left to right top to bottom: 1. 25% Wind speed, cloud cover off, mean f(w); 2. No Meteorology; 3. 25% Wind speed, cloud cover on, calculated f(w); 4. 25% Wind speed cloud cover off, calculated f(w); 5. 50% Wind speed, cloud cover off, calculated f(w); 6. 50% Wind speed, cloud cover on, calculated f(w).

Figure 1.18. Predicted versus observed salinity for 6 simulations during the summer time period for the mid USGS station. Observations are represented as points and predictions are represented as red lines. From left to right top to bottom: 1. 25% Wind speed, cloud cover off, mean f(w); 2. No Meteorology; 3. 25% Wind speed, cloud cover on, calculated f(w); 4. 25% Wind speed cloud cover off, calculated f(w); 5. 50% Wind speed, cloud cover off, calculated f(w); 6. 50% Wind speed, cloud cover on, calculated f(w).

Figure 1.19. Predicted versus observed salinity for 6 simulations during the summer time period for the south USGS station. Observations are represented as points and predictions are represented as red lines. From left to right top to bottom: 1. 25% Wind speed, cloud cover off, mean f(w); 2. No Meteorology; 3. 25% Wind speed, cloud cover on, calculated f(w); 4. 25% Wind speed cloud cover off, calculated f(w); 5. 50% Wind speed, cloud cover off, calculated f(w); 6. 50% Wind speed, cloud cover on, calculated f(w).

The model with a 50% reduction in wind speed, no cloud cover correction, and a calculated f(w) was used to estimate tidal exchange flow during the summer time period, because it had the highest overall agreement with respect to elevation. The discharge magnitude before

29

the opening was 0.120 ± 0.084 m^3/s at the Far South transect, 0.180 ± 0.117 m^3/s at the South transect, 1.458 ± 0.626 m^3/s at the Middle transect, and 0.793 ± 0.361 m^3/s at the North transect (all $\mu \pm$ sd; Fig. 1.20). Peak discharges for all transects occurred at simulation hour 443 and were 6.12 m^3/s for the Far South transect, 8.96 m^3/s for the South transect, 17.12 m^3/s at the Mid transect, and 23.97 m^3/s at the North transect (Fig. 1.20). Velocities and thus discharges increase and then subside quickly during the sector gate opening (Fig. 1.20-1.28). Increased velocities and a rise in elevation can be noted for three hours post opening followed by stabilization and slight decrease in elevation (Figs. 1.21-1.28). Strong eddies develop in hour 2 of the opening and are sustained throughout the opening (Figs. 1.24-1.26).
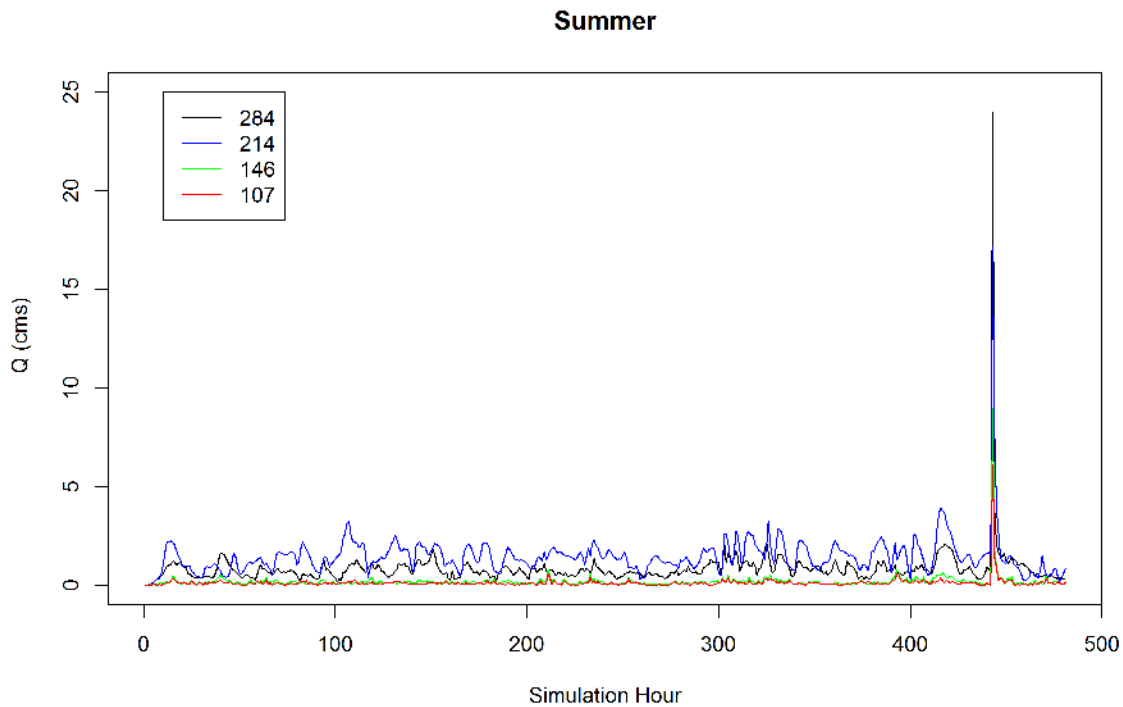
Figure 1.20. Total discharge (Q) in m^3/s at four transects in Bayou St. John during the summer period. Results from the best performing simulation with respect to elevation (50% reduction in Wind speed no cloud cover correction and a calculated f(w)) are displayed.

30
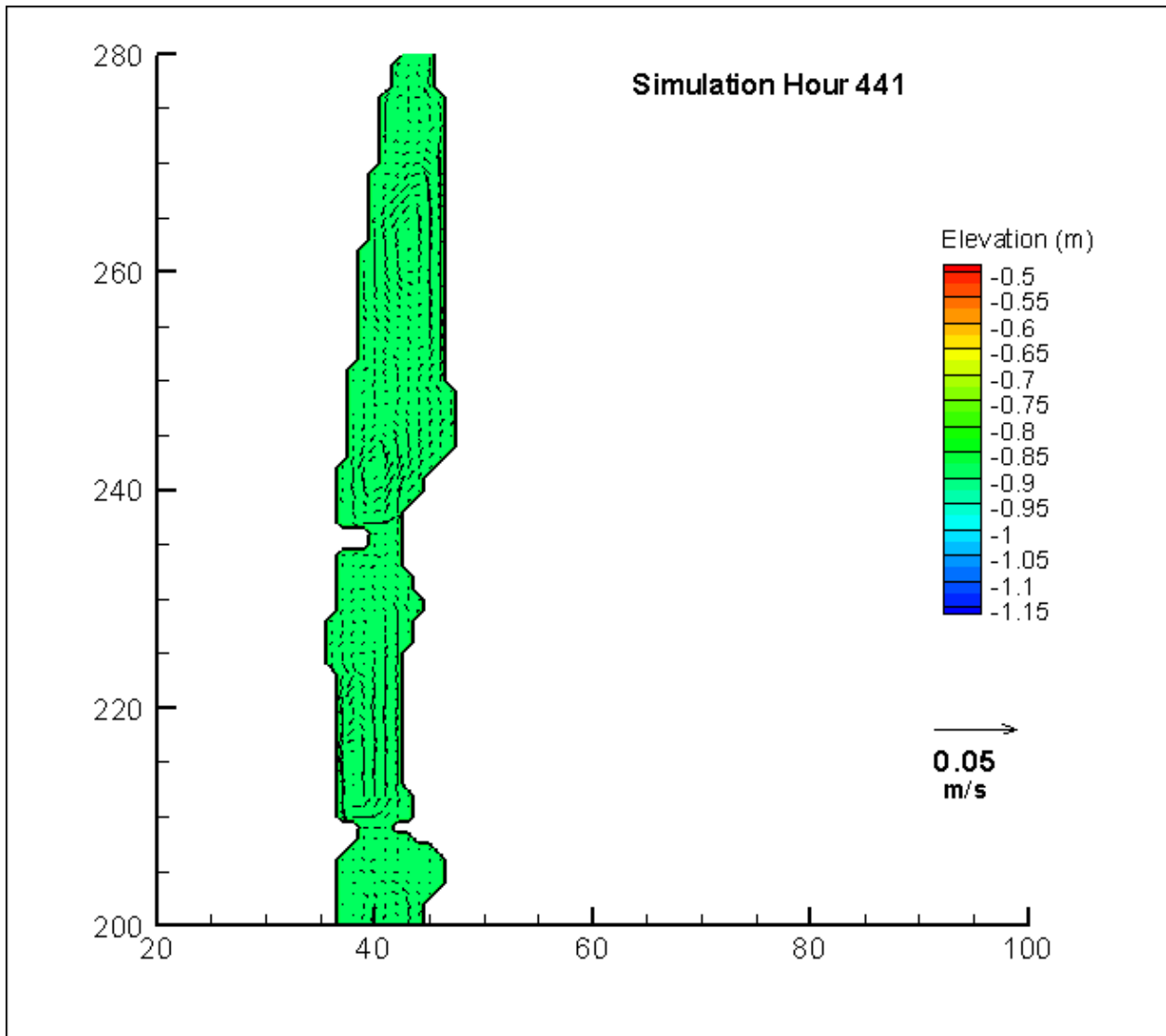
Figure 1.21. Tecplot image showing solutions for the summer period 50% reduction in meteorological forcing, no cloud cover correction, and a calculated f(w) simulation at hour 441 in the northern part of Bayou St. John. Axes indicate i,j coordinates of a Cartesian mesh with an extent of 70 x 300. This is 2 hours before sector gate opening and shows typical low energy conditions. Elevation is shown here as a contour and resultant velocity as a vector with appropriate legends.
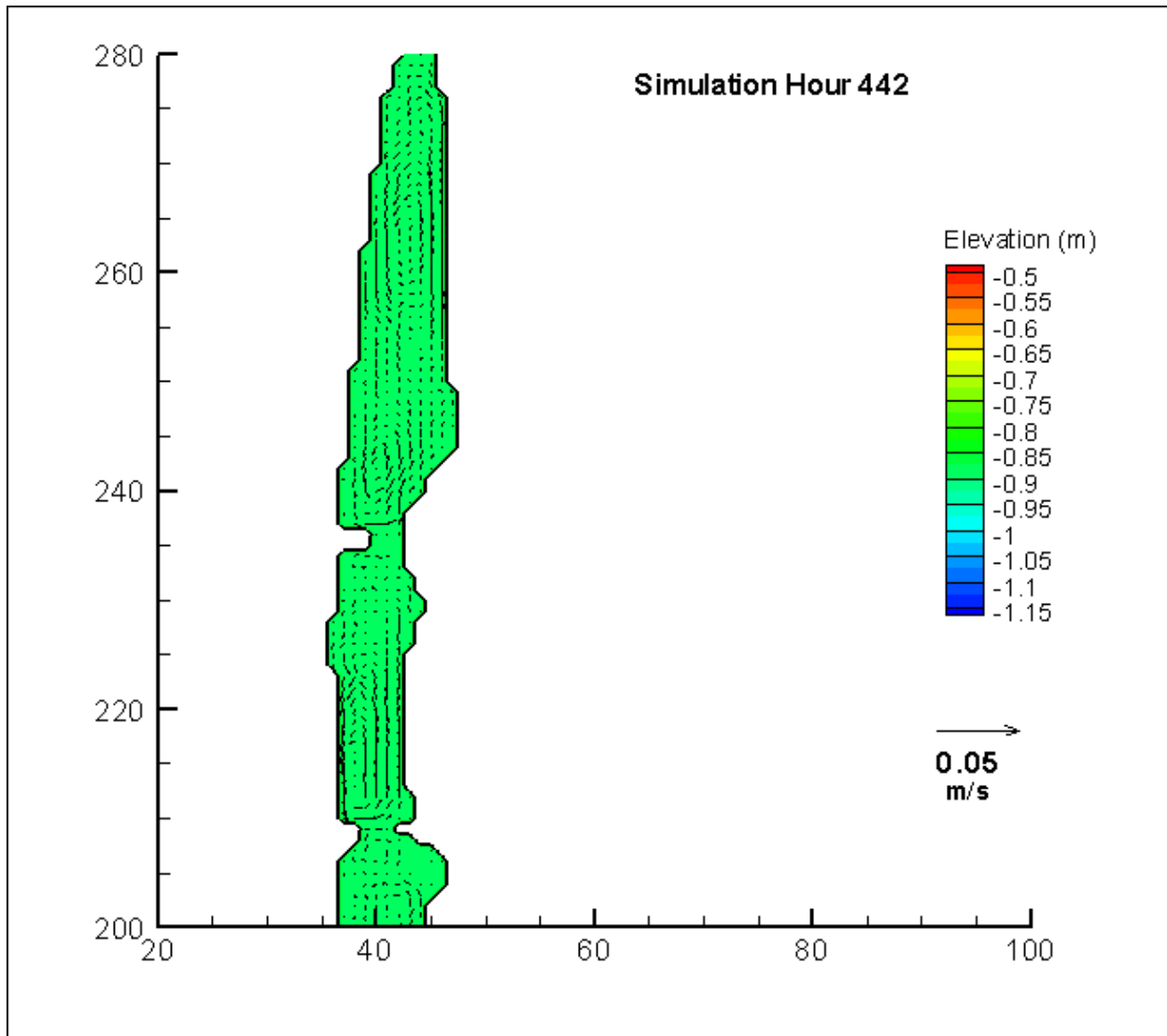
Figure 1.22. Solutions for the summer time period 50% reduction in meteorological forcing, no cloud cover correction, and a calculated f(w) simulation at hour 442 in the northern part of Bayou St. John. Axes indicate i,j coordinates of a Cartesian mesh with an extent of 70 x 300. This is one hour before the sector gate opening and shows typical low energy conditions. Elevation is shown here as a contour and resultant velocity as a vector with appropriate legends. Image created using TecPlot 360© graphical software.
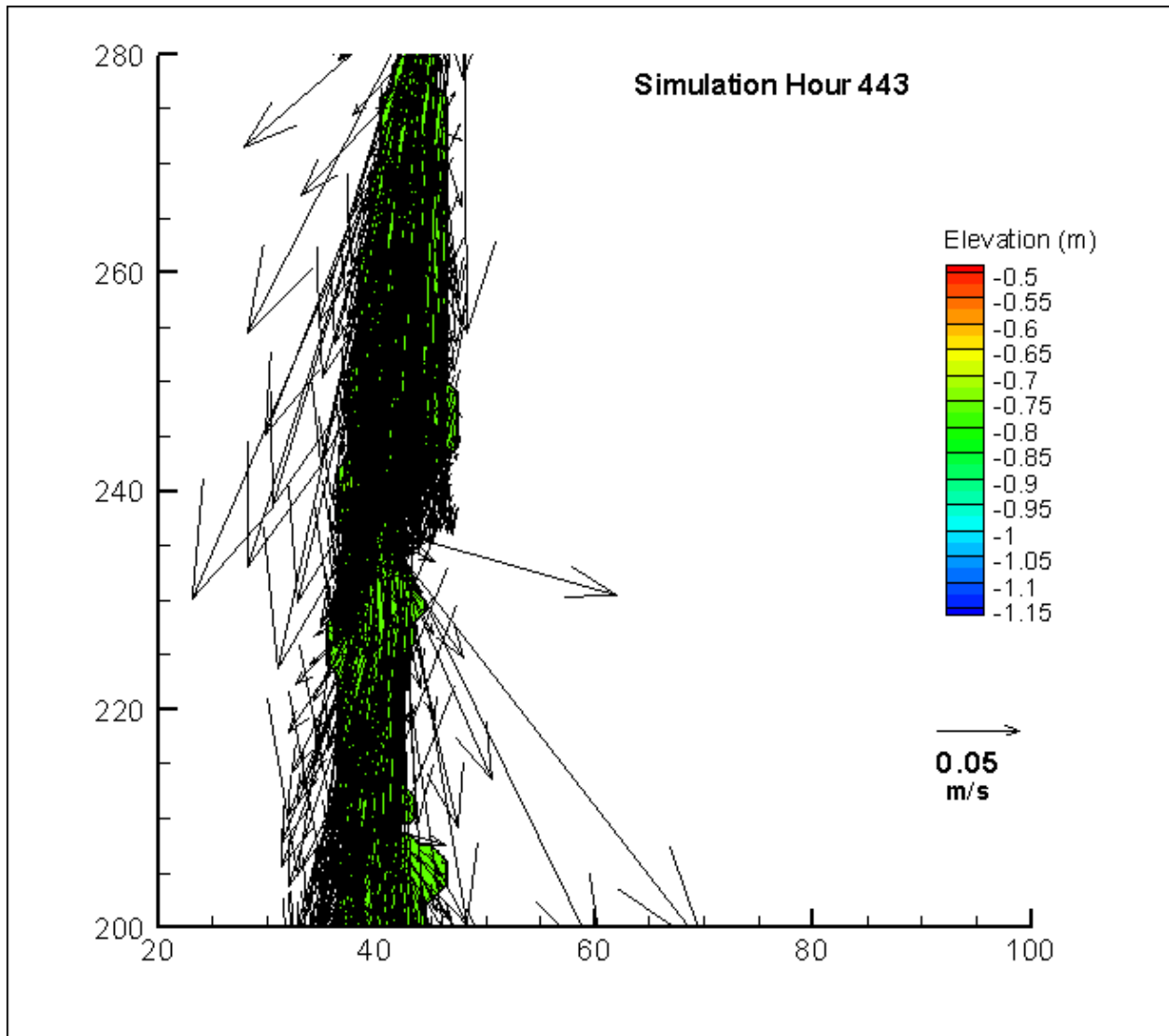
Figure 1.23. Solutions for the summer time period 50% reduction in meteorological forcing, no cloud cover correction, and a calculated f(w) simulation at hour 443 in the northern part of Bayou St. John. Axes indicate i,j coordinates of a Cartesian mesh with an extent of 70 x 300. This is during the beginning of the sector gate opening (hour 1). Elevation is shown here as a contour and resultant velocity as a vector with appropriate legends. Image created using TecPlot 360[©] graphical software.
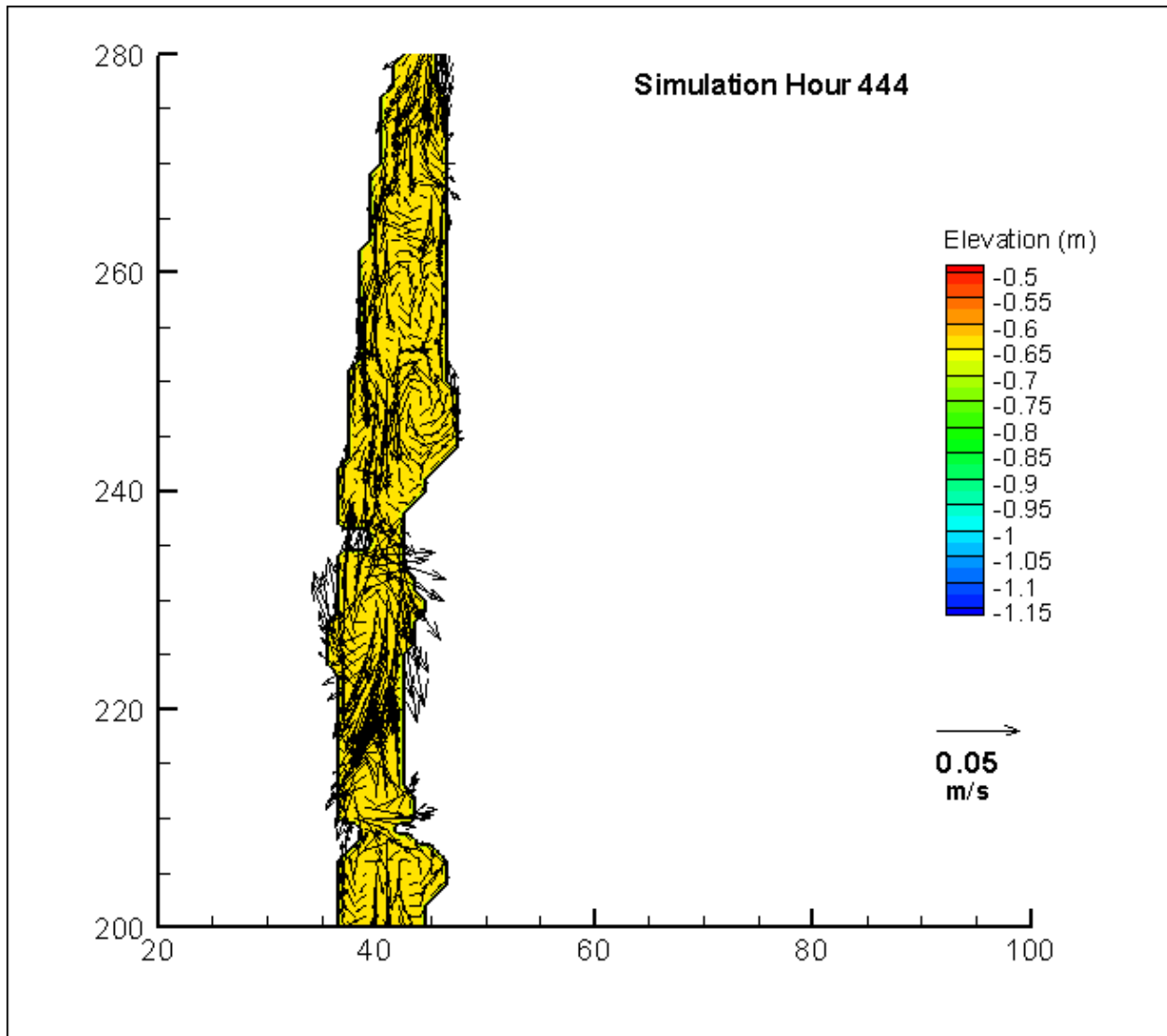
Figure 1.24. Solutions for the summer time period 50% reduction in meteorological forcing, no cloud cover correction, and a calculated f(w) simulation at hour 444 in the northern part of Bayou St. John. Axes indicate i,j coordinates of a Cartesian mesh with an extent of 70 x 300. This is during the sector gate opening (hour 2). Note the eddies appear more pronounced and have higher velocities when compared to solutions before the opening. Elevation is shown here as a contour and resultant velocity as a vector with appropriate legends. Image created using TecPlot 360[©] graphical software.
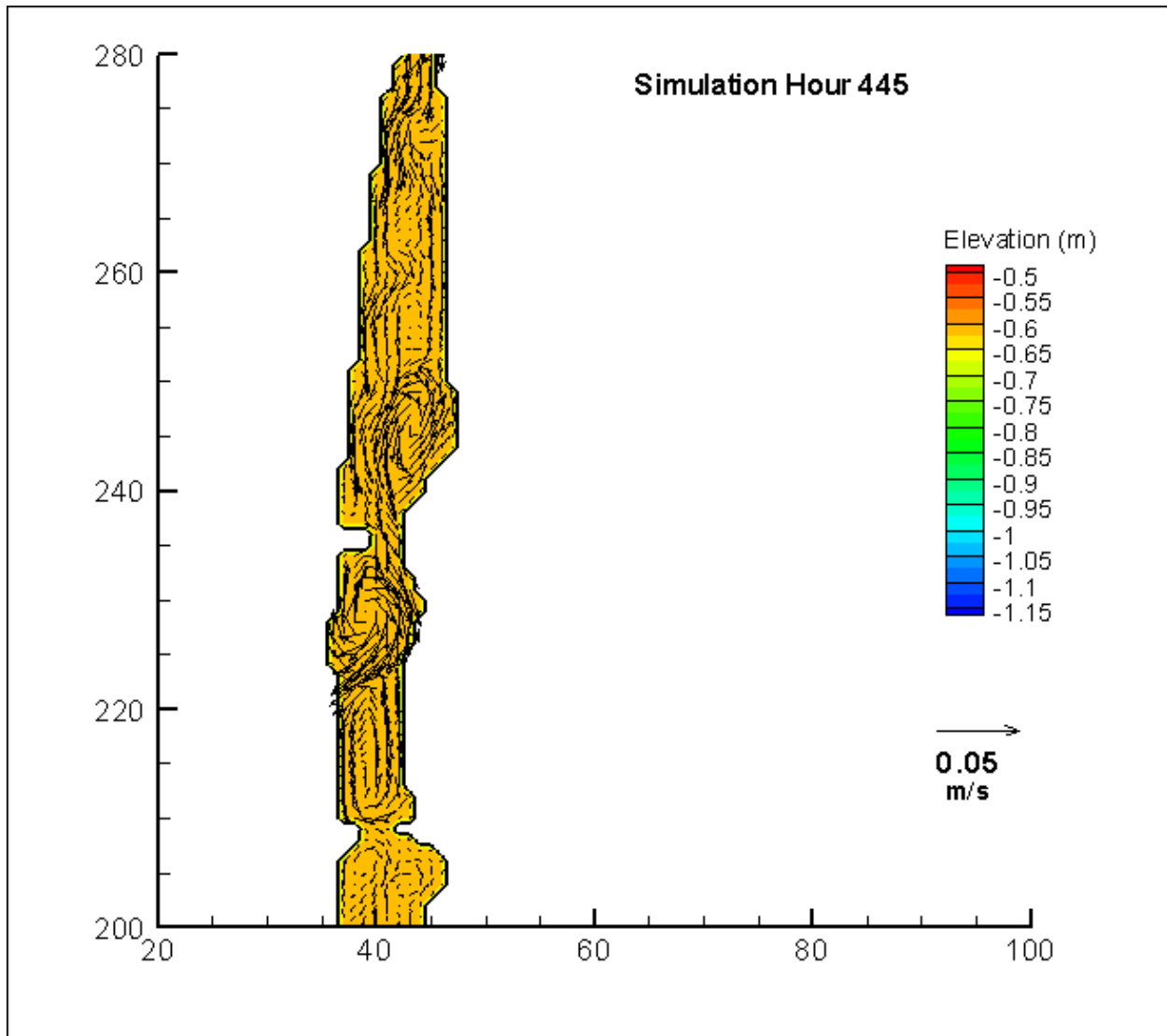
Figure 1.25. Solutions for the summer time period 50% reduction in meteorological forcing, no cloud cover correction, and a calculated f(w) simulation at hour 445 in the northern part of Bayou St. John. Axes indicate i,j coordinates of a Cartesian mesh with an extent of 70 x 300. This is at the end of the sector gate opening (hour 3). Note the eddies appear more pronounced and have higher velocities when compared to solutions before the opening. Elevation is shown here as a contour and resultant velocity as a vector with appropriate legends. Image created using TecPlot 360© graphical software.
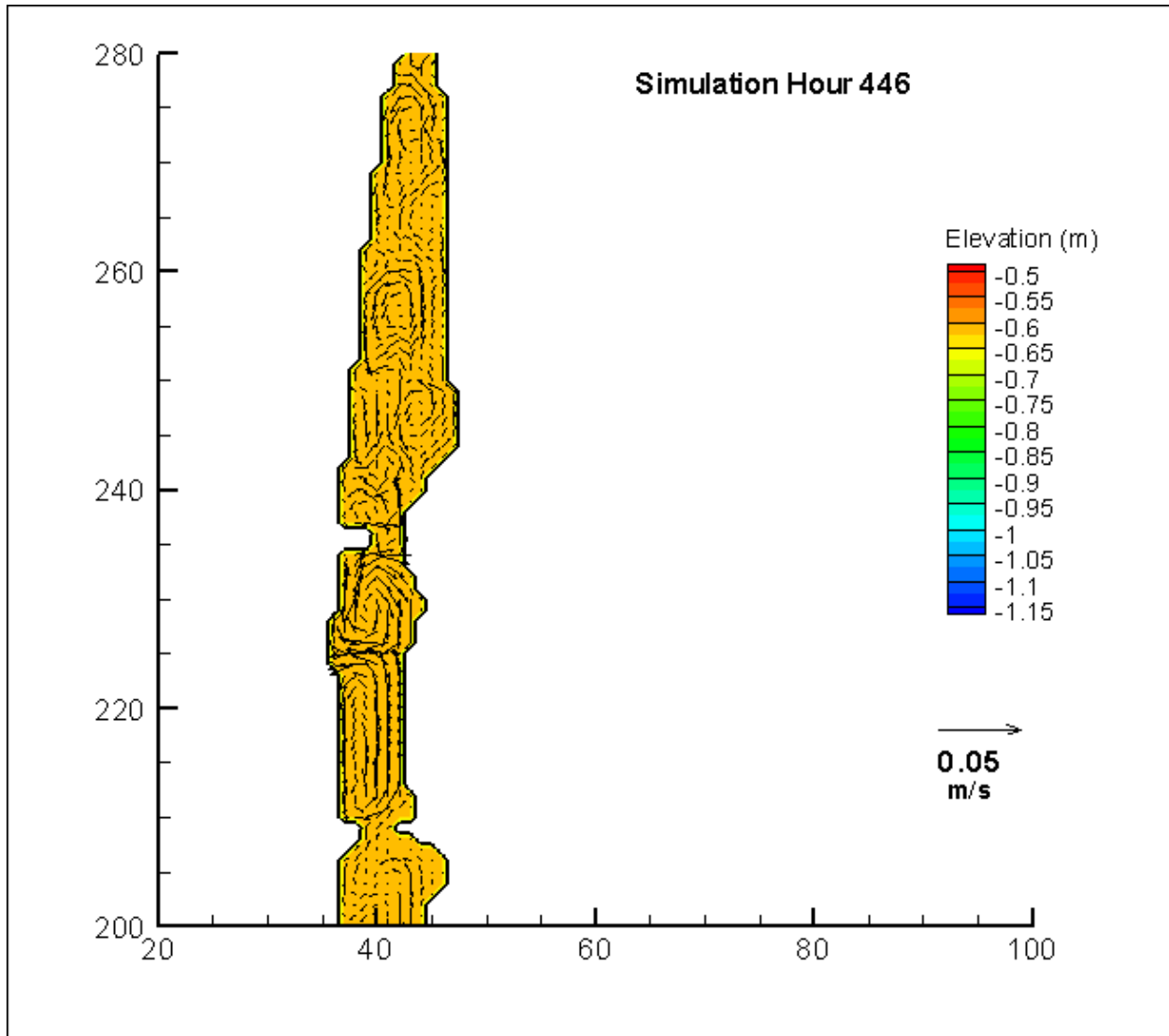
Figure 1.26. Solutions for the summer time period 50% reduction in meteorological forcing, no cloud cover correction, and a calculated f(w) simulation at hour 446 in the northern part of Bayou St. John. Axes indicate i,j coordinates of a Cartesian mesh with an extent of 70 x 300. This is at the end of the sector gate opening (hour 4). Note the velocities have decreased and stabilized. Elevation is shown here as a contour and resultant velocity as a vector with appropriate legends. Image created using TecPlot 360© graphical software.
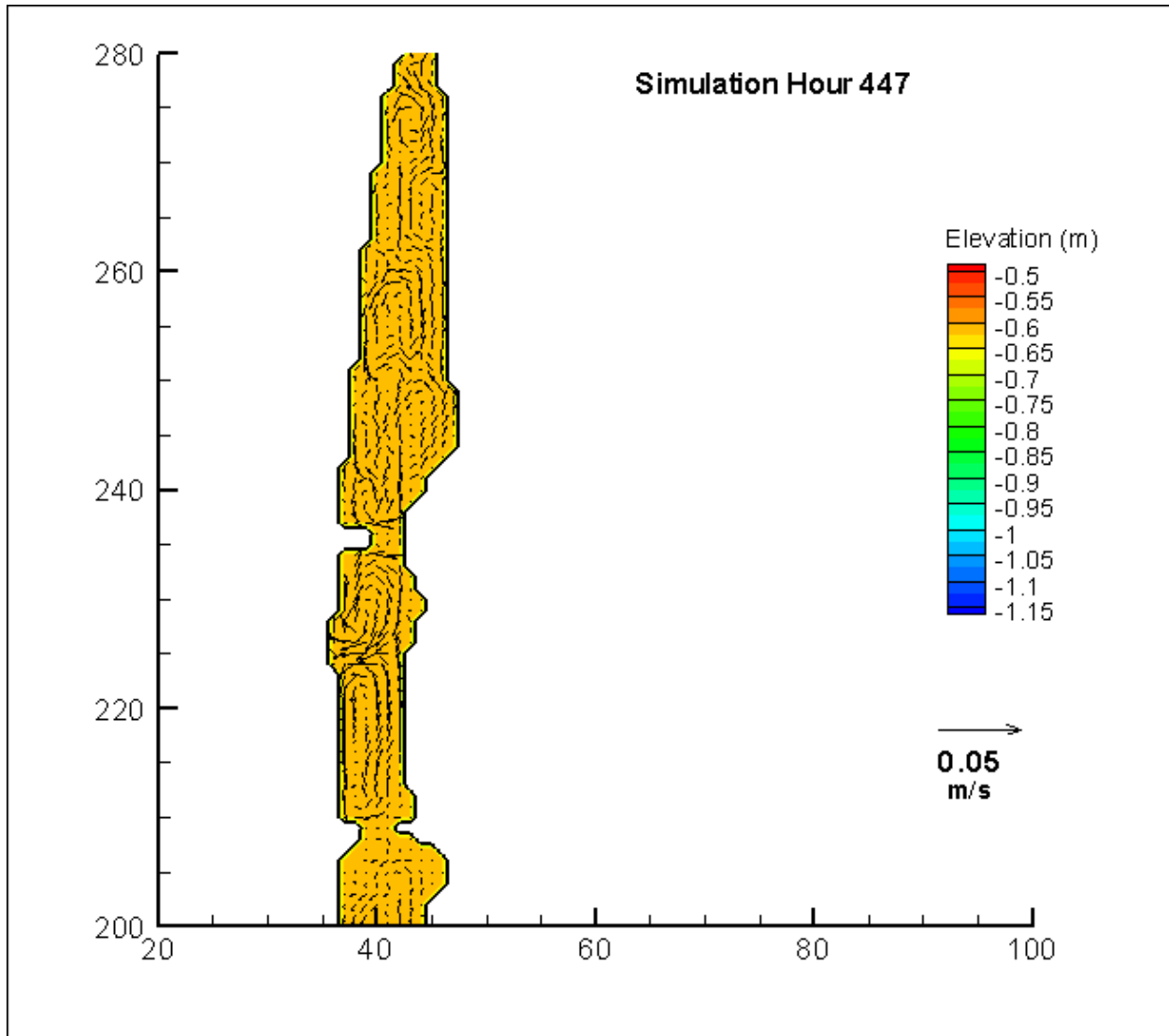
Figure 1.27. Solutions for the summer time period 50% reduction in meteorological forcing, no cloud cover correction, and a calculated f(w) simulation at hour 447 in the northern part of Bayou St. John. Axes indicate i,j coordinates of a Cartesian mesh with an extent of 70 x 300. This is after the sector gate opening. Note the velocities have stabilized with more turbulence than before the opening. Elevation is shown here as a contour and resultant velocity as a vector with appropriate legends. Image created using TecPlot 360© graphical software.
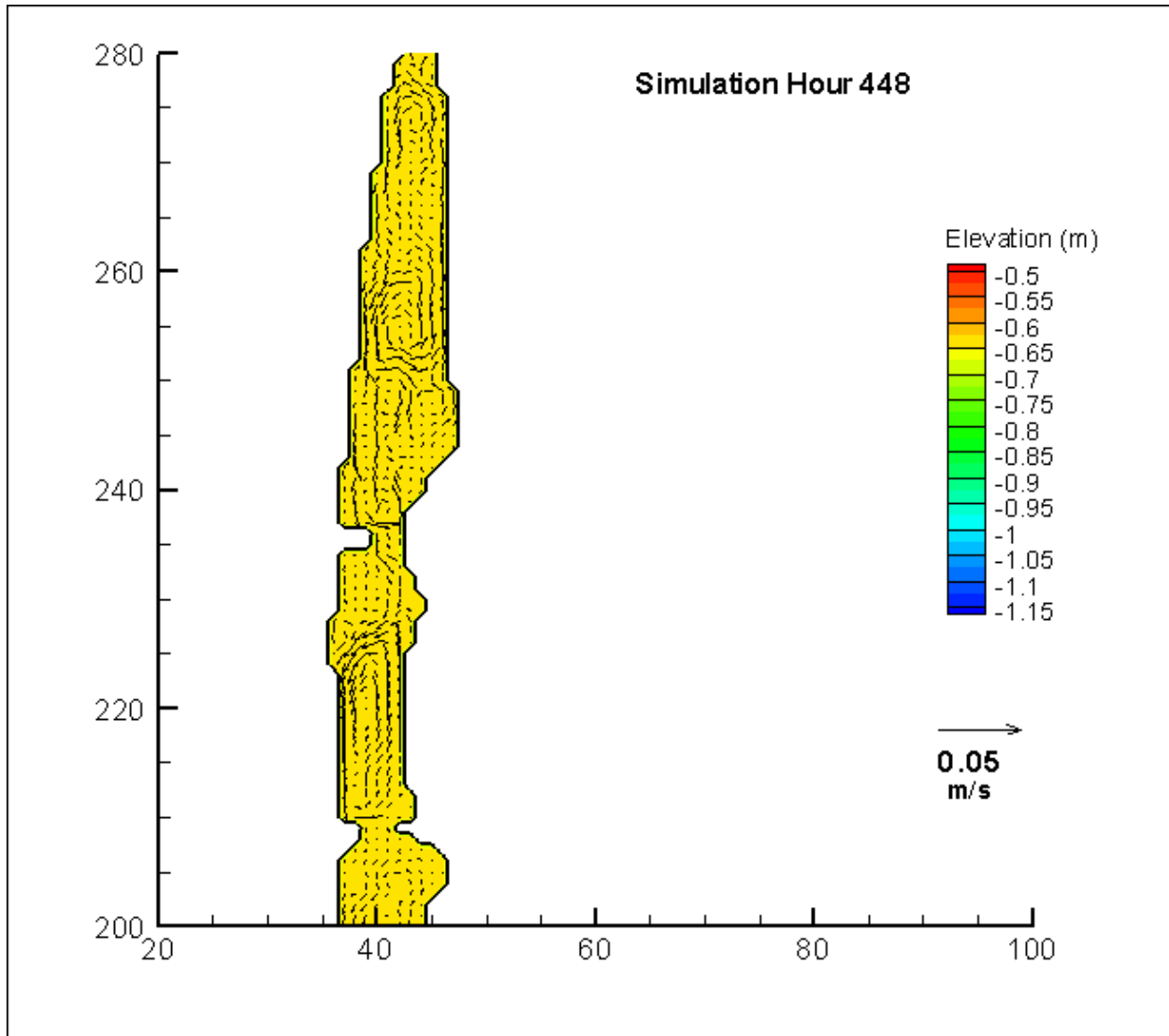
Figure 1.28. Solutions for the summer time period 50% reduction in meteorological forcing, no cloud cover correction, and a calculated f(w) simulation at hour 448 in the northern part of Bayou St. John. Axes indicate i,j coordinates of a Cartesian mesh with an extent of 70 x 300. This is after the sector gate opening. Note more turbulence is indicated here than before the opening (Figs. 1.20 and 1.21) and elevations have decreased since simulation hour 447 (Fig. 1.25). Elevation is shown here as a contour and resultant velocity as a vector with appropriate legends. Image created using TecPlot 360© graphical software.

Winter Simulations

Elevation predictions for all sites and all simulations had high agreement (Table 1.4).

Values for d_m ranged from 0.980 to 0.981 for the northern station, 0.935 and 0.938 for the middle

station, and 0.860 to 0.870 for the southern station. Corrected elevations were used at this station

as per the materials and methods. The simulation with a 75% reduction in wind speed, no cloud cover correction, and a mean f(w) value produced the best predictions for elevation overall (Figs. 1.29-1.31). It was within 0.001 of the highest d_m for the northern station and had the highest d_m for the other two stations. Overall, there was little variation in d_m among simulations. The largest among simulation variation was 0.01 and occurred at the middle site.

Table 1.4. Results of the winter period simulations for BSJ hydrology in response to a floodgate opening. The indices of agreement (d_m) of all simulations for elevation, temperature and salinity for each USGS field location are shown here. The best performing simulation for a given site and parameter are indicated by bold and italicized text.

Model	Location	Parameter	d_m	Model	Location	Parameter	d_m
25% Wind speed, Cloud Cover Off, Mean f(w)	North	Elevation	0.980	25% Wind speed, Cloud Cover Off, Calculated f(w)	North	Elevation	0.980
		Temperature	0.917			Temperature	0.917
		Salinity	0.307			*Salinity*	*0.314*
	Middle	*Elevation*	*0.938*		Middle	Elevation	0.936
		Temperature	*0.344*			Temperature	0.311
		Salinity	*0.031*			Salinity	0.007
	South	*Elevation**	*0.870*		South	Elevation*	0.860
		Temperature	*0.333*			Temperature	0.301
		Salinity	*0.070*			*Salinity*	*0.070*
No Meteorology	North	*Elevation*	*0.981*	50% Wind speed, Cloud Cover Off, Calculated f(w)	North	Elevation	0.980
		Temperature	0.897			*Temperature*	*0.928*
		Salinity	0.300			Salinity	0.313
	Middle	Elevation	0.937		Middle	Elevation	0.935
		Temperature	0.335			Temperature	0.257
		Salinity	0.009			Salinity	0.005
	South	*Elevation**	*0.870*		South	Elevation*	0.860
		Temperature	0.240			Temperature	0.290
		Salinity	*0.070*			*Salinity*	*0.070*
25% Wind speed, Cloud Cover On, Calculated f(w)	North	Elevation	0.980	50% Wind speed, Cloud Cover On, Calculated f(w)	North	Elevation	0.980
		Temperature	0.915			Temperature	0.917
		Salinity	0.311			*Salinity*	*0.314*
	Middle	Elevation	0.937		Middle	Elevation	0.936
		Temperature	0.308			Temperature	0.311
		Salinity	0.027			Salinity	0.006
	South	Elevation*	0.866		South	Elevation*	0.860
		Temperature	0.294			Temperature	0.301
		Salinity	*0.070*			*Salinity*	*0.070*

*indicates that corrected elevation was used, see Materials and Methods for details
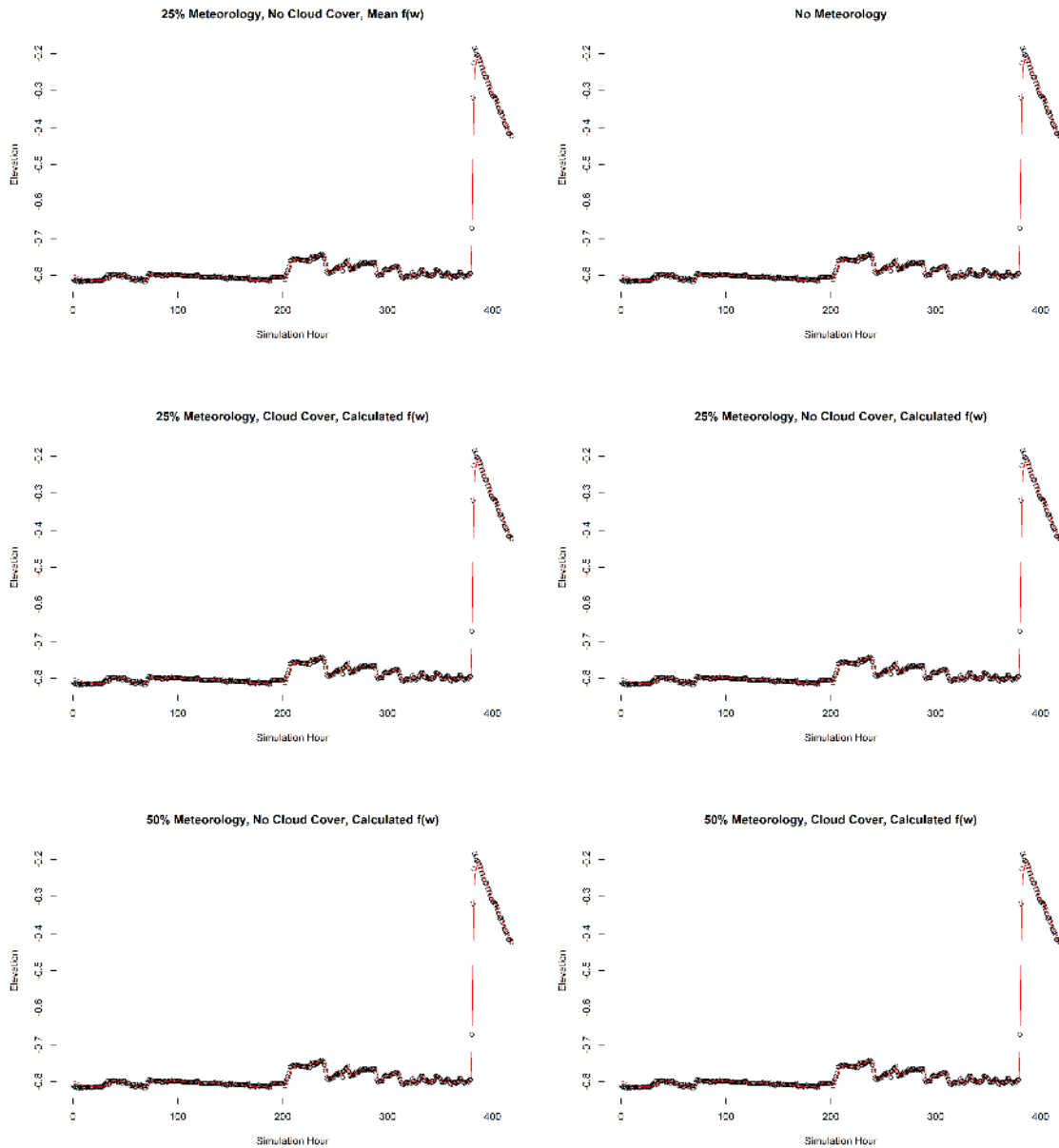
Figure 1.29. Predicted versus observed elevations (m) for 6 simulations during the winter time period for the northern USGS station. Observations are represented as points and predictions are represented as red lines. From left to right top to bottom: 1. 25% Wind speed, cloud cover off, mean f(w); 2. No Meteorology; 3. 25% Wind speed, cloud cover on, calculated f(w); 4. 25% Wind speed cloud cover off, calculated f(w); 5. 50% Wind speed, cloud cover off, calculated f(w); 6. 50% Wind speed, cloud cover on, calculated f(w).
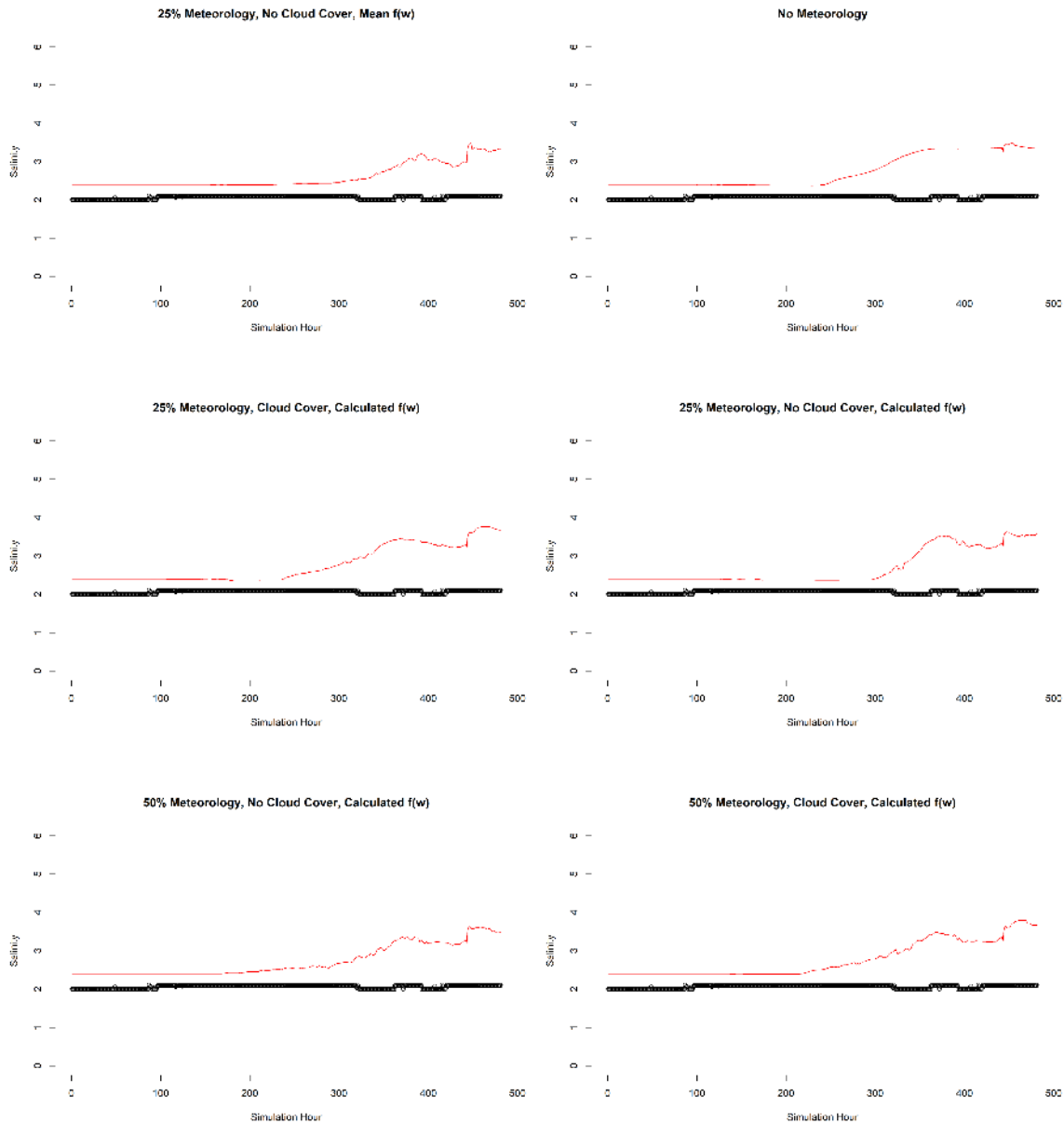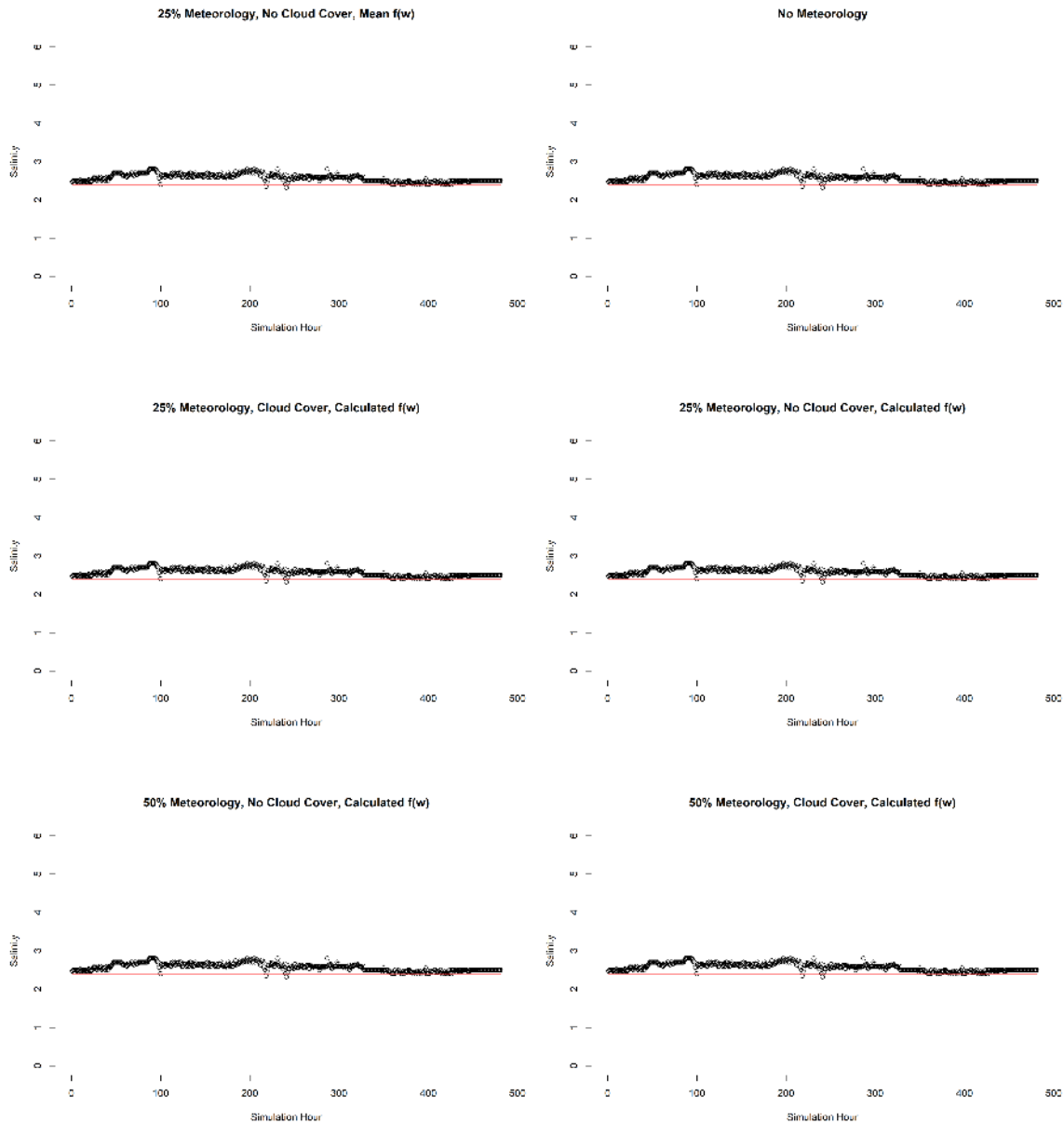
41
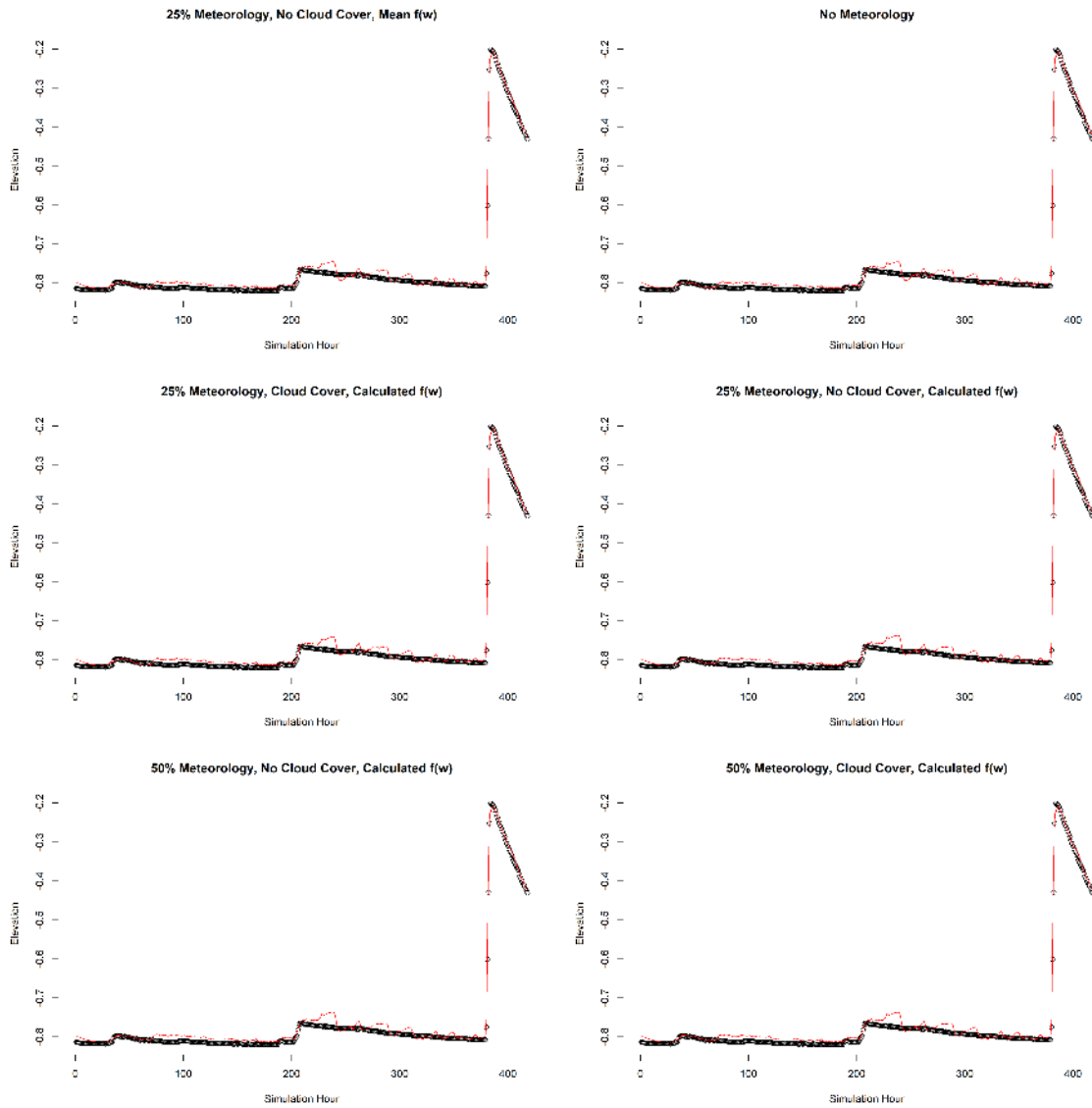
Figure 1.30. Predicted versus observed elevations (m) for 6 simulations during the winter time period for the mid USGS station. Observations are represented as points and predictions are represented as red lines. From left to right top to bottom: 1. 25% Wind speed, cloud cover off, mean f(w); 2. No Meteorology; 3. 25% Wind speed, cloud cover on, calculated f(w); 4. 25% Wind speed cloud cover off, calculated f(w); 5. 50% Wind speed, cloud cover off, calculated f(w); 6. 50% Wind speed, cloud cover on, calculated f(w).
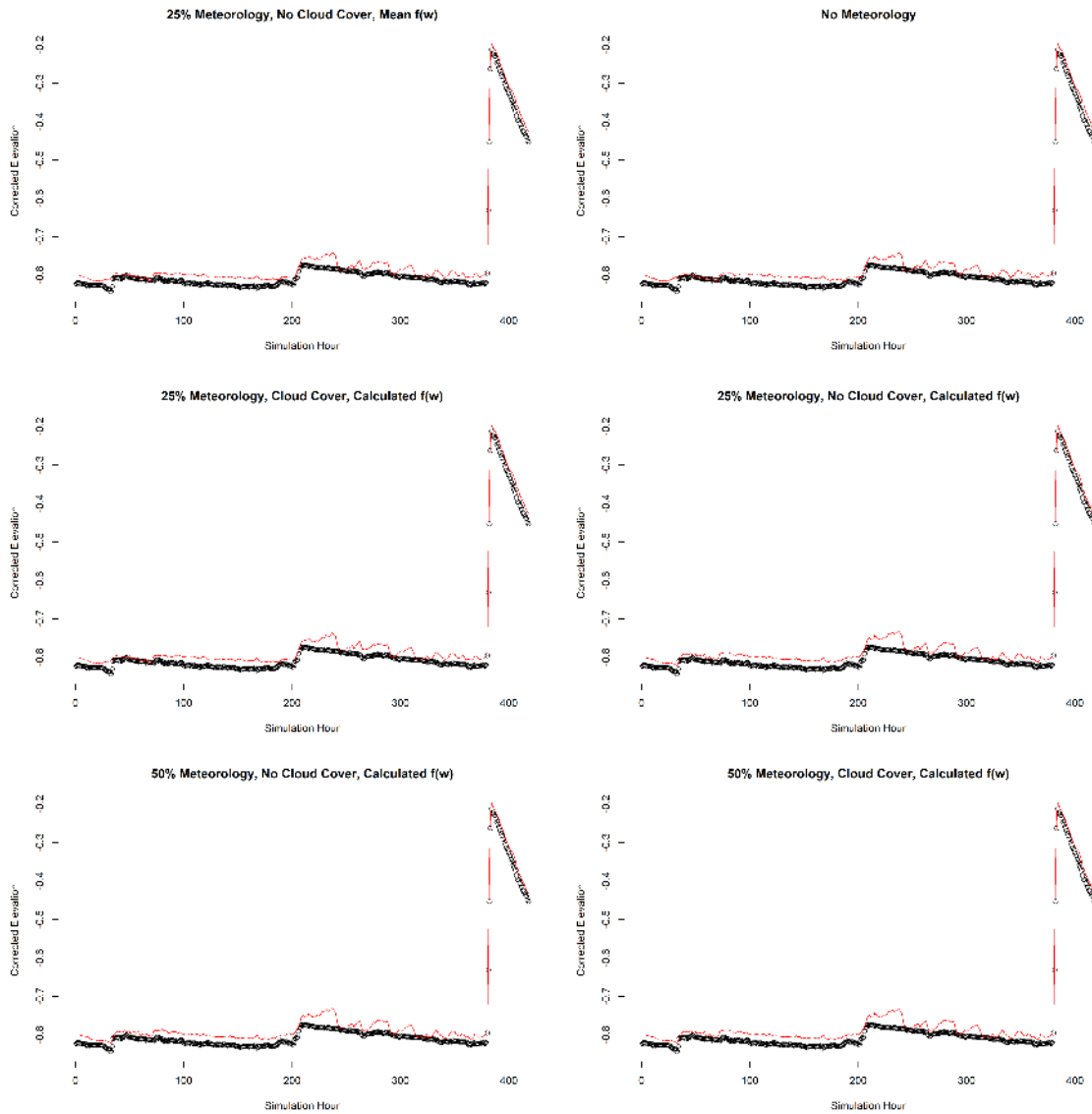
Figure 1.31. Predicted versus corrected observed elevations (m) for 6 simulations during the winter time period for the south USGS station. Observations are represented as points and predictions are represented as red lines. From left to right top to bottom: 1. 25% Wind speed, cloud cover off, mean f(w); 2. No Meteorology; 3. 25% Wind speed, cloud cover on, calculated f(w); 4. 25% Wind speed cloud cover off, calculated f(w); 5. 50% Wind speed, cloud cover off, calculated f(w); 6. 50% Wind speed, cloud cover on, calculated f(w).

Temperature predictions had more agreement than salinity, but produced low indices overall (Table 1.4). Values for d_m ranged from 0.897 to 0.928 for the northern station, 0.490 and 0.257 for the middle station, and 0.240 to 0.333 for the southern station. The model with a 75% reduced wind speed, no cloud cover correction, and a mean f(w) had the highest overall

agreement with temperature ($d_m = 0.917$, 0.344, and 0.333, for north, middle, and south, respectively; Figs. 1.32-1.34). Diurnal oscillations in temperature are not as evident during this time period. Simulations were accurate near the boundary, but a loss of heat can be noted for the two more southern stations (Figs. 1.32-1.34).
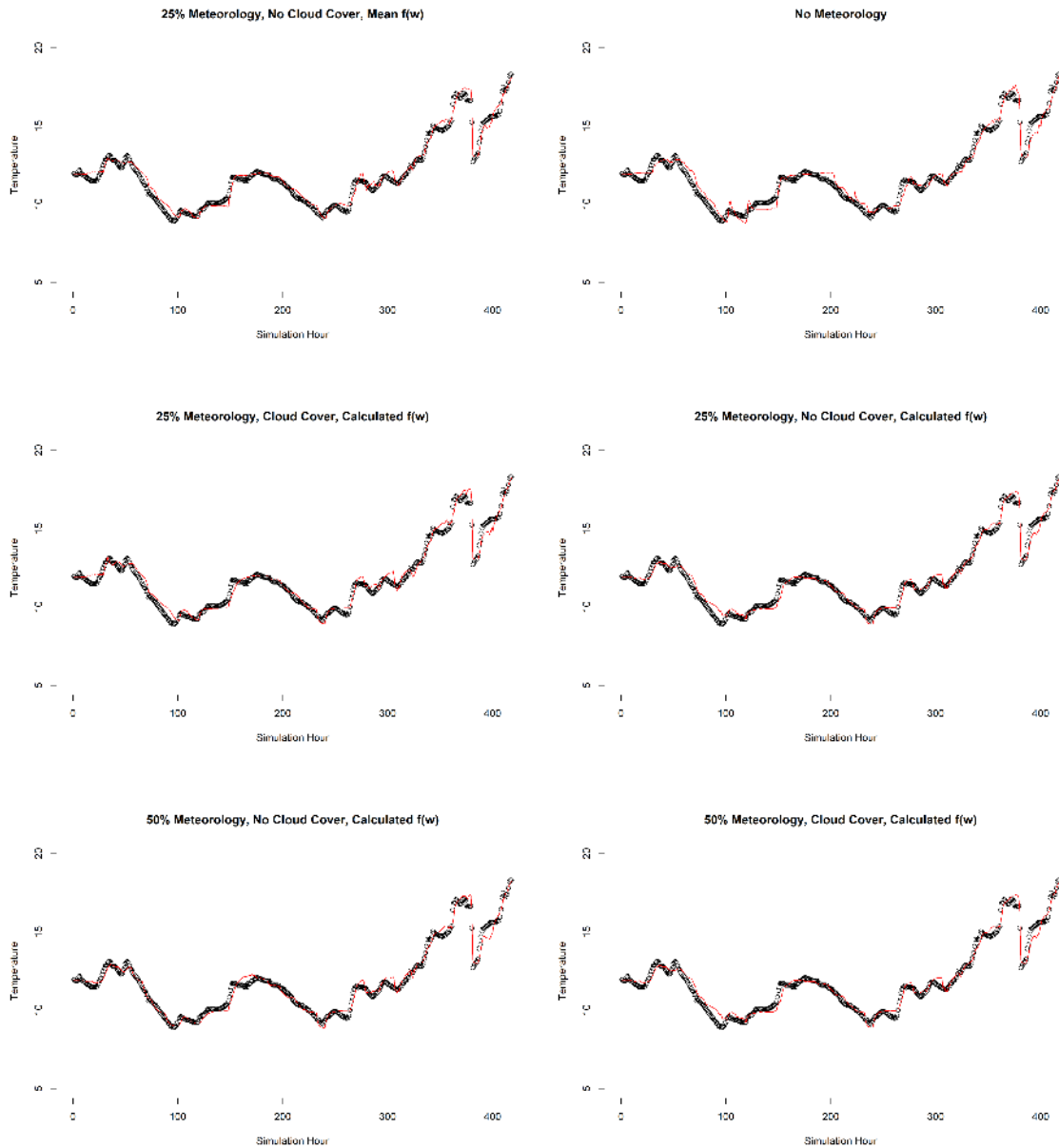
Figure 1.32. Predicted versus observed temperature (℃) for 6 simulations during the winter time period for the northern USGS station. Observations are represented as points and predictions are represented as red lines. From left to right top to bottom: 1. 25% Wind speed, cloud cover off, mean f(w); 2. No Meteorology; 3. 25% Wind speed, cloud cover on, calculated f(w); 4. 25% Wind speed cloud cover off, calculated f(w); 5. 50% Wind speed, cloud cover off, calculated f(w); 6. 50% Wind speed, cloud cover on, calculated f(w).
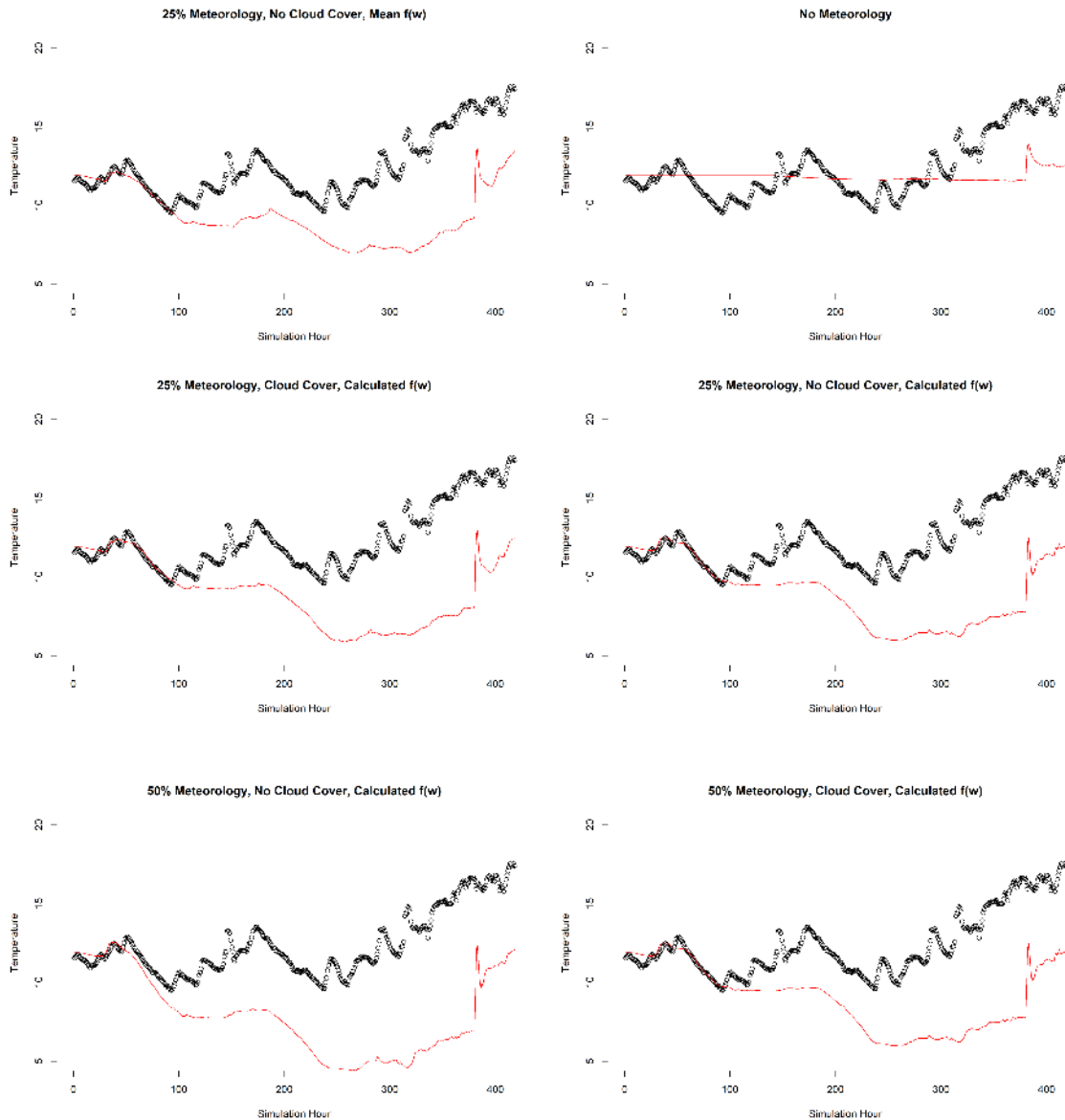
Figure 1.33. Predicted versus observed temperature (°C) for 6 simulations during the winter time period for the mid USGS station. Observations are represented as points and predictions are represented as red lines. From left to right top to bottom: 1. 25% Wind speed, cloud cover off, mean f(w); 2. No Meteorology; 3. 25% Wind speed, cloud cover on, calculated f(w); 4. 25% Wind speed cloud cover off, calculated f(w); 5. 50% Wind speed, cloud cover off, calculated f(w); 6. 50% Wind speed, cloud cover on, calculated f(w).
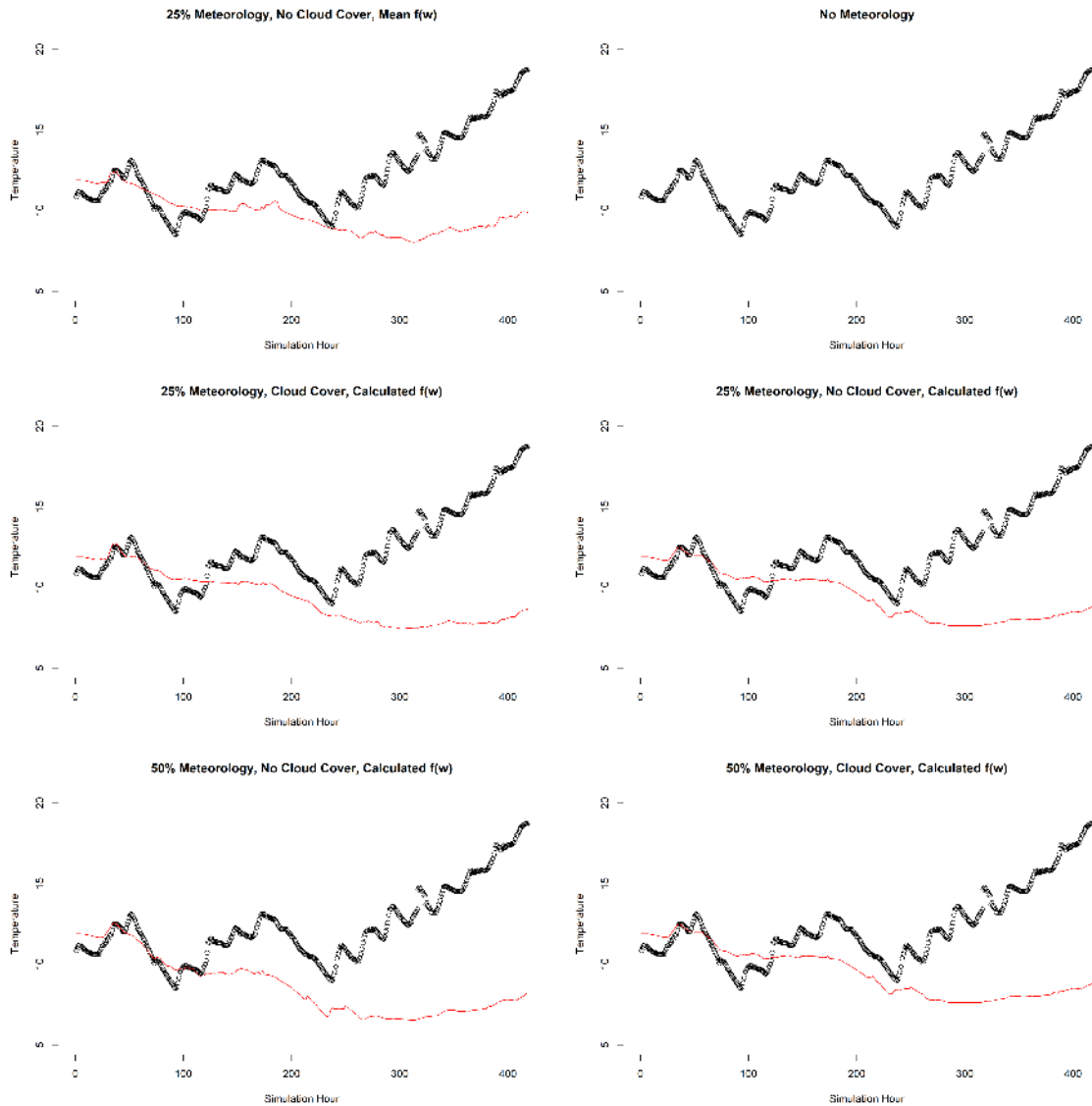
Figure 1.34. Predicted versus observed temperature (°C) for 6 simulations during the winter time period for the south USGS station. Observations are represented as points and predictions are represented as red lines. From left to right top to bottom: 1. 25% Wind speed, cloud cover off, mean f(w); 2. No Meteorology; 3. 25% Wind speed, cloud cover on, calculated f(w); 4. 25% Wind speed cloud cover off, calculated f(w); 5. 50% Wind speed, cloud cover off, calculated f(w); 6. 50% Wind speed, cloud cover on, calculated f(w).

Like the summer period, salinity had the lowest indices of agreement (Table 1.4). Values for d_m ranged from 0.300 to 0.314 for the northern station, 0.005 and 0.031 for the middle station, all simulations had values of 0.070 for the southern station. The model with a 75% reduction in wind speed, no cloud cover correction, and mean f(w) performed the best overall (Figs. 1.35-

1.37). All six simulations predicted the southern site's salinity to not change during the entire

simulation and thus produced the same d_m value (Fig. 1.37).
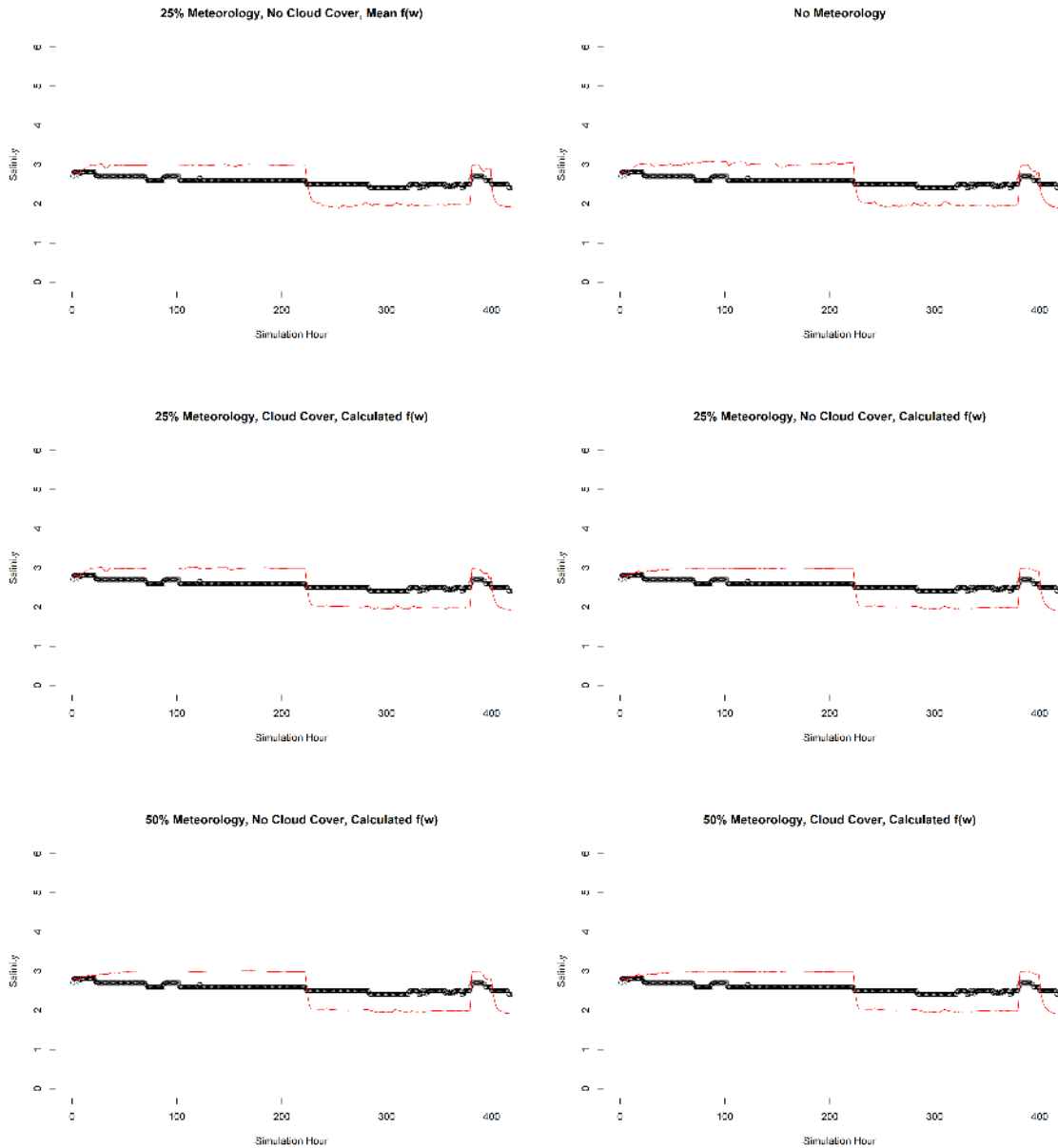
Figure 1.35. Predicted versus observed salinity for 6 simulations during the winter time period for the northern USGS station. Observations are represented as points and predictions are represented as red lines. From left to right top to bottom: 1. 25% Wind speed, cloud cover off, mean f(w); 2. No Meteorology; 3. 25% Wind speed, cloud cover on, calculated f(w); 4. 25% Wind speed cloud cover off, calculated f(w); 5. 50% Wind speed, cloud cover off, calculated f(w); 6. 50% Wind speed, cloud cover on, calculated f(w).
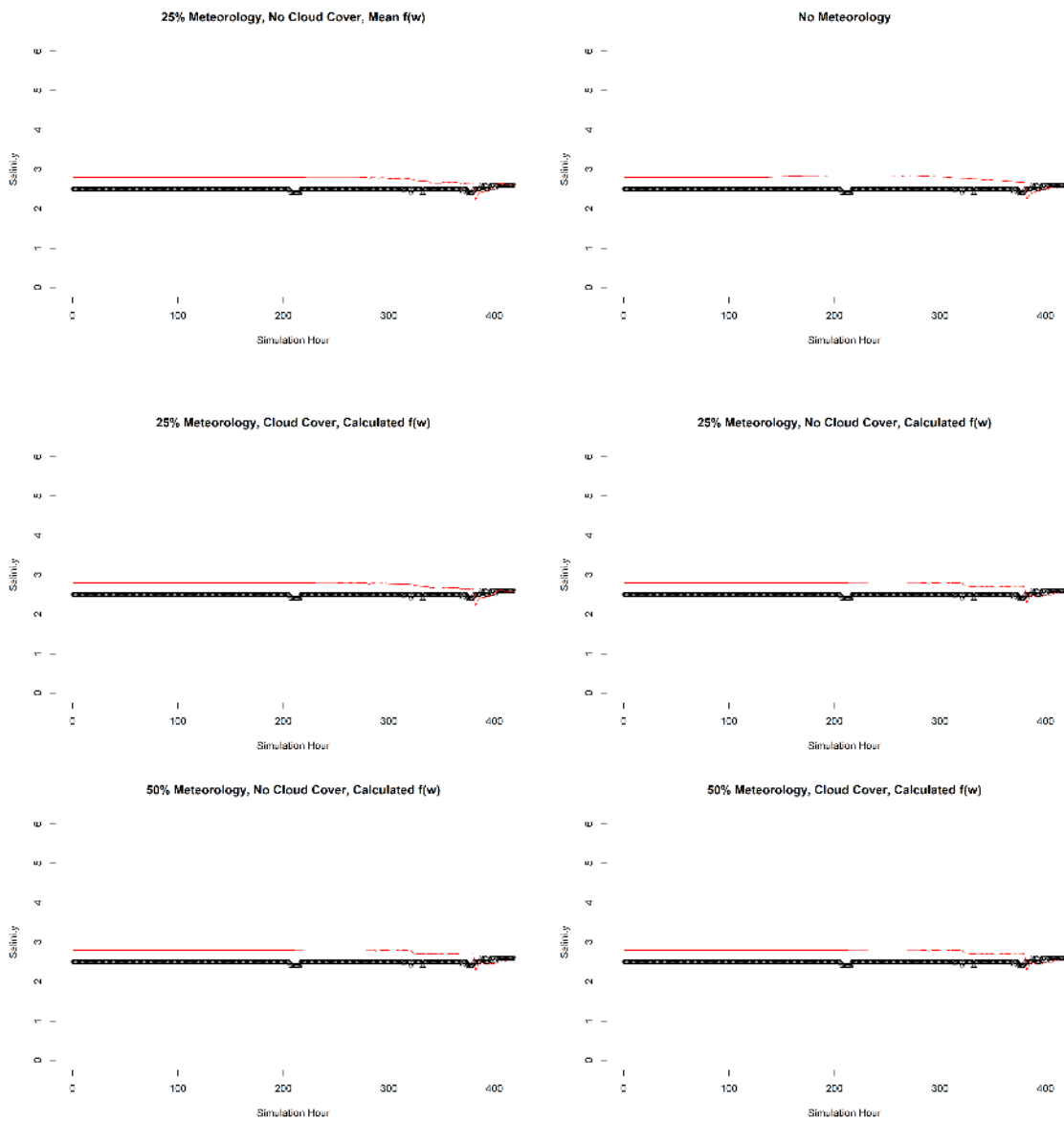
Figure 1.36. Predicted versus observed salinity for 6 simulations during the winter time period for the mid USGS station. Observations are represented as points and predictions are represented as red lines. From left to right top to bottom: 1. 25% Wind speed, cloud cover off, mean f(w); 2. No Meteorology; 3. 25% Wind speed, cloud cover on, calculated f(w); 4. 25% Wind speed cloud cover off, calculated f(w); 5. 50% Wind speed, cloud cover off, calculated f(w); 6. 50% Wind speed, cloud cover on, calculated f(w).
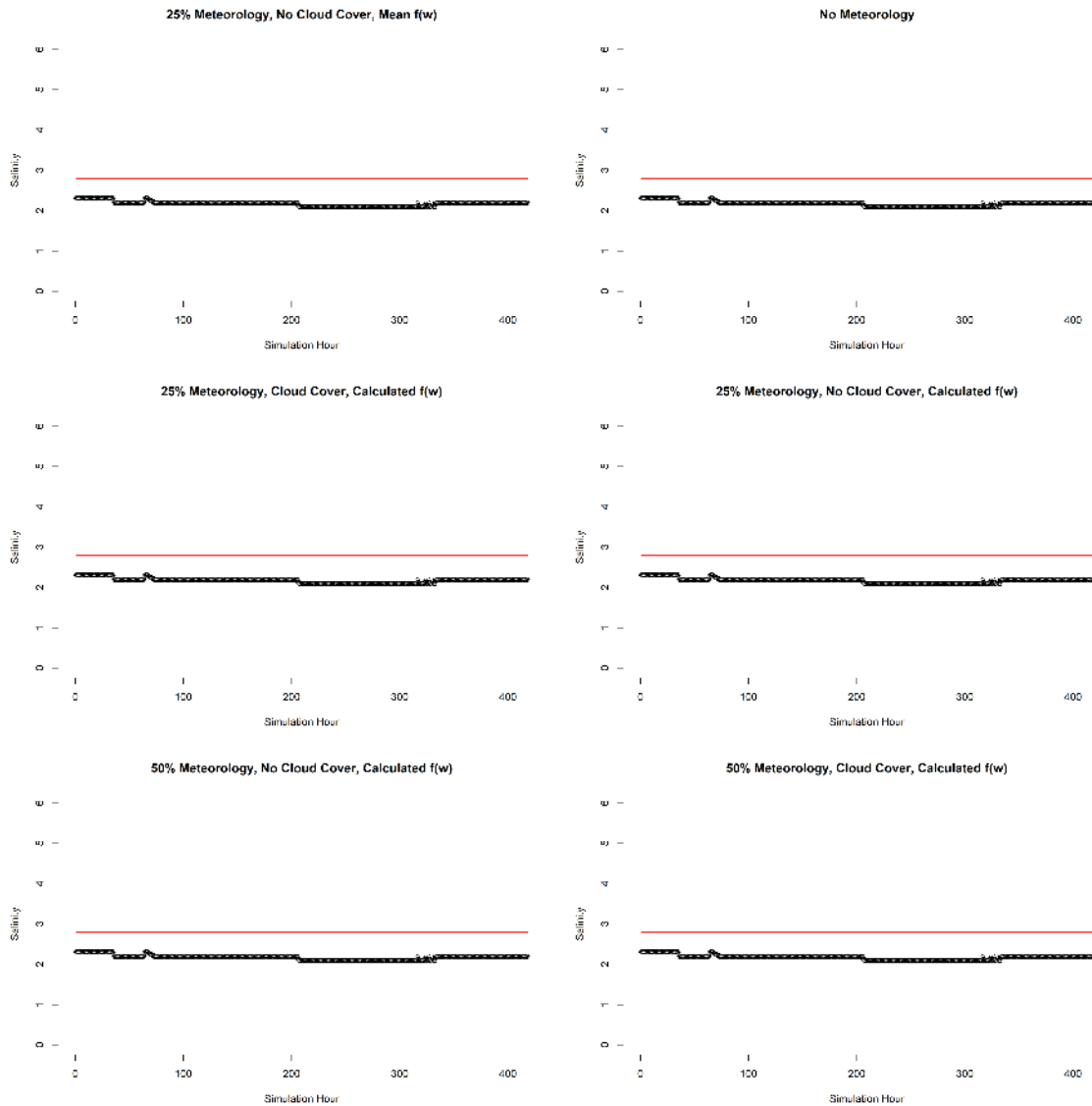
Figure 1.37. Predicted versus observed salinity for 6 simulations during the winter time period for the south USGS station. Observations are represented as points and predictions are represented as red lines. From left to right top to bottom: 1. 25% Wind speed, cloud cover off, mean f(w); 2. No Meteorology; 3. 25% Wind speed, cloud cover on, calculated f(w); 4. 25% Wind speed cloud cover off, calculated f(w); 5. 50% Wind speed, cloud cover off, calculated f(w); 6. 50% Wind speed, cloud cover on, calculated f(w).

Mean resultant velocity magnitude was $9.43 \times 10^{-3} \pm 6.71 \times 10^{-3}$ m/s (sd) with a range from 1.40×10^{-4} to 3.19×10^{-2} m/s before the sector gate opening (Fig. 1.38). During the opening, which lasted approximately four hours, mean resultant velocity magnitude was 0.356 ± 0.0854 (sd) m/s, with a range of 0.198 to 0.480 m/s. For the entire simulation period, the average

was $0.0132 \pm 0.02.93$ (sd) m/s. The model with a 50% reduction in wind speed, no cloud cover

correction, and a calculated f(w) value had the highest index of agreement ($d_m = 0.558$; Table

1.5; Fig. 1.39). When comparing each simulation with measured data for this parameter they

appear to be in phase, with simulated data consistently lower than measurements. This is

particularly evident when examining data before sector gate openings (Fig. 1.40).

Resultant Velocity Magnitude
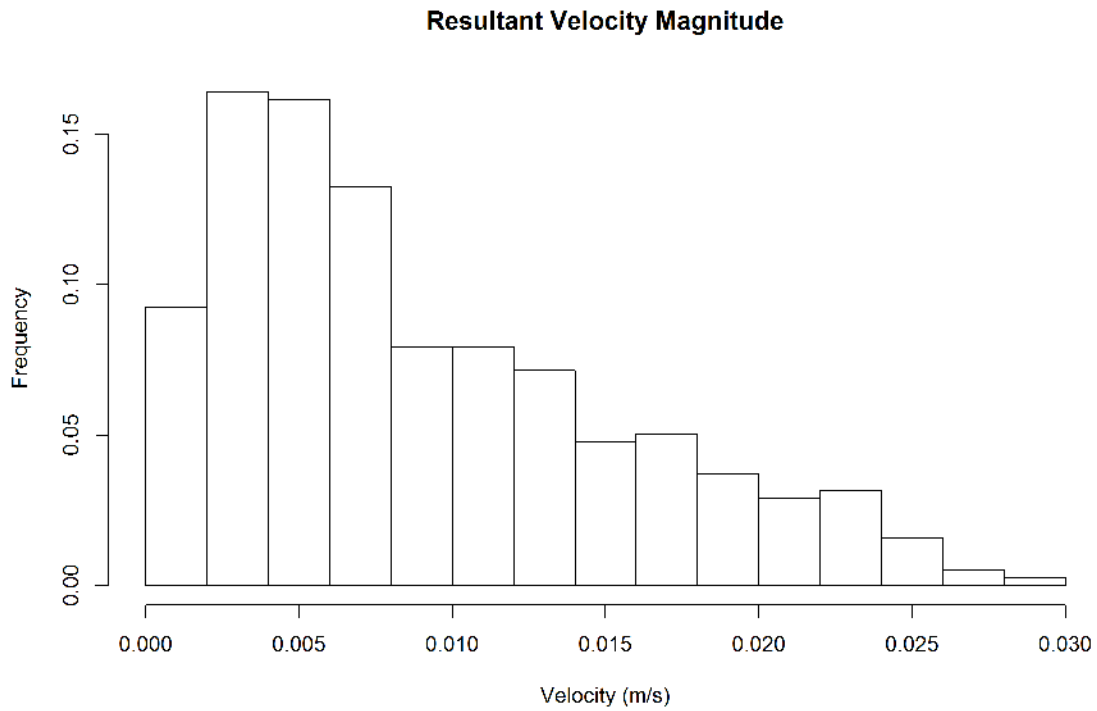
Figure 1.38. Frequency histogram of resultant vector velocity magnitudes (m/s) before the sector gate was opened during the winter time period. Velocities were calculated every 25 minutes using a Vector ADV velocimeter. Velocities were low overall and were well within the upper limit of the Vector ADV before the high energy sector gate opening.

Table 1.5. Indices of agreement (d_m) for average velocity from the winter simulations. Note that the model with 50% Wind speed, Cloud Cover Off, Calculated f(w) performed best and is indicated by bold and italicized font.

Simulation	d_m
25% Wind speed, Cloud Cover Off, Mean f(w)	0.541
No Meteorology	0.547
25% Wind speed, Cloud Cover On, Calculated f(w)	0.542
25% Wind speed, Cloud Cover Off, Calculated f(w)	0.549
50% Wind speed, Cloud Cover Off, Calculated f(w)	*0.558*
50% Wind speed, Cloud Cover On, Calculated f(w)	0.548
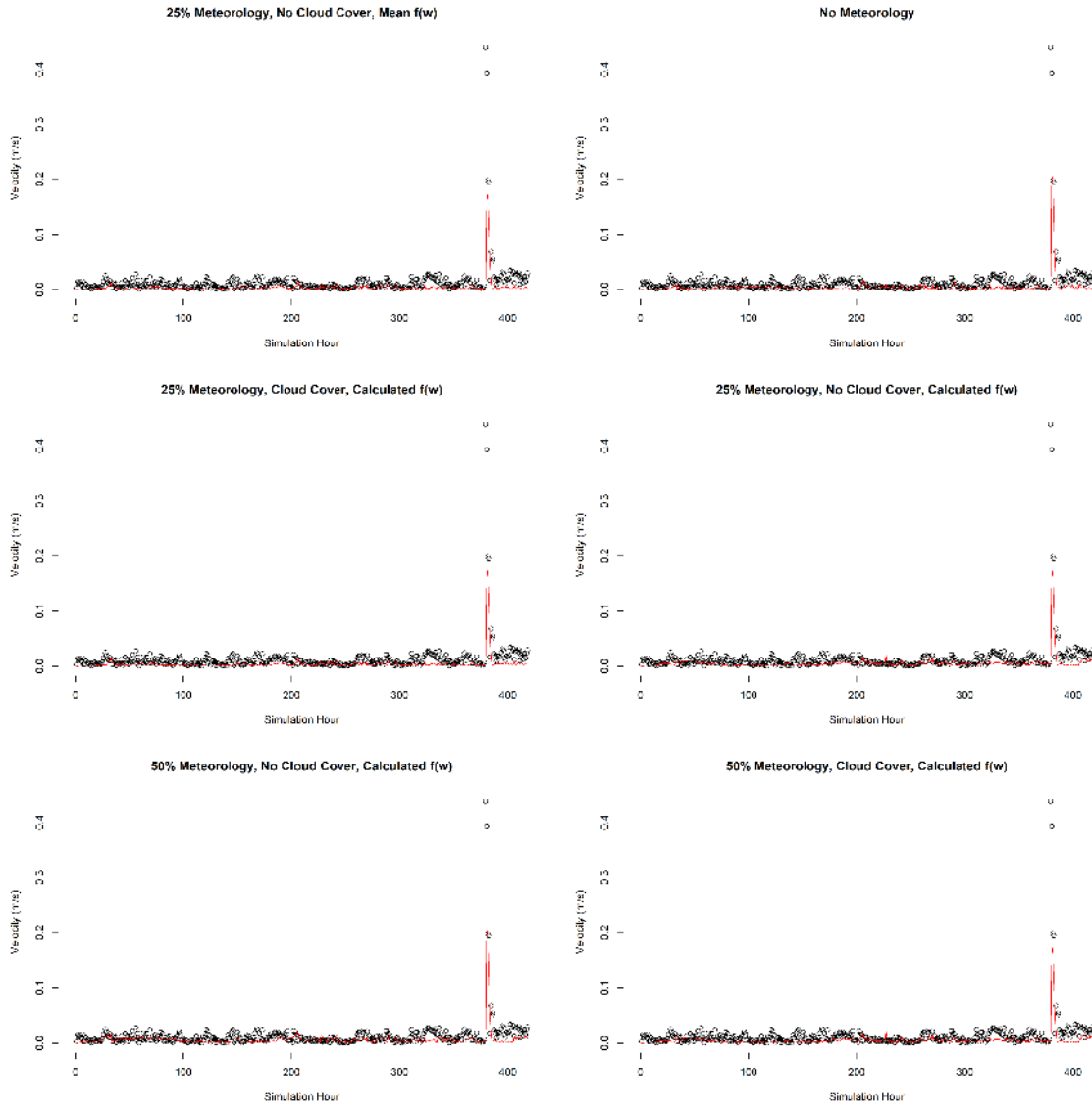
Figure 1.39. Predicted versus observed resultant vector velocity magnitudes (m/s) for 6 simulations during the winter time period near the Robert E. Lee Bridge. Observations are represented as points and predictions are represented as red lines. From left to right top to bottom: 1. 25% Wind speed, cloud cover off, mean f(w); 2. No Meteorology; 3. 25% Wind speed, cloud cover on, calculated f(w); 4. 25% Wind speed cloud cover off, calculated f(w); 5. 50% Wind speed, cloud cover off, calculated f(w); 6. 50% Wind speed, cloud cover on, calculated f(w).
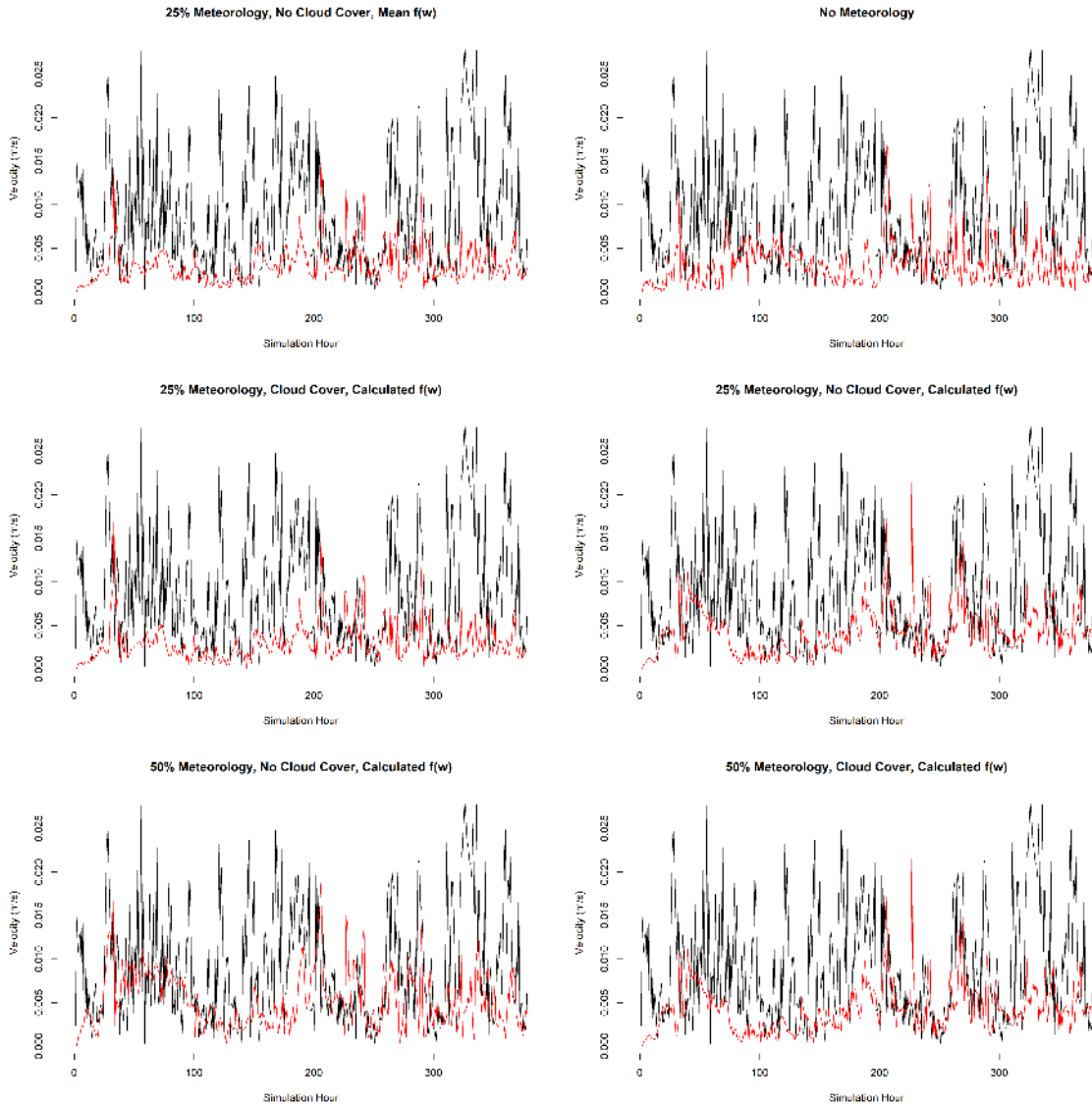
Figure 1.40. Predicted versus observed resultant vector velocity magnitudes (m/s) for 6 simulations during before sector gate opening during the winter period near the Robert E. Lee Bridge. Observations are represented as points and predictions are represented as red lines. From left to right top to bottom: 1. 25% Wind speed, cloud cover off, mean f(w); 2. No Meteorology; 3. 25% Wind speed, cloud cover on, calculated f(w); 4. 25% Wind speed cloud cover off, calculated f(w); 5. 50% Wind speed, cloud cover off, calculated f(w); 6. 50% Wind speed, cloud cover on, calculated f(w).

The model with a 50% reduction in wind speed, no cloud cover correction, and a calculated f(w) was used to estimate tidal exchange flow during the winter time period. The discharge magnitude before the opening was 0.207 ± 0.123 m^3/s at the Far South transect, 0.279 ± 0.148 m^3/s at the South transect, 1.997 ± 1.529 m^3/s at the Middle transect, and 1.239 ± 0.630

m^3/s at the North transect (all μ ± sd; Fig. 1.41). Peak discharges for all transects occurred at simulation hour 381 and were 6.02 m^3/s for the Far South transect, 9.10 m^3/s for the South transect, 18.60 m^3/s at the Mid transect, and 26.09 m^3/s at the North transect.
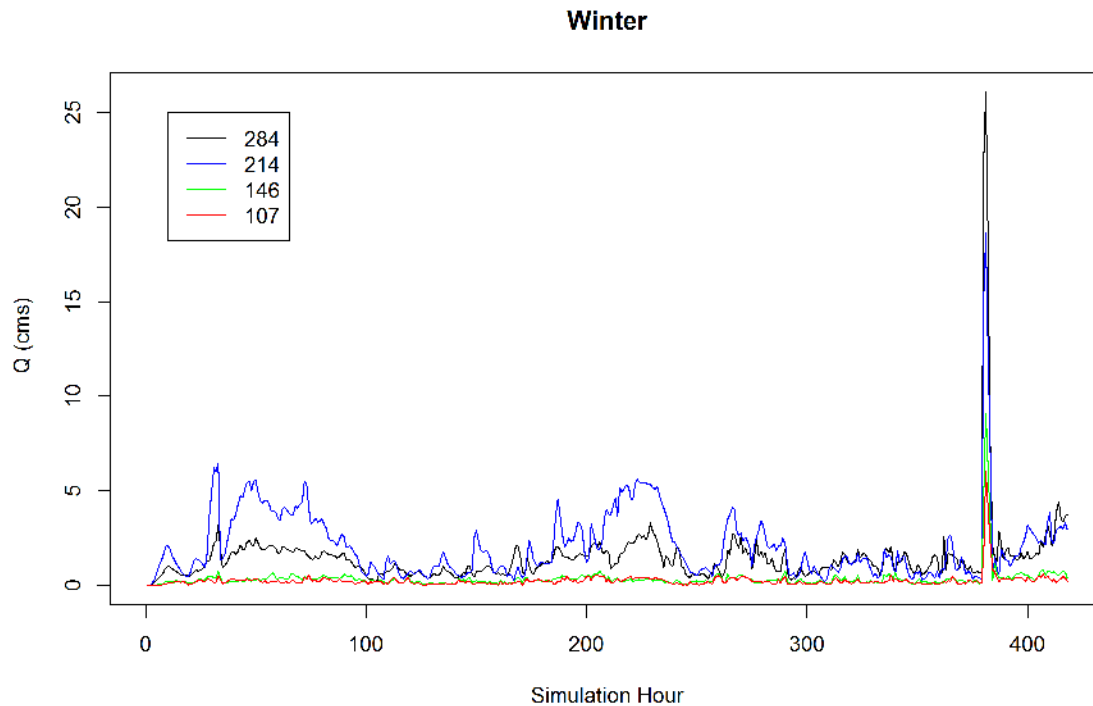
Winter

Figure 1.41. Total discharge (Q) in m^3/s at four transects in Bayou St. John during the winter period. The simulation with a 50% reduction in Wind speed no cloud cover correction and a calculated f(w). Results from the best performing simulation with respect to velocity (50% reduction in Wind speed no cloud cover correction and a calculated f(w)) are displayed. Notice the higher discharges observed at the middle site (214) during two cold fronts from simulation hour 22-85 and 166-240.

Velocities and thus discharges increased quickly and were sustained longer in the winter sector gate opening than the summer sector gate opening (Figs. 1.41-1.49). Increased velocities and a rise in elevation can be noted for five hours post opening followed by stabilization and a slight decrease in elevation (Figs. 1.44-1.49). Strong eddies develop in hour four of the opening and are sustained for three simulation hours (Figs. 1.47-1.49). It should be noted that the winter opening had higher and more sustained discharges and velocities with a sharper increase in

55

elevation following sector gate opening. Additionally, some complaints of docks flooding

occurred during this opening.
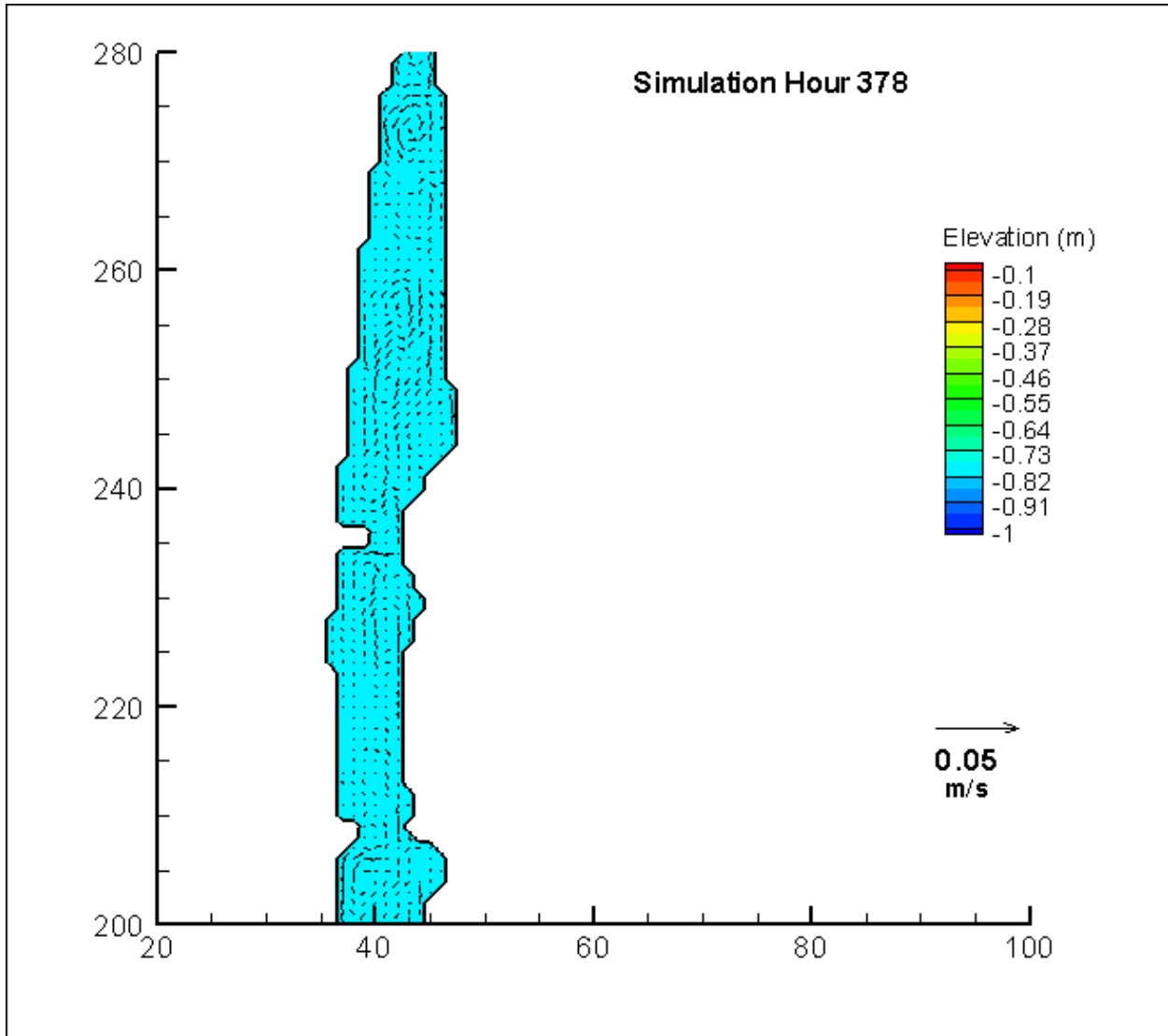
Figure 1.42. Solutions for the winter time period 50% reduction in meteorological forcing, no cloud cover correction, and a calculated f(w) simulation at hour 378 in the northern part of Bayou St. John. Axes indicate i,j coordinates of a Cartesian mesh with an extent of 70 x 300. This is 2 hours before sector gate opening and shows typical low energy conditions. Elevation is shown here as a contour and resultant velocity as a vector with appropriate legends. Image created using TecPlot 360© graphical software.
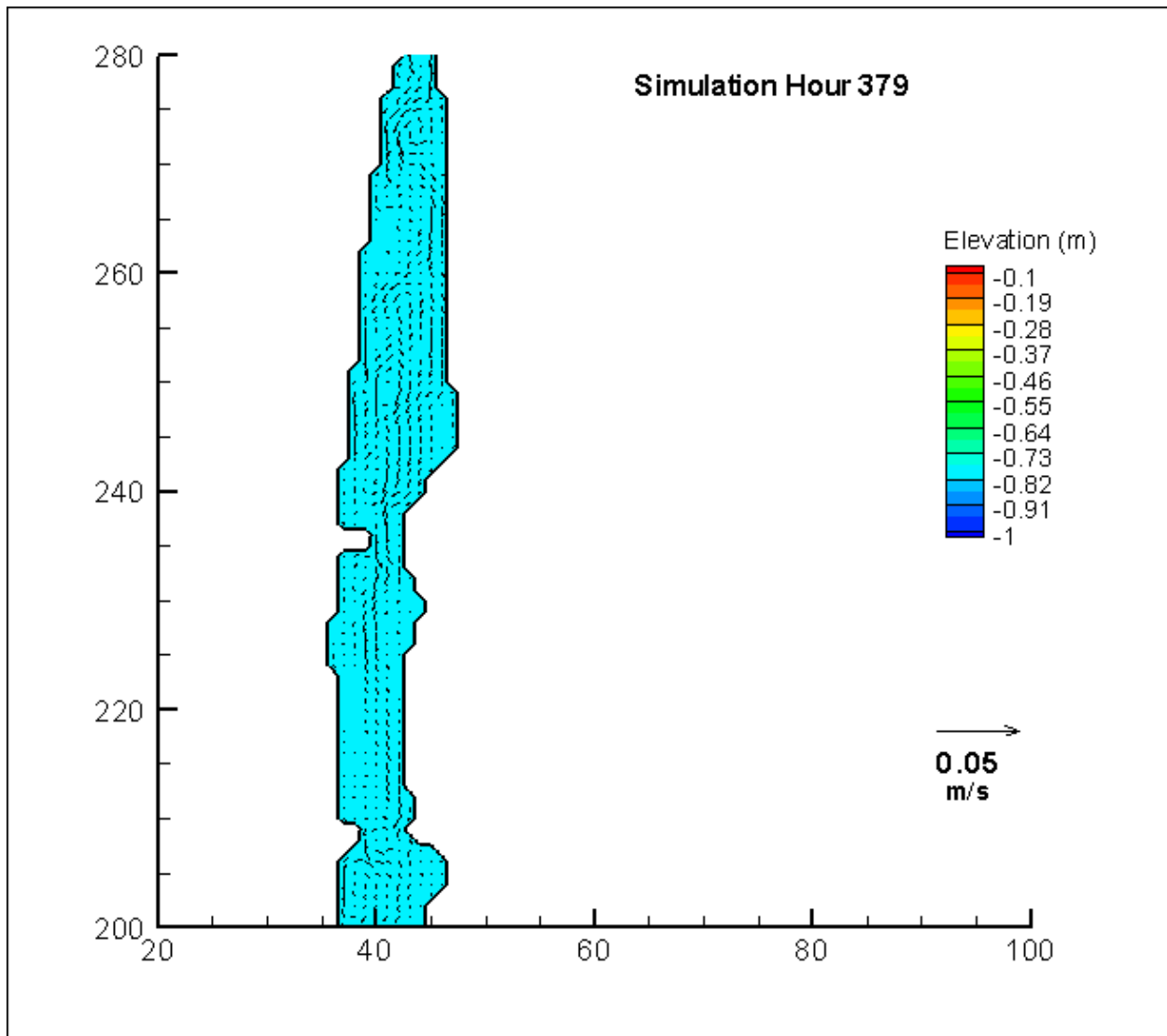
Figure 1.43. Solutions for the winter time period 50% reduction in meteorological forcing, no cloud cover correction, and a calculated f(w) simulation at hour 379 in the northern part of Bayou St. John. Axes indicate i,j coordinates of a Cartesian mesh with an extent of 70 x 300. This is 1 hour before sector gate opening and shows typical low energy conditions. Elevation is shown here as a contour and resultant velocity as a vector with appropriate legends. Image created using TecPlot 360© graphical software.
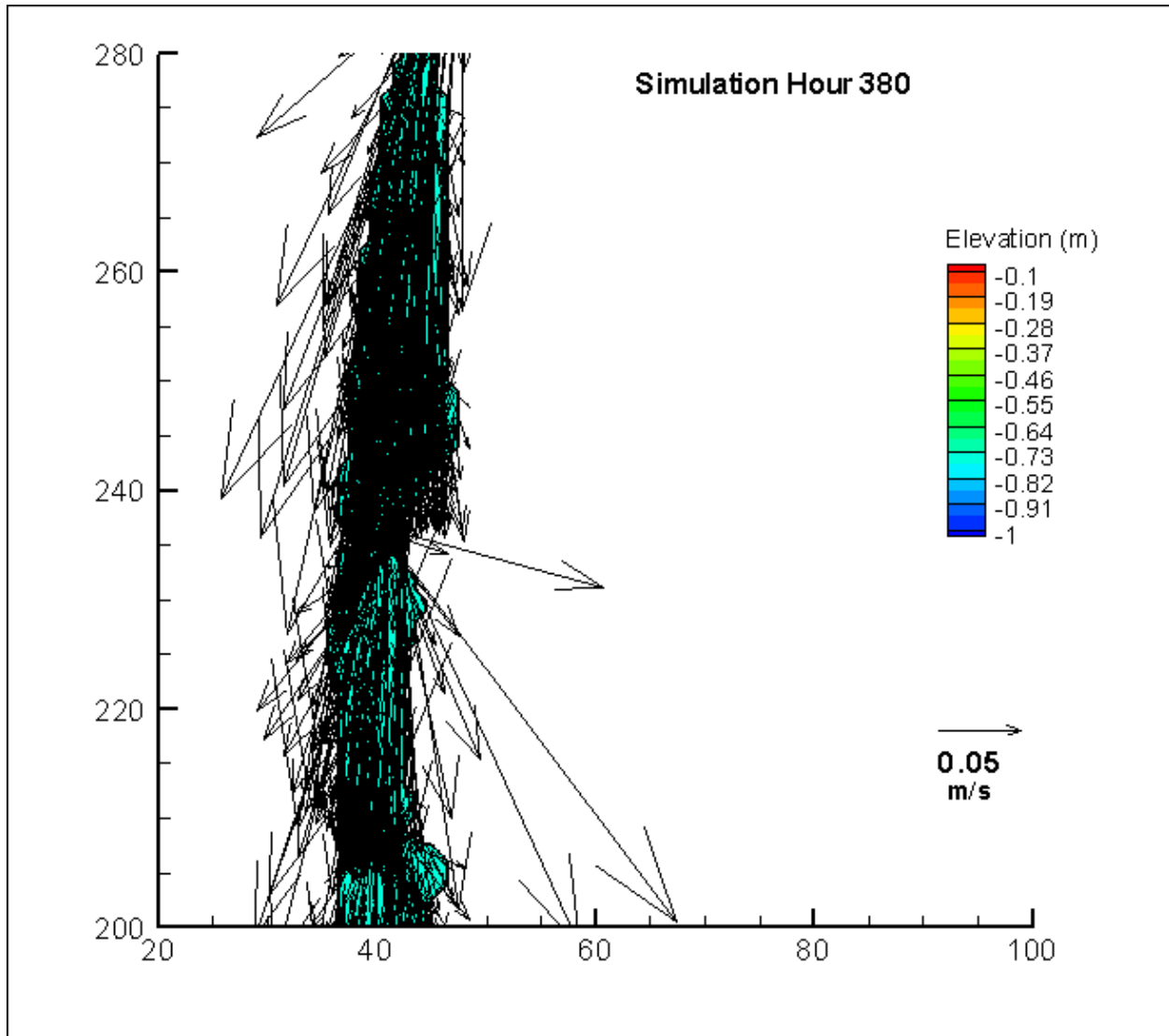
Figure 1.44. Solutions for the winter time period 50% reduction in meteorological forcing, no cloud cover correction, and a calculated f(w) simulation at hour 380 in the northern part of Bayou St. John. Axes indicate i,j coordinates of a Cartesian mesh with an extent of 70 x 300. This is the first hour of the sector gate opening. Elevation is shown here as a contour and resultant velocity as a vector with appropriate legends. Image created using TecPlot 360© graphical software.
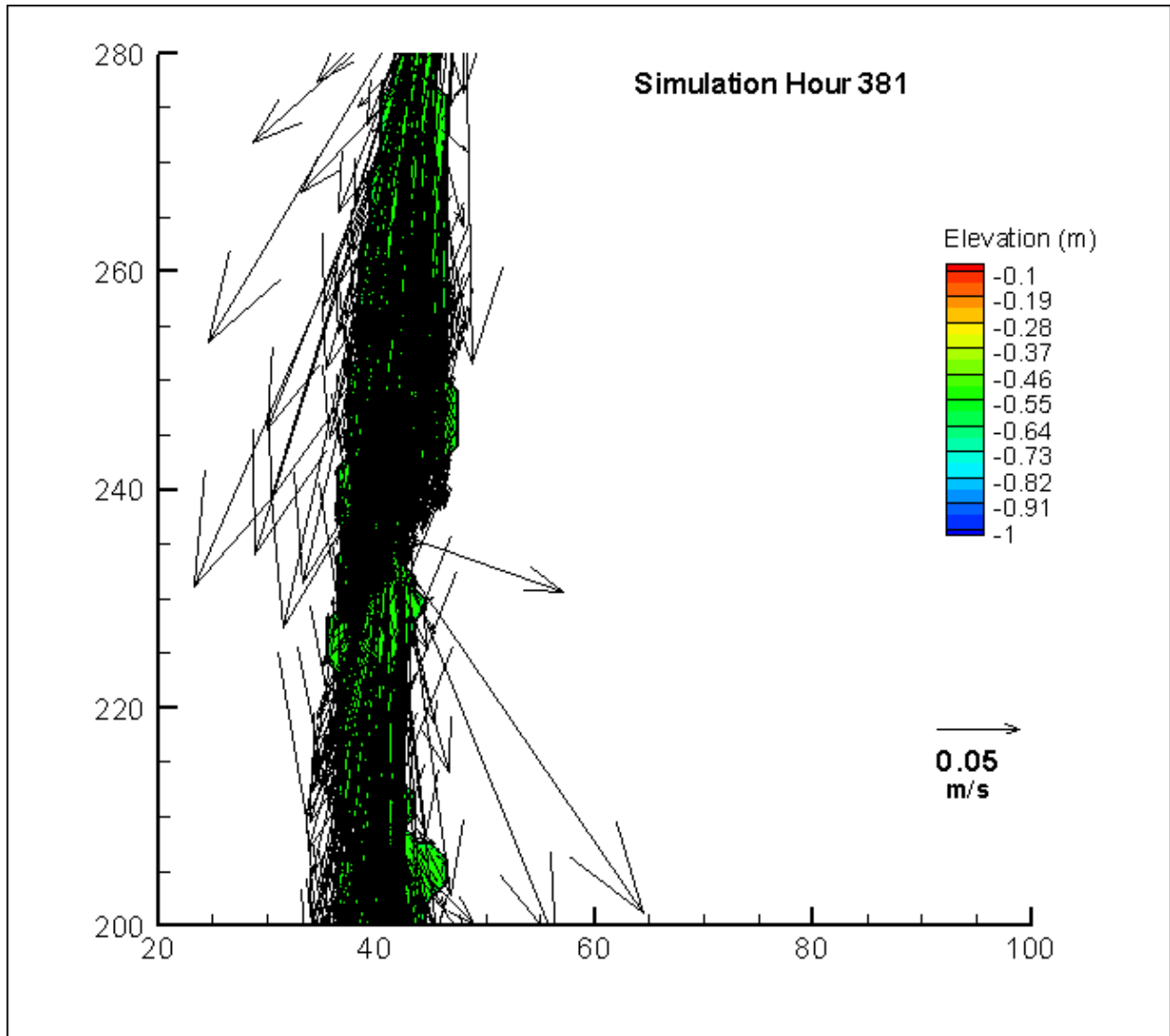
Figure 1.45. Solutions for the winter time period 50% reduction in meteorological forcing, no cloud cover correction, and a calculated f(w) simulation at hour 381 in the northern part of Bayou St. John. Axes indicate i,j coordinates of a Cartesian mesh with an extent of 70 x 300. This is hour 2 of the sector gate opening. Elevation is shown here as a contour and resultant velocity as a vector with appropriate legends. Image created using TecPlot 360[©] graphical software.
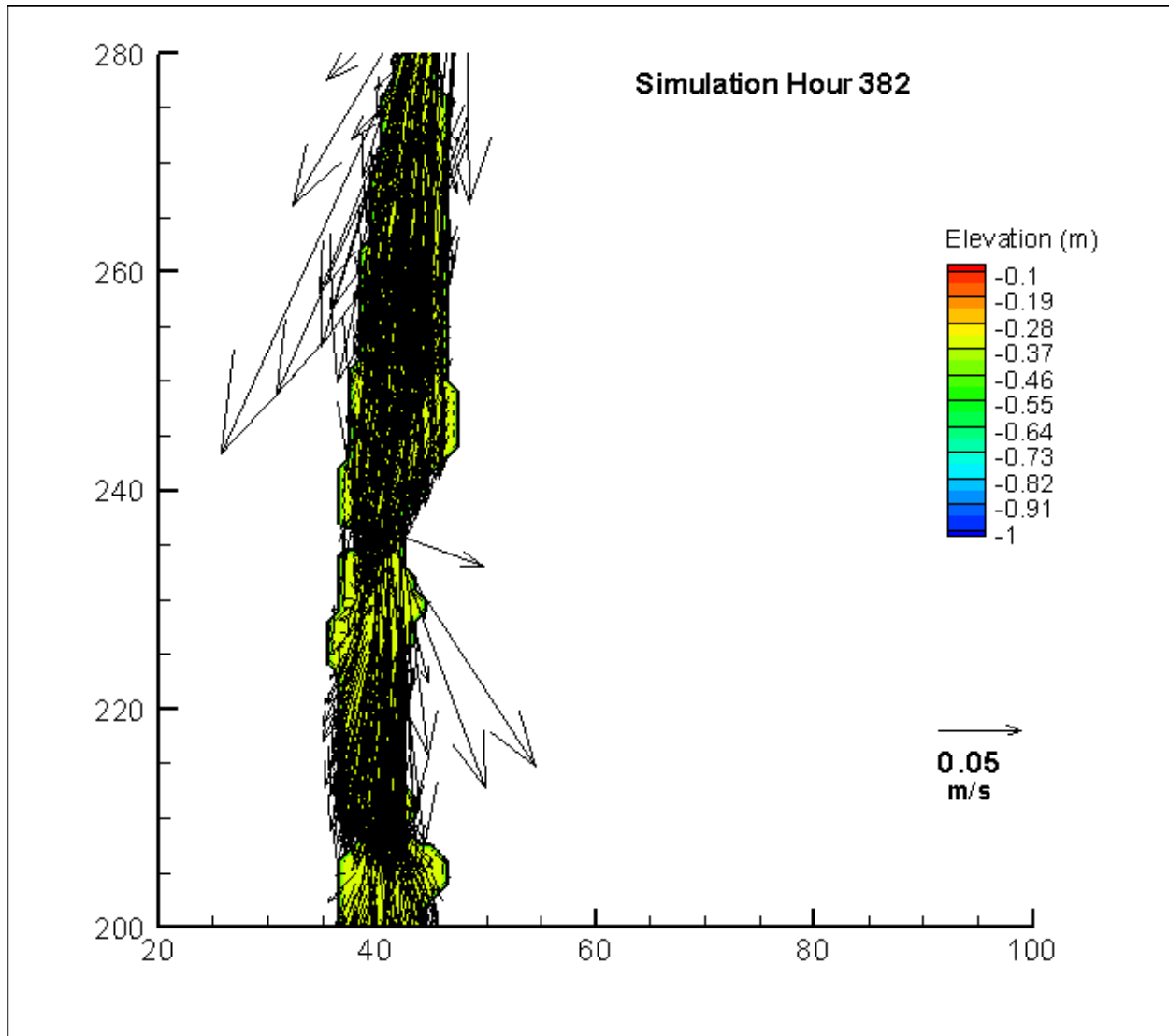
Figure 1.46. Solutions for the winter time period 50% reduction in meteorological forcing, no cloud cover correction, and a calculated f(w) simulation at hour 382 in the northern part of Bayou St. John. Axes indicate i,j coordinates of a Cartesian mesh with an extent of 70 x 300. This is hour 3 of the sector gate opening. Elevation is shown here as a contour and resultant velocity as a vector with appropriate legends. Image created using TecPlot 360[©] graphical software.
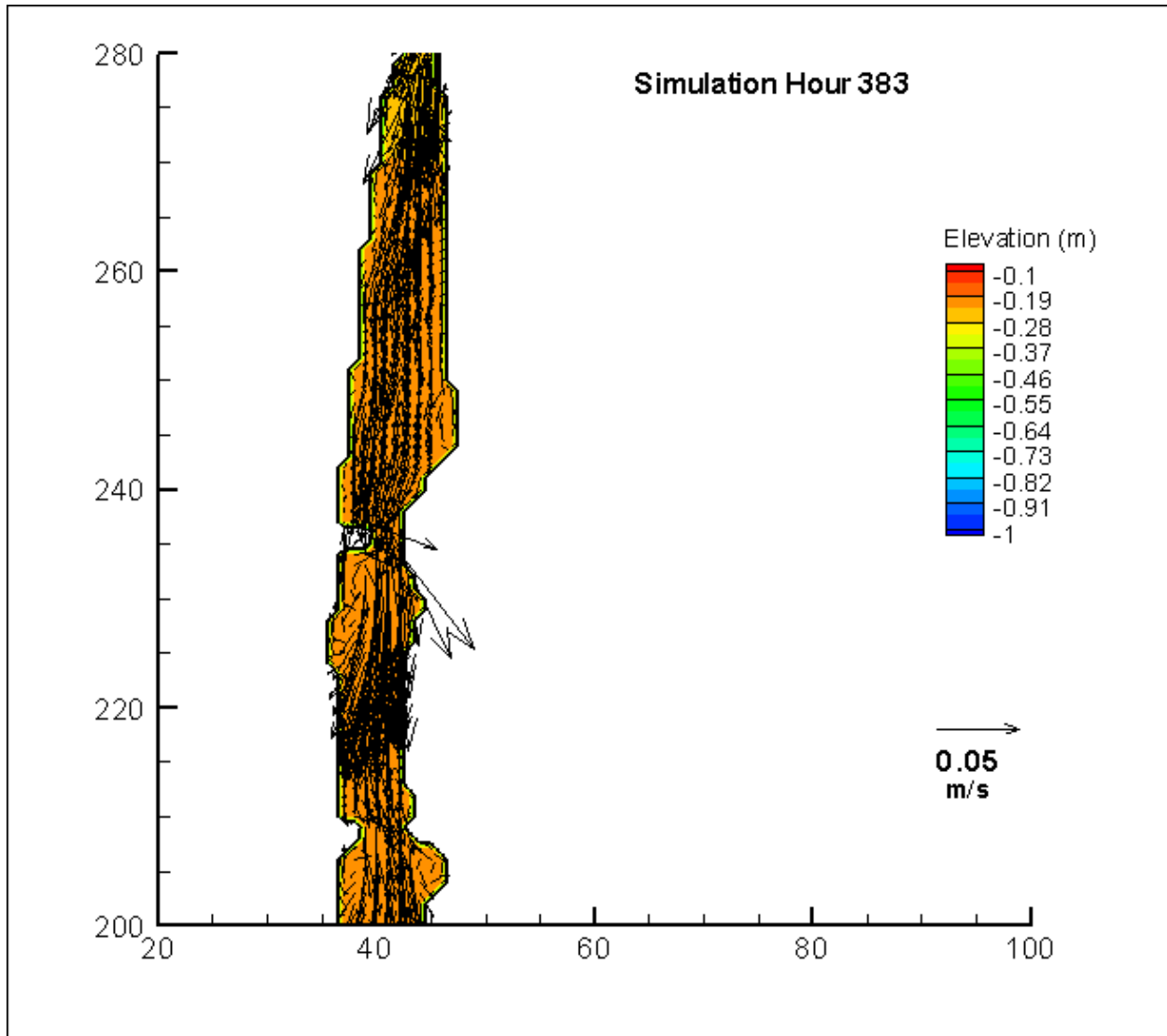
Figure 1.47. Solutions for the winter time period 50% reduction in meteorological forcing, no cloud cover correction, and a calculated f(w) simulation at hour 383 in the northern part of Bayou St. John. Axes indicate i,j coordinates of a Cartesian mesh with an extent of 70 x 300. This is hour 4 of the sector gate opening. Elevation is shown here as a contour and resultant velocity as a vector with appropriate legends. Image created using TecPlot 360[©] graphical software.
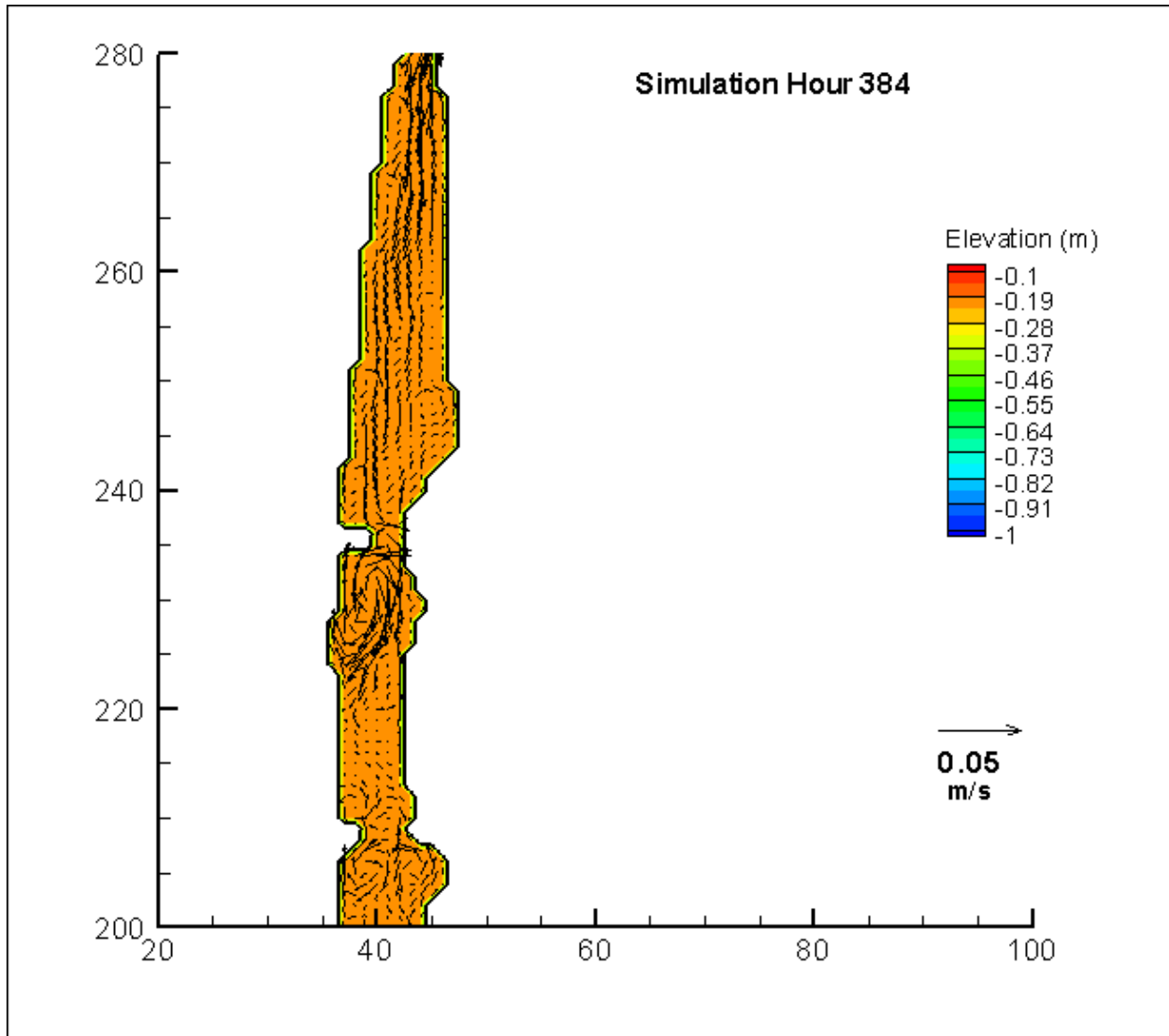
Figure 1.48. Solutions for the winter time period 50% reduction in meteorological forcing, no cloud cover correction, and a calculated f(w) simulation at hour 384 in the northern part of Bayou St. John. Axes indicate i,j coordinates of a Cartesian mesh with an extent of 70 x 300. This is hour 5 after the sector gate was opened. Elevation is shown here as a contour and resultant velocity as a vector with appropriate legends. Image created using TecPlot 360© graphical software.
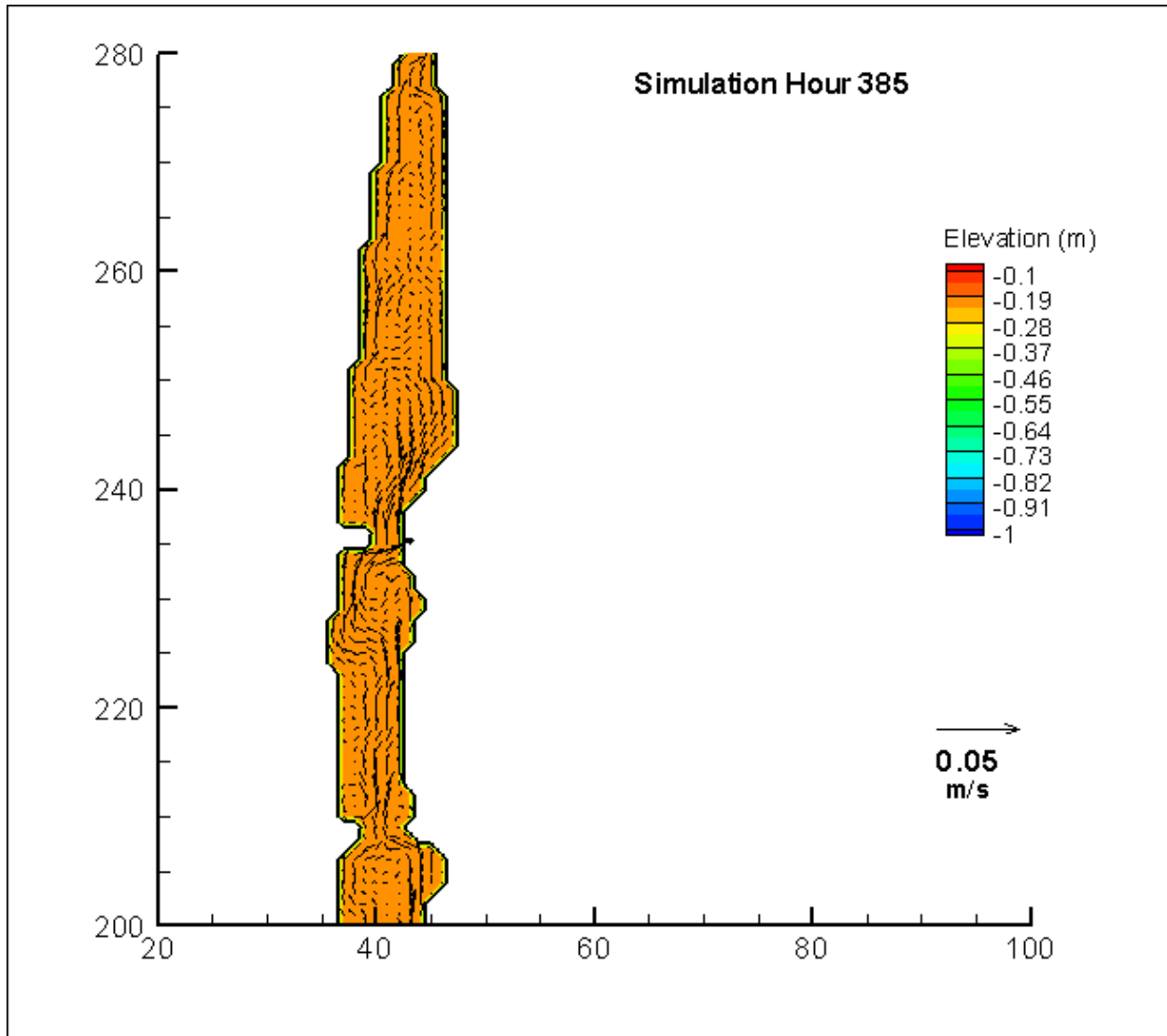
Figure 1.49. Solutions for the winter time period 50% reduction in meteorological forcing, no cloud cover correction, and a calculated f(w) simulation at hour 385 in the northern part of Bayou St. John. Axes indicate i,j coordinates of a Cartesian mesh with an extent of 70 x 300. This is hour 6 after the sector gate was opened. Note how velocities have stabilized with more turbulence observed than pre-opening (Figs. 1.41 and 1.42). Elevation is shown here as a contour and resultant velocity as a vector with appropriate legends. Image created using TecPlot 360[©] graphical software.

Two 5-point moving average plots were created to compare results here to a previous

study that used 3D simulations to determine how removal of the outdated flood control structure

would affect exchange and water fluxes in the Bayou (Fig. 1.50; Schroeder, 2011). Only along

the Bayou discharges were plotted here for easier comparison. Less flow was observed in the

current study, than what was previously predicted (Figs. 1.50, 1.51). Discharge values from a

previous study show that flow was often an order of magnitude lower at the two southern

transects (Schroeder, 2011). Overall, lower flows were observed at the southern transect in the

current study, but were much closer to flows for the mid and north transects. Negative flows are

also shown for the summer period at the mid transect and this could be due to eddy formation

(Figs. 1.20 and 1.21).
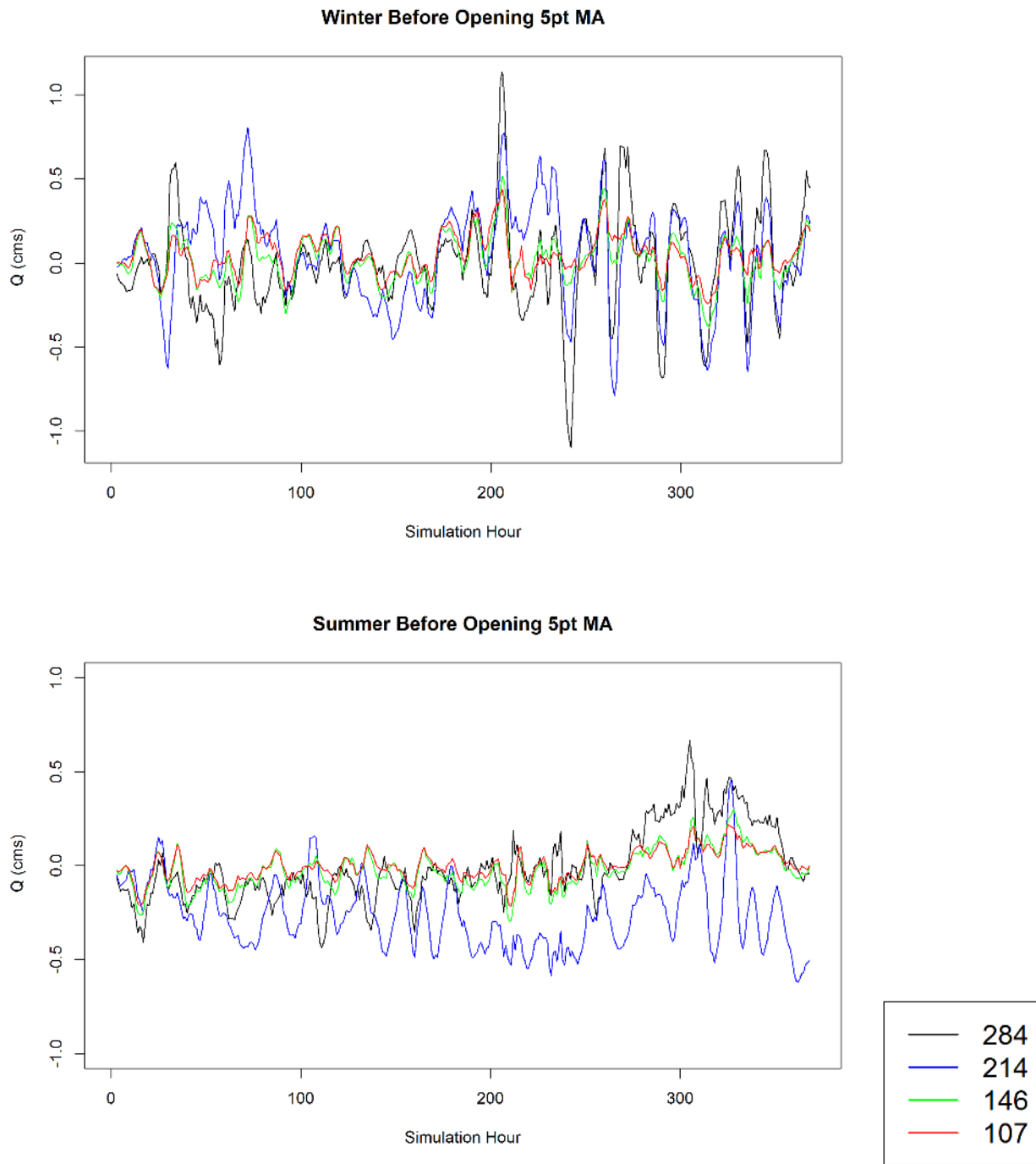
Figure 1.50. Five-point moving average of discharge (Q) in m^3/s at four transects in Bayou St. John during the winter and summer periods is shown above. Both show simulation hours 1 to 370, which is before sector gate opening for both scenarios. The simulation with a 50% reduction in wind speed no cloud cover correction and a calculated f(w) is used because it performed best for velocity in the winter and elevation in the summer.
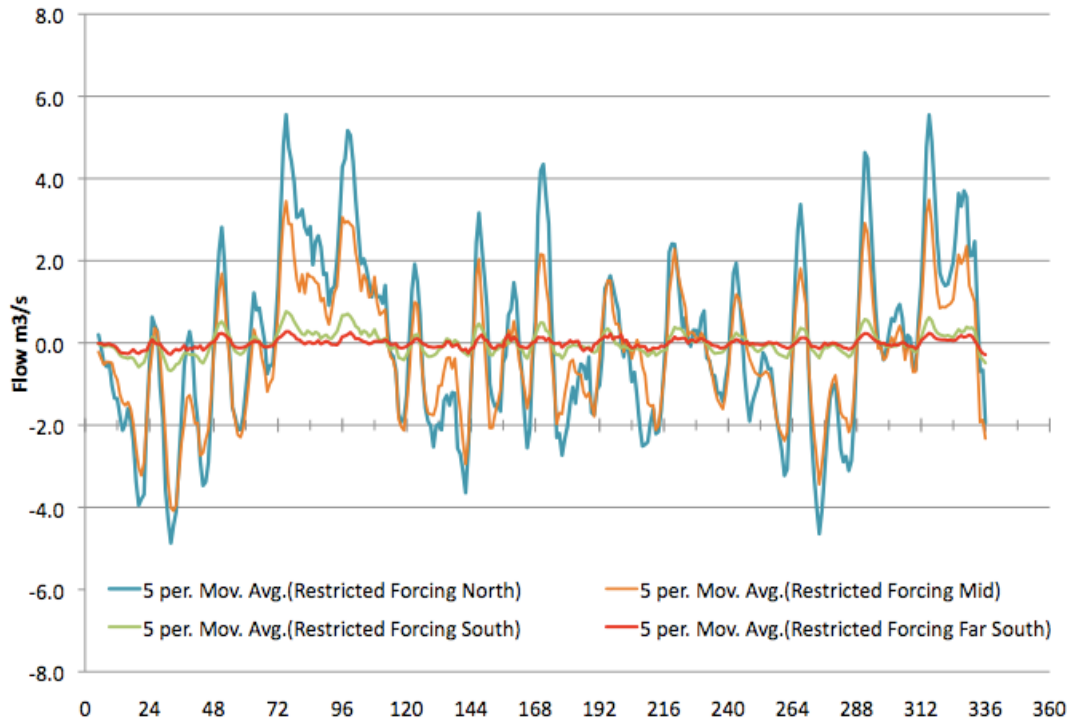
Figure 1.51. Five-point moving averages for discharge during the restricted zone forcing simulation from a previous study (Figure 27 in Schroeder, 2011). This adapted figure used the same four transects, with North corresponding to 284, Mid referring to 214, South referring to 146, and Far South Referring to 107. When compared to the current study (Fig. 1.49), much higher discharges were observed.

Discussion

This study characterizes the hydrological conditions for a semi-impounded waterway in

southern Louisiana under different conditions. Hydrologic conditions were affected by both

natural (i.e., cold fronts) and anthropogenic (i.e., sector gate openings and sluice valve operation)

sources. It provides a generalized understanding that could be used for future management of

exchange flow using sector gate openings and sluice valve management (BKI, 2011). It also can

be used as a case study for future flood control projects in other parts of Louisiana. Sea level rise

and subsidence have and are predicted to cause future land loss in coastal Louisiana (González

and Törnqvist, 2006). To protect coastal communities, more flood control structures are planned

(CPRA, 2012). Many communities in coastal Louisiana are deeply connected to local waterways

66

and wetlands with livelihoods dependent on natural environments (Gramling and Hagelman, 2005). Therefore, they would be benefit from flood control measures that maintain ecosystem functioning.

The distribution of flow across Bayou St. John was similar for both openings, with higher flows being observed during the winter opening. Discharge was highest at the North transect and decreased southerly. Higher discharges for each transect were observed during the winter opening and this opening had a longer duration of high flows. This is likely indicative of a longer or wider (or both) sector gate opening or larger head differential. A larger head differential existed before the summer opening (1.20 m) than the winter opening (0.42 m). A longer period of high discharges during the winter opening suggests a longer opening occurred. Higher peak velocities and larger discharges observed in the winter opening with a smaller head differential suggest a wider sector gate opening also occurred.

Wind stress during cold fronts has been suggested as a large influence on coastal processes and exchange in coastal Louisiana (Georgiou et al., 2005; Feng and Li, 2010). A previous study found that subtidal flow caused by east-west winds explained a large amount of variation in water levels in nearby Lake Pontchartrain (Chuang and Swenson, 1981). Two large cold fronts passed during the winter simulation period from approximately 5 February to 7 February 2014 and 10 February to 13 February 2014 (simulation hours 33 – 85 and 166 – 240, respectively). Their effects appear to have the largest influence of water flow and discharge throughout the Bayou outside of sector gate openings. Although no spike in either discharge or flow was noted at the south or far south transects. Higher discharges and velocities were observed at the Mid than the North transect during passage of the cold fronts. This suggests that

the large fetch north of the Mid transect affects flow and discharge more than distance from the Lake.

When there was no cold front and no flood gate opening, flows calculated using resultant velocities were consistently higher in the Mid transect. A previous study that simulated discharges with and without a flood control structure suggested that discharges would be higher in the North for both situations (Schroeder, 2011). Higher flows overall and more tidal periodicity suggest there was more exchange in the previous study. Less exchange would decrease the effect of Lake Pontchartrain on the Bayou, thus increasing the relative effects of wind stress. More similar along Bayou flows (i.e., more similar flows at the four transects in the current study) also could indicate less connectivity. Comparing other observations between studies suggests the latter may be more likely. Large oscillations due to tidal periodicity are not apparent at all stations during the summer period, but some oscillations were observed at the northern station during the winter period after simulation hour 200. However it is difficult to be sure that this was not due to the influence of sluice valves, weirs, or pumps. When comparing to data from a previous study (Schroeder, 2011), much less tidal periodicity was observed in the current study. Again, the lack of tidal oscillations could be due to less exchange. It is likely that the sluice valves were more closed or closed more often during the current study causing less exchange between BSJ and the Lake. The overall influence of sluice valve management was not an objective of the current study, however, it could be an important consideration to maintain connectivity and increase exchange with Lake Pontchartrain.

During flood gate openings, the difference between maximum elevations among USGS monitoring stations was higher during the summer opening than the winter opening. This is especially evident when comparing the north and south monitoring stations for both events, with

a 0.105 m difference in the summer and a 0.027 m difference in the winter. This large difference suggests an initial pulse was released, but dissipated before reaching the southern end of BSJ for the 19 August 2013 opening. This could be because the summer opening was shorter in duration or had a smaller opening.

Several similarities were apparent across all simulations for both time periods. Predictions for elevation were consistently accurate across simulations and stations. This is likely due to the small amount of variation in elevation and to the simple bathymetry of the Bayou. Predictions for both salinity and temperature were best at the northern station and were greatly reduced for the mid and south stations. This trend is likely because the model boundary was closest to the northern USGS station. Salinity was poorly constrained. This is likely to be because of small variation and model sensitivity. Salinity varied 1.1 during the summer and 0.4 in the winter. The model calculates salinity to the nearest 0.1. Small observed variations with respect to model sensitivity may be why there were low indices of agreement. Even though constraining salinity was a primary objective of the current study, low agreement is acceptable because of such small variability. While chemically these changes may be large (median $\pm$ 22% in summer and median $\pm$ 8% in winter) they are probably not hydrological or biological drivers. Diurnal oscillations in temperature were not captured by the simulations. Using a more sensitive heat flux calculation or a smaller time step could produce these effects. Heat was lost across all simulations. This is possibly due to poor estimation of atmosphere-water heat flux.

Evidence from both simulation time periods may suggest that when heat flux is negative, too much heat is lost from the system. In the summer, simulations with cloud cover corrections retained more heat and produced more accurate temperature predictions. During this time period, temperature was more stable with a slightly decreasing trend overall. Additionally, heat

flux was consistently low (often negative) during this time period. Cloud cover essentially penalizes heat flux. It could be inferred from this that cloud cover is lessening the effects of the negative heat flux values, creating more accurate predictions. In the winter, regardless of cloud cover calculations, all simulations lost heat. Simulations with more stable meteorological forcings (e.g., 25% wind speed mean f(w) values, and the simulation with no meteorology) performed best. Temperature varied more during this time period with large fluctuations occurring during cold fronts. Cloud cover in this case, dampened the effects of heating and cooling periods more evenly, but too much heat was lost. Therefore, the better performance of cloud cover corrected models in the summer (time with mostly negative heat flux) and models with stabilized meteorological forcings during the winter (time with highly variable, but overall neutral heat flux) suggest that heat is lost too quickly across simulations. This may be alleviated with dampening negative heat flux values or intensifying positive heat flux values. It should be noted that careful consideration needs to be taken before doing this and a more robust set of simulations should be used if these manipulations are studied. Surface temperatures were also similar across USGS stations, so accurate estimations may be calculated using the nearest gage or a one dimensional linear interpolation. This method would exclude any vertical stratification, which may be an important characteristic (Schroeder, 2011).

Velocity measurements during the flood gate opening of the winter period exceeded the upper limit for the ADV Vector. The accuracy of any measurements during the flood gate opening should be viewed cautiously. Despite this, velocity predictions have a high index of agreement and were conservative overall. All wintertime simulations predict a maximum velocity below 0.3 m/s, suggesting predictions were conservative during sector gate openings. Conservative velocity predictions occurred outside of the opening as well with similar trending.

Based on these findings, it can be concluded that velocity and discharge solutions for the summer 50% Wind speed, Cloud Cover Off, Calculated f(w) simulation is conservative but accurate.

This study characterizes the hydrologic characteristics of two early flood gate openings in BSJ as a part of an adaptive management plan to increase connectivity with Lake Pontchartrain. Both simulations indicate that velocity, flow, and elevation can be accurately predicted using a three dimensional ECOMSED model under different flow regimes and seasons. This information is important for future management of the sluice gates and flood control structure. The results presented here can also be used to compare the biological response to these restoration efforts (e.g., Smith, 2012; Chapter 2).

References Cited

Blumberg, AF and GL Mellor. (1987) "A description of a three-dimensional coastal ocean circulation model" in *Three dimensional coastal ocean models*. Ed. N.S. Heaps. AGU, Washington, D.C. 1-16.

Brogan, SJ. 2010. Red Drum (*Sciaenops ocellatus*) Habitat use in an urban system; behavior of reintroduced fish in Bayou St. John, New Orleans. Thesis. University of New Orleans.

Burk-Kleinpeter Incorporated (BKI) 2011. Bayou St. John Water Management Study Phase 1. Prepared for the Orleans Levee District. 56 pp.

Cdo.ncdc.noaa.gov. Quality Controlled Local Climatological Data. http://cdo.ncdc.noaa.gov/qclcd/QCLCD?prior=N. Accessed on 15 June 2014.

Chuang, WS and EM Swenson. 1981. Subtidal water level variations in Lake Pontchartrain, Louisiana. *Journal of Geophysical Research* 86.C5: 4198-4204.

Coastal Protection and Restoration Authority (CPRA). 2012. Louisiana's Comprehensive Master Plan for a Sustainable Coast (Final): 2012 Coastal Master Plan. http://www.coastalmasterplan.louisiana.gov/.

Coops, H and SH Hosper. 2002. Water-level management as a tool for the restoration of shallow lakes in the Netherlands. *Lake and Reservoir Management* 18.4: 293-298.

Dick, TM and OO Osunkoya. 2000. Influence of tidal restriction floodgates on decomposition of mangrove litter. *Aquatic Botany* 68: 273-280.

Feng, Z and C Li. 2010. Cold-front-induced flushing of the Louisiana Bays. *Journal of Marine Systems* 82: 252-264.

Fontenot, LR. 2004. An evaluation of reference evapotranspiration models in Louisiana. Thesis. University of New Orleans. New Orleans, LA. 83 pp.

Georgiou, IY, DM FitzGerald, and GW Stone. 2005. The impact of physical processes along the Louisiana coast. *Journal of Coastal Research* 44: 72-89.

González, JL, and TE Törnqvist. 2006. Coastal Louisiana in crisis: subsidence or sea level rise? *Eos Trans. AGU* 87.45: 493-498.

Gramling, R and R Hagelman. 2005. A working coast: People in the Louisiana wetlands. *Journal of Coastal Research, Special Issue 44*, 112-133.

Layman, CA, DA Arrington, and MA Blackwell. 2005. Community-based collaboration restores tidal flow to an island estuary (Bahamas). *Ecological Restoration* 23.1: 58-59.

Lellis-Dibble, KA, KE McGlynn, and TE Bigford. 2008. Estuarine Fish and Shellfish Species in U.S. Commercial and Recreational Fisheries: Economic Value as an Incentive to Protect and Restore Estuarine Habitat. U.S. Dep. Commerce, NOAA Tech. Memo. NMFSF/SPO-90, 94 pp.

Llanso, RJ, SS Bell, FE and Vose. 1998. Food Habits of Red Drum and Spotted Seatrout in a restored mangrove impoundment. *Estuaries* 21.2: 294-306.

Martinez, L, S O'Brien, and S Brogan. 2008. Bathymetric survey of Bayou St. John. Internal Report. University of New Orleans. New Orleans, LA. 5 pp.

Schroeder, RL. 2011. Exchange flows in an urban water body Bayou St. John response to the removal of flood control structures, future water elevation control and water quality. Thesis. University of New Orleans.

Sinicrope, TL, PG Hine, RS Warren, and WA Niering. 1990. Restoration of an impounded salt marsh in New England. *Estuaries* 13: 25–30.

Smith, PW. 2012. Fish assemblage dynamics and Red Drum habitat selection in Bayou St. John and associated urban waterways located within the city of New Orleans, Louisiana. Thesis. University of New Orleans.

Ward, KA. Ecology of Bayou St. John. Thesis. University of New Orleans. 1982.

Warren, RS, PE Fell, R Rozsa, AH Brawley, AC Orsted ET Olson, V Swamy, WA Niering. 2002. Salt marsh restoration in Connecticut: 20 years of science and management. *Restoration Ecology* 10.3: 437-513.

Zambrano-Bigiarini, M (2014). hydroGOF: Goodness-of-fit functions for comparion of simulated and observed hydrological time series. R package version 0.3-8. http://CRAN.R-project.org/package=hydroGOF.

Chapter 2

Red Drum (*Sciaenops ocellatus*) Behavior and Activity at Multiple Scales in a Semi-natural Urbanized Oligohaline Waterway in New Orleans, LA

Introduction

Protection from storms and flooding is a priority in coastal areas and multiple strategies are planned for the future. Often, these protection measures come with an environmental cost. As such, coastal protection plans should consider these impacts. For instance, the Louisiana Comprehensive Master Plan emphasizes the integration of ecosystem functioning with flood control protection (CPRA, 2012). Some plans include the construction of more flood control structures that will disconnect natural estuaries from corridors to marine and freshwater habitats. Reducing connectivity in estuaries has been shown to decrease diversity and a loss of estuarine dependent organisms (Layman et al., 2004; Valentine-Rose et al., 2007). The majority (68%) of commercial fishery landings by value in the US is estuarine dependent (Lellis-Dibble et al., 2008).

Red Drum is an economically valuable estuarine dependent species common to Gulf of Mexico and southern Atlantic US coastal waters (Matlock, 1987). It has been shown that they thrive in habitats with varying water quality (Thomas, 1991; Bacheler et al., 2009). As such, they have been successfully reared in aquaculture environments and in some states (e.g., Texas) widespread stocking of aquaculture reared fish is common (Thomas, 1991; McEachron et al., 1998). In natural environments, it has been suggested that this species requires high (> 20) salinity waters to complete their lifecycle and move offshore at maturity (Boothby and Avault, 1971; Matlock, 1987; Peters and McMichael Jr., 1987; Wilson and Nieland, 1994). However,

during their juvenile and subadult stages, they are more common in oligohaline inshore

environments and often remain near coastlines as adults (Pearson, 1928; Bass and Avault, Jr,

1975; Matlock, 1987; Beckman et al., 1988). Bacheler et al. (2009) found distance from shore to

be a strong explanatory variable of the spatial distribution of Red Drum. Their proximity to

shore and coastal areas makes them susceptible to anthropogenic impacts.

Acoustic telemetry has been widely used to better determine site fidelity, habitat use, and

behavior of many different fish species (Zeller et al., 1997; Lowe et al., 2003; Dresser and

Kneib, 2007; Wetherbee et al., 2007; Bacheler et al., 2009; Brogan, 2010). A number of

different techniques have been employed, including manual tracking (e.g., Coral Trout

[*Plectropomus leopardus*]; Zeller et al., 1997) and remote tracking (e.g., Lemon Sharks

[*Negaprion brevirostris*]; Wetherbee et al., 2007). Two such studies exist on site fidelity and

habitat use for Red Drum (*Sciaenops ocellatus*) using acoustic telemetry. Across years and at the

basin-level scale, Red Drum habitat use was associated with shallow depth, closer distances from

shore, and salinity (Bacheler et al., 2009). At finer temporal and spatial scales, Red Drum

activity was found to be tidally dependent, with specific habitats being used at specific tides

(Dresser and Kneib, 2007). Across studies, juvenile Red Drum have exhibited high site fidelity

and usually occupy small home ranges ($\sim < 5$ km^2; Matlock, 1987; Adams and Tremain, 2000;

Dresser and Kneib, 2007).

Bayou St. John (BSJ) is an urbanized, narrow water body with little to no tidal fluctuation

and limited up-estuary connectivity. Up-estuary connectivity is controlled via a sector gate and

sluice valves, with water surface elevations maintained artificially low. This limited connectivity

prevents much tidal fluctuation and little variation in salinity with respect to time or space (see

Chapter 1 for more details). As such, it does not contain, nor is it connected to suitable spawning

habitat for Red Drum. These conditions do not allow for adequate estimation of habitat selection, as not all habitats are made available. However, by holding salinity, distance from shore, and solar-lunar tidal periodicity constant, it allows for the study of Red Drum activity and site fidelity without these effects.

Here, I examined Red Drum activity and behavior in BSJ across multiple scales using acoustic telemetry. I aimed to determine if Red Drum have high site fidelity in BSJ by testing their Sedentariness, a measure of inactivity, across a broad temporal scale. Using a large dataset, I compared their behavior to other studies. Absent of tidal periodicity, I characterized their response to changes in temperature and flow characteristics. I also analyzed their response to artificially elevated discharges. Specifically, I asked:

1. How did Red Drum detections vary across a broad (18 month) time period in Bayou St. John? Was there variability among tagging groups, individual fish, or day night periods? What were the general patterns in detections across months?

2. How did Red Drum Sedentariness, a measure of inactivity, vary across a broad (18 month) time period in Bayou St. John? Did this vary among tagging groups, individual fish, or day night periods? What were the general patterns in Sedentariness across months?

3. Were Red Drum detections associated with temperature and subtidal flow characteristics? Did these relationships vary among sites and between day night periods?

4. How did high energy sector gate openings effect Red Drum behavior? Did their site preference change surrounding these events?

Materials and Methods

Study Site

Bayou St. John is an urban waterway located in the north-central portion of the City of New Orleans, Louisiana (Fig. 2.1). Much of its banks have been stabilized by concrete and it is surrounded by houses and roadways with 16 bridges crossing it. It is approximately 6.5 km long and for most of its length has a north-south orientation. The width of the bayou varies from 45 m to 200 m. The northern extremity is partially connected to Lake Pontchartrain via a sector gate containing three sluice valves used to manage BSJ's water elevation. The most southern point ends at the corner of Jefferson Davis Parkway and Lafitte Street (29 58' 23.9" N, -90 5' 28.53" E). For a complete description of the Bayou and its hydrodynamic properties see Chapter 1. Five VEMCO VR2W 69 kHz acoustic receivers were moored from 1 July 2012 through 20 May 2014 (Fig. 2.1). These were used to detect pings emitted from Red Drum fitted with internal transmitters.
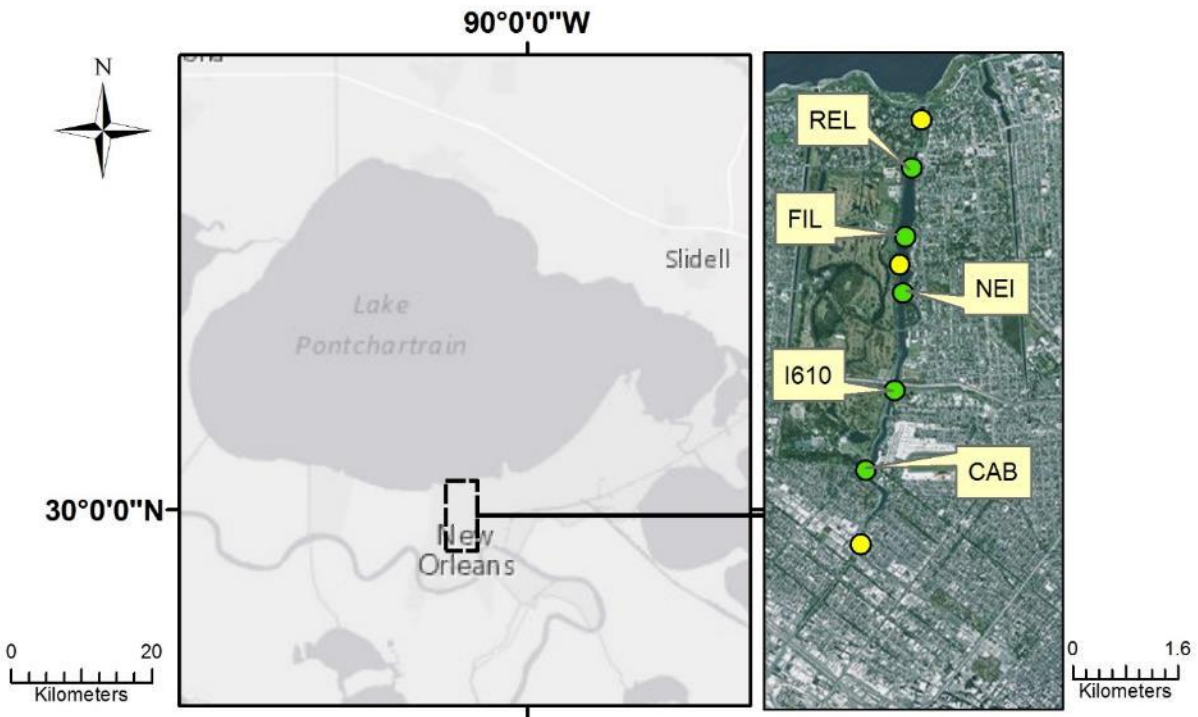
Figure 2.1. Map created using ArcMap 10 showing the extent of Bayou St. John within the local area. Note its position relative to New Orleans, LA and Lake Pontchartrain. On the inset, Green dots mark moored receiver locations with their respective site names and yellow dots mark continuous water quality stations within the Bayou maintained by USGS.

Surgery

I surgically implanted internal VEMCO V13-1x-A69-1610 transmitters with a random delay of 50 to 130 seconds and estimated battery life of 818 days into the peritoneal cavity of 22 Red Drum (IACUC 09-009; approved 13 August 2009, renewed and updated 13 August 2011; Appendix I). All fish were tagged from 5 November 2011 to 2 February 2014, were 444 to 710 mm SL, and weighed between 1100 and 4820 g (Table 2.1). Transmitters weighed 11.11 grams in air which was less than 2% of the body weight of the smallest fish studied. All fish acoustically tagged were collected using rod and reel outside of BSJ, but within the Lake Pontchartrain Basin. All fish that were not donated (see below for more information) were kept in aerated holding tanks made of water collected at the collection site until they were brought

back to the laboratory. Each fish was carefully monitored for health and condition and only fish that appeared in good condition were considered for surgery. Given low level of angling and difficultly with recapture (Brogan, 2010) MS-222 (Tricaine methanesulfonate) was used as an anesthetic. An anesthetic (100 mg/l MS-222) and maintenance bath (65 mg/l MS-222) were prepared and all surgery equipment was sanitized using ethanol before surgery. Fish were placed in the anesthetic bath and closely monitored for approximately five minutes or until completely sedated. Once sedated, each fish were measured, weighed, externally tagged with a Floy FT-1-94 dart tag, and placed dorsal side down on a wedge on the surgery table. The maintenance bath was aerated and continually pumped across the fish's gills during surgery. Scales were removed with forceps along the fish's ventral surface and a 2 cm incision was made. Then, the transmitter was placed in the peritoneal cavity and shifted posteriorly. Careful consideration was given to avoid the colon-anus junction during transmitter placement. The incision was then closed using Ethicon® 36 mm ½ circle taper point with absorbable chromic gut sutures. After surgery fish were placed in an aerated recovery tank, a mixture of BSJ water and holding tank water, and monitored for approximately one hour. Rejuvenade Next Generation® was added to the recovery tank to reduce stress. Once recovered, all fish were transported to BSJ and released near site REL (Fig. 2.1). Eleven fish were donated as part of the Louisiana IFA Redfish Tour and LA Saltwater Series Events. At these events, fish were donated after being caught and weighed as a part of a fishing tournament. Fish were transported from the weigh-in site to the Nekton Research Laboratory (NRL) in aerated tanks. Once in the lab the same protocol was followed as was for fish collected by NRL personnel in the field. Help from personnel with the Audubon Aquarium of the Americas was used in handling, tagging, and the transportation of donated fish.

Table 2.1. Date and location of collection and surgery date, weight, length and VEMCO transmitter ID for all fish. Season denotes whether each fish was detected during the summer, winter, or both periods for the short term and sector gate response sections. Locations are approximate with some fish (denoted by a * or **) being from tournament weigh ins.

ID	Date	Location	Season	FL (mm)	Weight (g)
31681	5 Nov 2011	Chalmette, LA*	None	510	1700
31678	5 Nov 2011	Chalmette, LA*	None	645	3460
31679	5 Nov 2011	Chalmette, LA*	None	654	3515
31682	5 Nov 2011	Chalmette, LA*	Both	641	3515
31680	5 Nov 2011	Chalmette, LA*	Both	643	3630
31683	5 Nov 2011	Chalmette, LA*	None	660	3700
31698	22 Jan 2012	Bayou Platte, LA	Summer	590	2250
31697	22 Jan 2012	Bayou Platte, LA	None	690	4150
31691	23 Jun 2012	Delacroix, LA**	Summer	444	1100
31692	23 Jun 2012	Delacroix, LA**	Both	456	1175
31695	23 Jun 2012	Delacroix, LA**	None	634	3070
31693	23 Jun 2012	Delacroix, LA**	Summer	652	3350
31696	23 Jun 2012	Delacroix, LA**	Both	656	3750
31700	11 Nov 2013	Bayou Platte, LA	Winter	520	1400
31701	11 Nov 2013	Bayou Platte, LA	None	491	1400
31703	11 Nov 2013	Bayou Platte, LA	Winter	505	1450
31699	11 Nov 2013	Bayou Platte, LA	Winter	524	1500
31702	11 Nov 2013	Bayou Platte, LA	Winter	529	1760
31708	11 Nov 2013	Bayou Platte, LA	Winter	535	1810
31707	2 Feb 2014	Reggio, LA	Winter	533	1620
26301	2 Feb 2014	Reggio, LA	Winter	565	2300
26300	2 Feb 2014	Reggio, LA	Winter	710	4820

All fish responded well after surgery and were subsequently released into BSJ. All fish except one were detected at more than one receiver in BSJ for at least a month after release. Fish number 31701 was recaptured 6 days after release by an angler between the old and new flood control structures. This fish was only detected at site REL. Fish 31693, 31707, and 31708 were also recaptured and reported by anglers, but remained at liberty in the Bayou for longer than one month. Fish 31693 was turned in and had a prolapsed gut. Fish number 31701 was not turned

in, but pictures were taken and no prolapsing could be seen and there was evidence of incision healing.

Range Test

Four VEMCO V13 transmitters were fitted with external caps designed by VEMCO for range testing. The range calculator from VEMCO was used to determine appropriate distances to moored transmitters (http://vemco.com/range-calculator/; Table 2.2). Range approximations by VEMCO are for open marine systems. Using this guide, distances of 250 m, 400 m, 550 m and 675 m were chosen. To reduce potential interference with tagged fish, range test transmitters were moored within the two southern receiver locations (sites I610 and CAB), because there were typically far fewer fish detections at these locations (Smith, 2012; current study). One transmitter per buoy was moored at four different locations within BSJ from 5 May 2014 to 20 May 2014 (Fig. 2.2). Two transmitters were located within the range of the I610 receiver station (550 m and 675 m) and two within the CAB receiver station (250 m, 400 m; Fig. 2.2). Careful attention to line of site was given and through water line of site was maintained for each mooring location. However, in three of the four locations a bridge was between the receiver and transmitter (Fig. 2.2). For each receiver the proportion of pings emitted per transmitter was estimated. Each transmitter is set to send a ping randomly between 50 and 130 seconds. For analyses, time between pings was assumed to be every 130 seconds. This is conservative, because it represents less than all of the pings emitted. The percentage of pings recorded was calculated

$$p = \left(\frac{n}{\frac{t}{130}} \right) * 100 \qquad\qquad (2.1)$$

,where p is the percentage of pings recorded, n is the number of pings recorded, and t is the

duration of deployment in seconds.

Table 2.2. Results for theoretical range of transmitters from VEMCO's website (http://vemco.com/range-calculator/). Note that the transmitters used here were 147 dB. These values were used as a guide when planning the range test for the current study.

Transmitter Power (dB)			
147		153	
Wind Speed (knots)	Range (m)	Wind Speed (knots)	Range (m)
Calm	539	Calm	700
3 to 6	522	3 to 6	682
11 to 16	406	11 to 16	551
28 to 34	282	28 to 34	406

Figure 2.2. Map generated using ArcMap 10 showing mooring locations for the range test. Distances of 250, 400, 550, and 675 m were tested. Yellows transmitters were associated with receiver at site CAB (southern site) and red indicates transmitters associated with the receiver at I610 (northern site).

The 250 m transmitter for site CAB was the only one receiver-transmitter combination that recorded any pings. For the entire deployment, 1.8% of pings were detected, suggesting that the coverage range for VEMCO receivers is much lower in BSJ than open ocean conditions. Pings were only recorded from 8 May at 0150 to 8 May 2014 at 1245. Using equation 1, during this time period a maximum of 60.2% of pings were recorded. For the analysis part of the *Fine Scale Detectability* section, a maximum range of 200 m was assumed for each receiver.

Detection Metrics

For analysis, the number of pings per fish ID per hour was totaled. Only hours when three or more pings were observed were included. Each hour was also binned as either daytime or nighttime. Daytime hours for November through March were from 0600 to 1759 CST. Daytime hours for April through October were 0500 to 1859 CST. After this, two different metrics were calculated. "Detectability" was used to estimate how often a tagged fish was observed for each day or night period. It was calculated by dividing the number of hours a fish was detected (i.e., the number of hours in which three or more detections were observed from at least one receiver location) by the number hours for that day or night. A modification of Andrews' et al. (2010) "Sedentariness" was used to estimate to estimate the amount of time a fish spent at one location and was calculated for each day/night period as follows:

$$S = \frac{D_s}{D_t} \tag{2.2}$$

where S is Sedentariness, D_s is the number of hours in which a fish was detected in the same location as its previous location, and D_t is the total number of hours in which a fish was detected for each diurnal/nocturnal period.

Large Scale Analysis

To better understand if Detectability and Sedentariness were different among tagging groups, individuals, diurnal/nocturnal periods, or across time, two Generalized Linear Mixed Models (GLMMs) with binomial distribution and logit link using lme4 and lmerTest in R were used (Bates et al., 2014; Kuznetsova et al., 2014; R Core Team, 2015). Before analysis, each of the proportions (i.e., Detectability and Sedentariness) was expanded to the number of successes and failures. Each of the two models share a similar design, where Fish ID, day/night, and an interaction between day/night and Fish ID were treated as fixed effects and Month-Year and an interaction between Fish ID and Tagging Group were treated as random effects. Month-Year here refers to the month and year in which each period occurred and was used to remove serial autocorrelation. The most parsimonious model was selected using Bayesian Information Criterion (BIC; Schwarz, 1978) as this has been suggested for mark-recapture fisheries data (Muthukumarana et al., 2008). Before analysis, the number of detections for each fish was determined to ensure an adequate sample size was available. In other words, I plotted the number of detections per day by site and fish id across the entire study period. If a fish was not consistently detected over this temporal period, it was not included.

Fine Scale Detectability

Two other periods of interest were analyzed at a finer scale. Results from three dimensional hydrodynamic models were used to understand the relationship between Red Drum detections and flow characteristics. These simulations covered time from 1 August 2013 to 21 August 2013 (termed summer period here) and 3 February 2014 – 21 February 2014 (termed winter period here). On the 19th of each month, a sector gate opening occurred. These openings altered the overall hydrology and produced much higher currents than under normal conditions.

For this section, data before sector gate openings only was used. Two parameters, resultant magnitude velocity (referred to as velocity), and the horizontal derivative of velocity with respect to space (referred to as cross stream gradient), related to flow were considered and selection of parameter(s) was based on simple regression. It was likely these parameters were closely related to each other and if this was the case, one was chosen to represent changes in both. Generalized estimating equations (GEEs) in geepack for R statistical software (Højsgaard et al., 2006, R Core Team, 2015) were used for all GEEs. Here, GEEs were used to test how flow, temperature, and day/night influence Detectability at each site during the summer and winter simulations. Temperature was not well constrained for either season (Chapter 1), so a linear interpolation was used between the two nearest real time water data gages was used (Fig. 2.1). Model grid size is 20 m x 20 m with output every hour. Average flow values within 200 m each receiver were used. Before analysis, the number of detections for each site and each fish was visualized to be sure an adequate sample size was available. Overall model design was the same for each season/site combination with a binomial response and logit link function. For each hour, Detectability for each fish-site combination was calculated and used as a response variable for all GEEs. Flow, temperature, day/night, and all one-way interactions were used as predictor variables. Three different correlation structures, independence, AR-1, and exchangeable, were used for each modeling scenario and a goodness of fit criterion called the Correlation Information Criterion (CIC) was used to determine the best fitting correlation structure (Hin and Wang, 2009). After the appropriate correlation structure was chosen, corrected quasi likelihood under the independence model criterion (QICc) was used to determine the best subset of predictor variables.

Response to Sector Gate Openings

Analyses were also performed to determine if sector gate openings had an effect on Detectability of tagged fish at each site. Detectability per fish-site before and after sector gate opening were tested using GEEs for both the summer and winter period (Højsgaard et al., 2006, R Core Team, 2015). A binomial structure with a logit link was utilized. Detectability was treated as a response variable, before/after opening, day/night, site, and all one way interactions were used as predictor variable ($\alpha = 0.05$). CIC was used to select correlation structure among the same three options in the previous section. After the appropriate correlation structure was chosen, QICc was used to determine the best subset of predictor variables. Again, the number of detections for each fish was determined before analysis to ensure an adequate sample size was available.

Results

Large Scale Detections

From 1 July 2012 through 31 December 2013, a total of 431,545 detections were recorded form 15 fish. After filtering the database by hour-fish and removing all hour-fish combinations with less than 3 detections, there were 418,008 detections. Five fish were consistently observed throughout the study with 348,208 detections. These detections were used in the GLMMs and were the focus of the large scale detection analyses.

A plot of monthly mean Detectability per fish indicated a slight separation of fish into two groups, with Fish ID 31680 and 31692 having consistently higher monthly mean detectability than 31682, 31698, and 31691 (Fig. 2.3). Monthly mean Detectability for day/night periods indicated for most months little difference in Detectability was observed (Fig. 2.4).

Monthly mean Detectability per release group shows that overall, the Chalmette (n = 2) and

Delacroix (n = 2) release groups were detected more often than the Platte (n = 1) group (Fig.

2.5). The most parsimonious model included all random effects and the month-year fixed effect

(BIC = 29,774; Table 2.3).
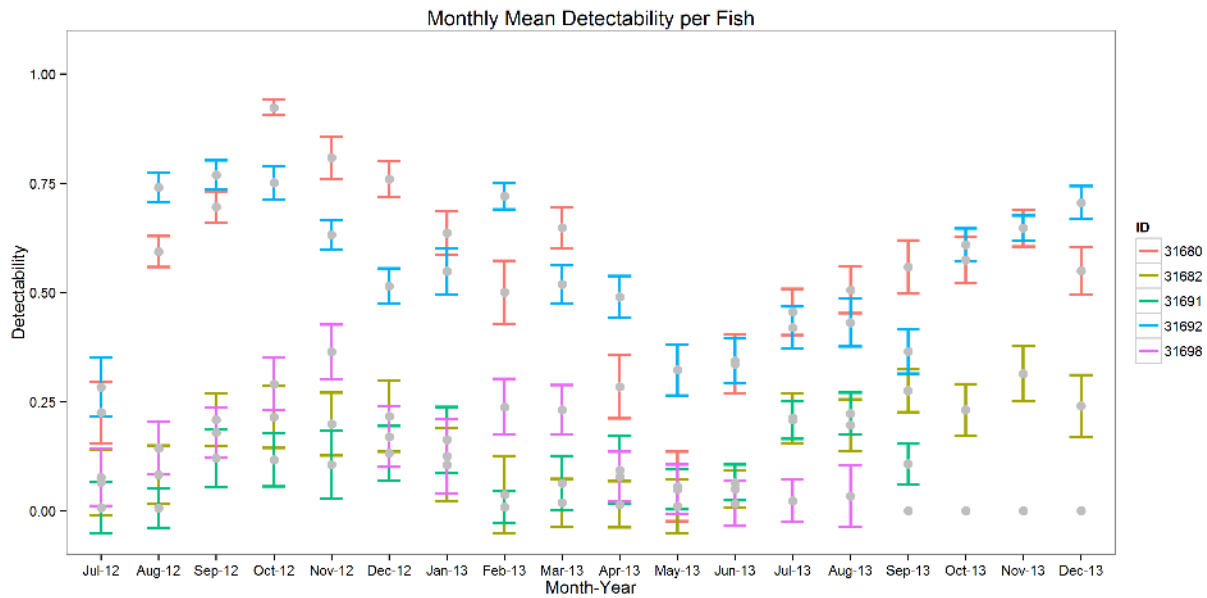
Figure 2.3. Monthly mean Detectability for each of the five fish that were consistently detected from 1 July 2012 through 31 December 2013. The gray point represents the mean for each fish-month and the error bars indicate standard error.
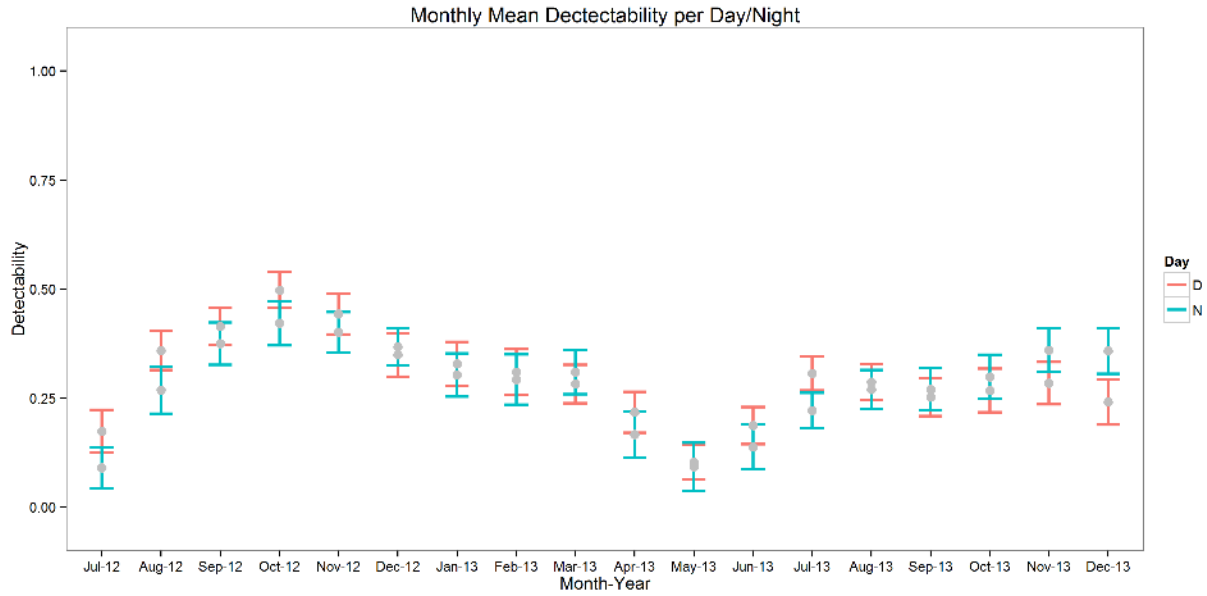
Figure 2.4. Monthly mean Detectability for day/night periods of fish that were consistently detected from 1 July 2012 through 31 December 2013. The gray point represents the mean for each fish-month and the error bars indicate standard error.
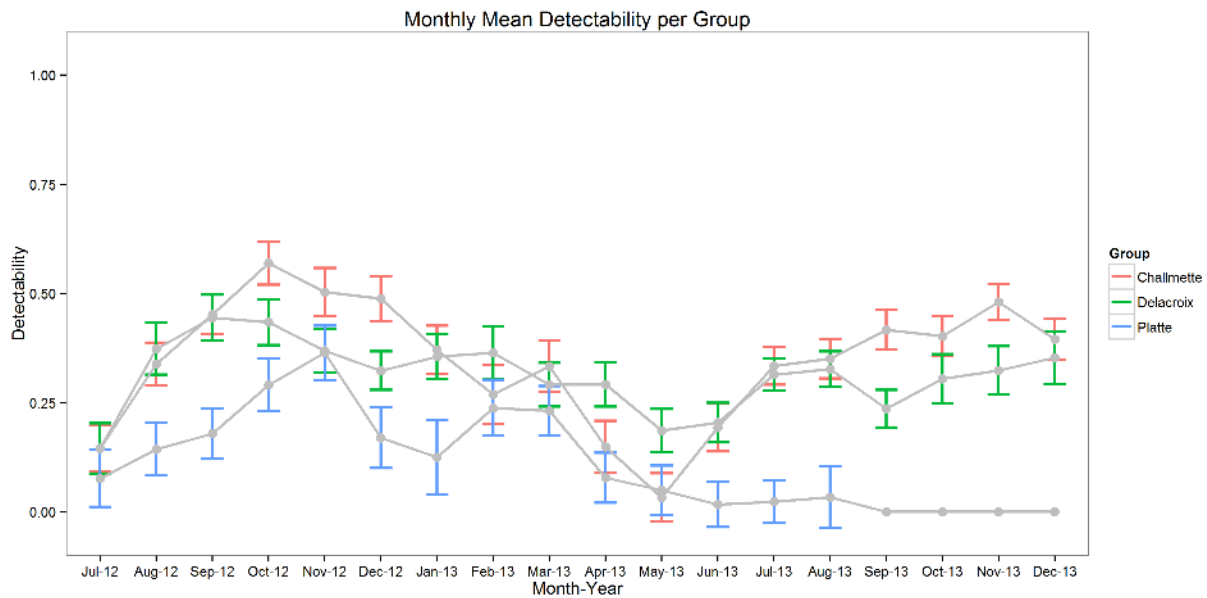
Figure 2.5. Monthly mean Detectability for Tagging Groups of fish that were consistently detected from 1 July 2012 through 31 December 2013. The gray point represents the mean for each fish-month and the error bars indicate standard error.

Table 2.3. Fixed effects results of the most parsimonious (BIC = 29,774) large scale Detectability generalized linear mixed model (GLMM). The design of this GLMM treated detections as a response variable, and individual fish id, day/night period, and an interaction between individual and day/night were treated as fixed effects. Month-year was treated as random effects.

Fixed Effects Large Scale Detectability		
	Estimate	SE
(Intercept)	0.18	0.15
ID31682	-2.00	0.04
ID31691	-2.97	0.05
ID31692	-0.26	0.04
ID31698	-2.31	0.05
DayN	-0.13	0.04
ID31682:DayN	-0.24	0.06
ID31691:DayN	0.29	0.08
ID31692:DayN	0.50	0.05
ID31698:DayN	-0.34	0.07

Monthly mean Sedentariness per fish suggested that sedentariness varied less among tagged fish and across months than Detectability (Fig. 2.6). No clear grouping was apparent. Monthly mean Sedentariness for day/night periods indicated mean Sedentariness was higher during the night for most months (Fig. 2.7). Monthly mean Sedentariness per Tagging Group did not show any clear separation among Groups (Fig. 2.8). Across plots and categories, Sedentariness was often higher than 0.5 indicating that when a fish was detected, it was more often detected at the same site as it was for the previous detection. This suggested that overall fish were inactive with high levels of site fidelity. Day/night as a random factor and month-year as a fixed factor were the only variables in the most parsimonious GLMM (BIC = 7,750.6). Higher mean Sedentariness was observed during the night, suggesting fish were less active during the night (Table 2.4).
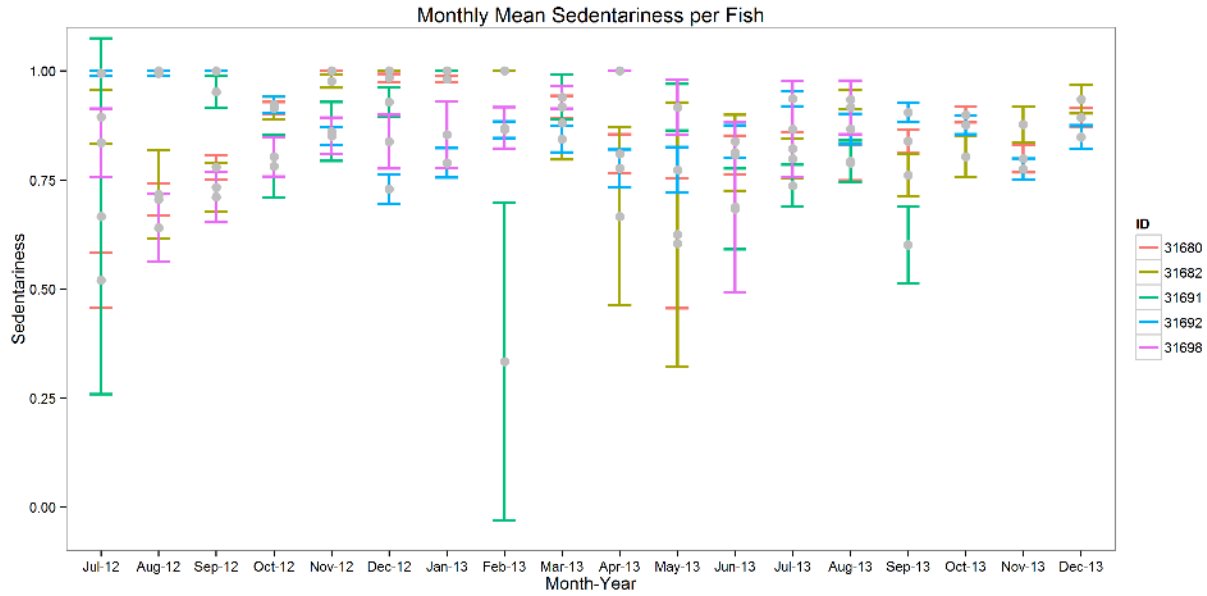
Figure 2.6. Monthly mean Sedentariness for each of the five fish that were consistently detected from 1 July 2012 through 31 December 2013. The gray point represents the mean for each fish-month and the error bars indicate standard error.
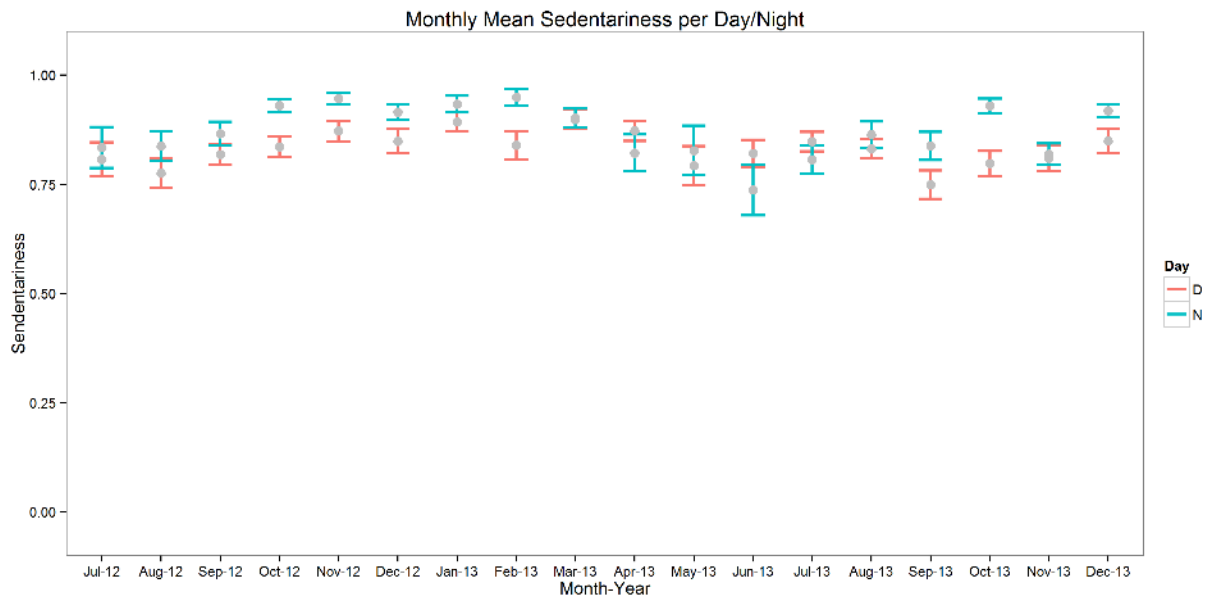
Figure 2.7. Monthly mean Sedentariness for day/night periods of fish that were consistently detected from 1 July 2012 through 31 December 2013. The gray point represents the mean for each fish-month and the error bars indicate standard error.
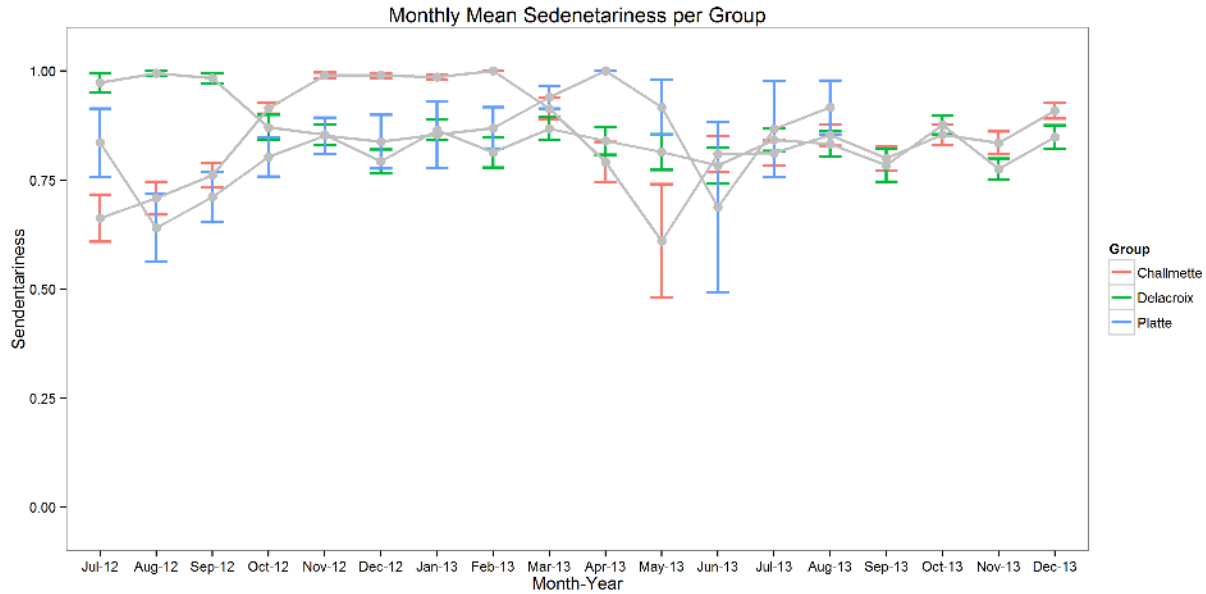
Figure 2.8. Monthly mean Sedentariness for Tagging Groups of fish that were consistently detected from 1 July 2012 through 31 December 2013. The gray point represents the mean for each fish-month and the error bars indicate standard error.

Table 2.4. Fixed effect results of the most parsimonious (BIC = 7,751) for the large scale Sedentariness generalized linear mixed model (GLMM).   The design of this GLMM initially treated Sedentariness as response variable, and individual fish id, day/night period, and an interaction between individual and day/night as fixed effects and month-year as a fixed effect.

Fixed Effects Large Scale Sedentariness		
	Estimate	SE
(Intercept)	1.68	0.09
Day/Night	0.55	0.05

Fine Scale Detectability

A total of 6,256 detections from five fish were observed during the summer period. Four fish, 31680, 31682, 31691, and 31692, were consistently detected during the summer period 6,062 times. Before the sector gate opening, there were 1,564 detections at REL, 3,744 detections at FIL, 269 at NEI, 56 at I610, and 34 at CAB (Figs. 2.9-2.13). Four fish, 31680, 31682, 31691, and 31692, were detected at REL and all five were detected at FIL (Figs. 2.14 and

91

2.15). Two fish, 31692 and 31698 were detected at NEI (Fig. 2.16). Only fish 31692 was

detected at I610 and CAB on 10 August to 11 August 2013 (Figs. 2.17 and 2.18).

Figure 2.9. Daily mean detections at site REL for fish IDs that were consistently detected throughout the summer period (1 August 2013 – 21 August 2013). The gray point represents the mean for each fish-day and the error bars indicate standard error.

Figure 2.10. Daily mean detections at site FIL for fish IDs that were consistently detected throughout the summer period (1 August 2013 – 21 August 2013). The gray point represents the mean for each fish-day and the error bars indicate standard error.

Figure 2.11. Daily mean detections at site NEI for fish IDs that were consistently detected throughout the summer period (1 August 2013 – 21 August 2013). The gray point represents the mean for each fish-day and the error bars indicate standard error.

Figure 2.12. Daily mean detections at site I610 for fish IDs that were consistently detected throughout the summer period (1 August 2013 – 21 August 2013). The gray point represents the mean for each fish-day and the error bars indicate standard error.

Figure 2.13. Daily mean detections at site CAB for fish IDs that were consistently detected throughout the summer period (1 August 2013 – 21 August 2013). The gray point represents the mean for each fish-day and the error bars indicate standard error.

Figure 2.14. Daily mean Detectability at site REL for fish IDs that were consistently detected throughout the summer period (1 August 2013 – 21 August 2013). The gray point represents the mean for each fish-day and the error bars indicate standard error.

Figure 2.15. Daily mean Detectability at site FIL for fish IDs that were consistently detected throughout the summer period (1 August 2013 – 21 August 2013). The gray point represents the mean for each fish-day and the error bars indicate standard error.

Figure 2.16. Daily mean Detectability at site NEI for fish IDs that were consistently detected throughout the summer period (1 August 2013 – 21 August 2013). The gray point represents the mean for each fish-day and the error bars indicate standard error.
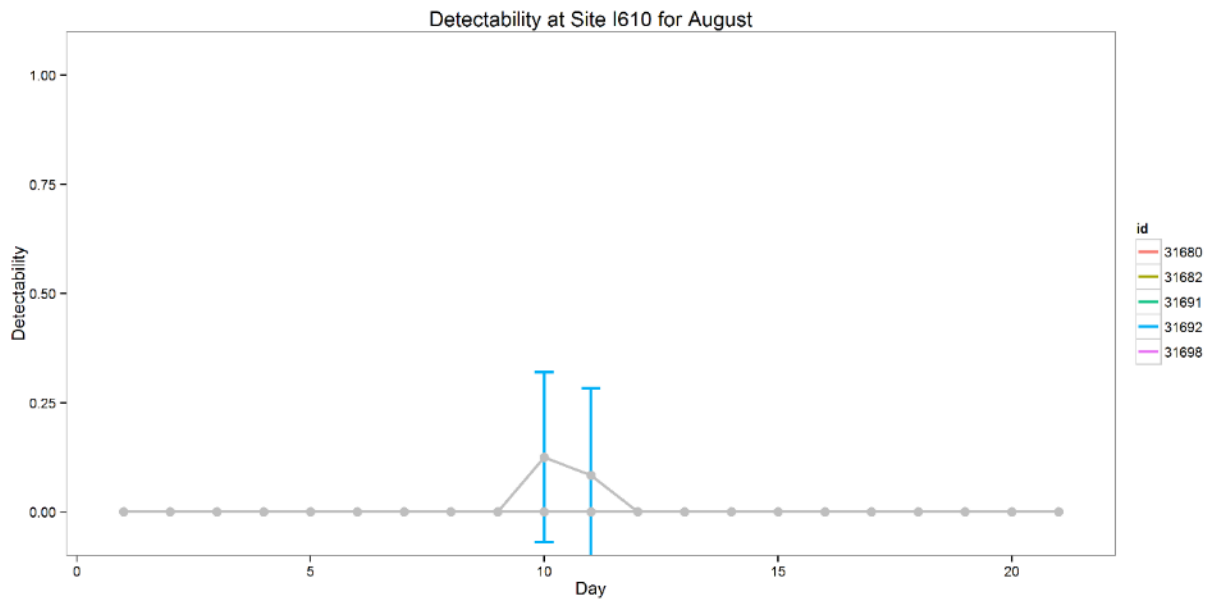
Figure 2.17. Daily mean Detectability at site I610 for fish IDs that were consistently detected throughout the summer period (1 August 2013 – 21 August 2013). The gray point represents the mean for each fish-day and the error bars indicate standard error.
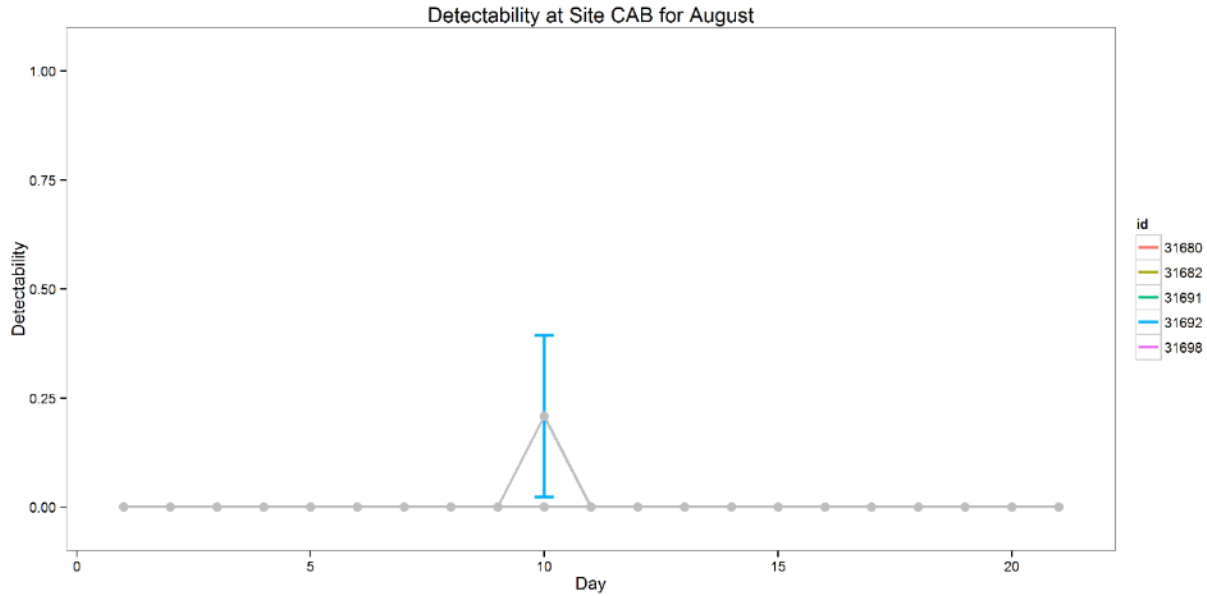
Figure 2.18. Daily mean Detectability at site CAB for fish IDs that were consistently detected throughout the summer period (1 August 2013 – 21 August 2013). The gray point represents the mean for each fish-day and the error bars indicate standard error.

A regression between velocity and cross stream gradient indicate high correlation during the summer period for both sites where fish were consistently detected, REL ($R^2 = 0.995$) and FIL ($R^2 = 0.997$; Table 2.5). Plots of 21 point weighted moving averages for both flow variables across time further demonstrate the similarity of their patterns across all five sites (Figs. 2.19 and 2.20). Weights are decreasing arithmetically from the center, where a weight of 10 was used. For GEE analyses, only velocity was used as a predictor variable, but any effects noticed were treated as representative of both velocity and cross stream gradient metrics.

Table 2.5. Summary of results from four regressions testing the relationship between two flow metrics, resultant magnitude of velocity and the horizontal derivative of velocity with respect to space. These metrics were regressed for all site (REL and FIL) and seasons (summer and winter) combinations. Note the high correlation coefficients for all combinations.

Regression Results between Velocity and Flow Gradient

Summer			
Site	t-value	p	R^2
REL	309	< 2E-16	0.995
FIL	387	< 2E-16	0.997
Winter			
Site	t-value	p	R^2
REL	130	< 2E-16	0.976
FIL	133	< 2E-16	0.977
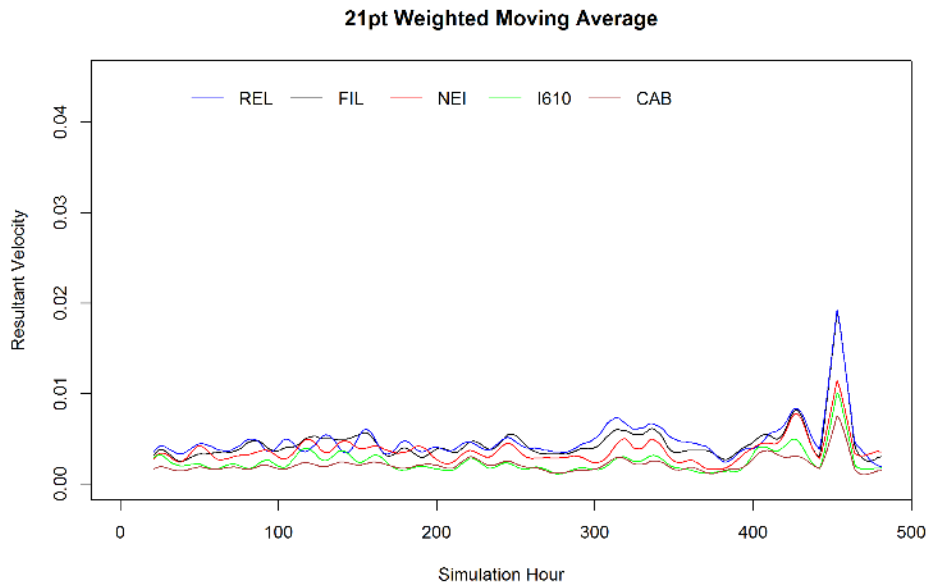
Figure 2.19. Twenty one-point weighted moving average for resultant magnitude of velocity m/s (referred to as velocity in the text) for each site during the summer simulation period. Weights decreased arithmetically from the center, where a weight of 10 was used.
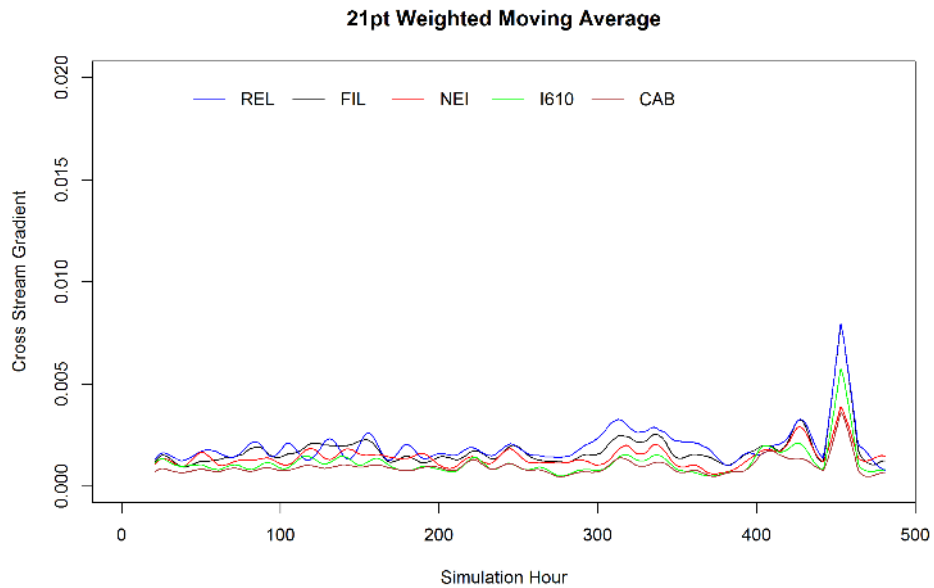
Figure 2.20. Twenty one-point weighted moving average with linear weighting for the horizontal derivative of velocity with respect to space m/s (referred to as cross stream gradient in the text) for each site during the summer simulation period. Weights decreased arithmetically from the center, where a weight of 10 was used.

Due to consistent Detectability across time, GEEs were performed for two different sites (REL and FIL) for the summer period. The AR-1 correlation structure performed better than exchangeable or independence for REL (CIC; 13.5, 28.8, 62; respectively). Temperature, velocity, and an interaction between velocity and temperature were predictor variables included in the most parsimonious model (QICc=1120.9; Table 2.6). Velocity and temperature had positive correlations with Detectability. For the GEE during the summer period at site FIL an AR-1 correlation structure performed better than exchangeable or independence (CIC; 19.7, 48.64, 87.77; respectively). Similar to site REL, Temperature, velocity, and an interaction between them were the only variables included in the most parsimonious model for site FIL during the summer (QICc=1590.2; Table 2.7). A positive correlation between Detectability and velocity was observed among fish, but a negative correlation was observed between Detectability and temperature (Table 2.7).

99

Table 2.6. Results of the most parsimonious model (QICc=1,137) from the pre-opening summer period generalized estimating equation (GEE) for site REL with an AR-1 correlation structure and a CIC of 13.1. Detectability was used as a response variable. Velocity, temperature, day/night period, and all one-way interactions were treated as predictor variables.

GEE Results Summer REL		
	Estimate	SE
Intercept	-7.81	8.71
Temperature	0.18	0.28
Velocity	9.35	4.24
Temp:Velocity	-0.31	0.14

Table 2.7. Results of the most parsimonious model (QICc=1,590.2) from the pre-opening summer period generalized estimating equation (GEE) for site FIL with an AR-1 correlation structure and a CIC of 15.8. Detectability was used as a response variable. Velocity, temperature, day/night period, and all one-way interactions were initially considered as predictor variables.

GEE Results Summer FIL		
	Estimate	SE
Intercept	6.54	5.75
Temperature	-0.23	0.17
Velocity	16.33	8.53
Temp:Velocity	-0.56	0.28

In winter, 48,497 detections were observed from 12 fish. One fish, 31696, was observed consistently at site NEI only (n=14,441). It was excluded from analyses because it is suspected that it is either a shed tag or a deceased fish near the NEI receiver. Eleven fish, 26300, 26301, 31680, 31682, 31692, 31699, 31700, 31702, 31703, 31707, and 31708, were detected consistently throughout this period (n=34,056). Before the sector gate opening, 2,418 Detections were observed at REL, 26,870 at FIL, and 342, excluding fish 31696, at NEI (Figs. 2.21-2.23). No detections were observed at I610 or CAB during this period. Eleven fish, all but 31696, were detected at both REL and FIL (Figs. 2.24-2.25). Only two fish were detected at NEI, 31696 and 31692 (Fig. 2.26).
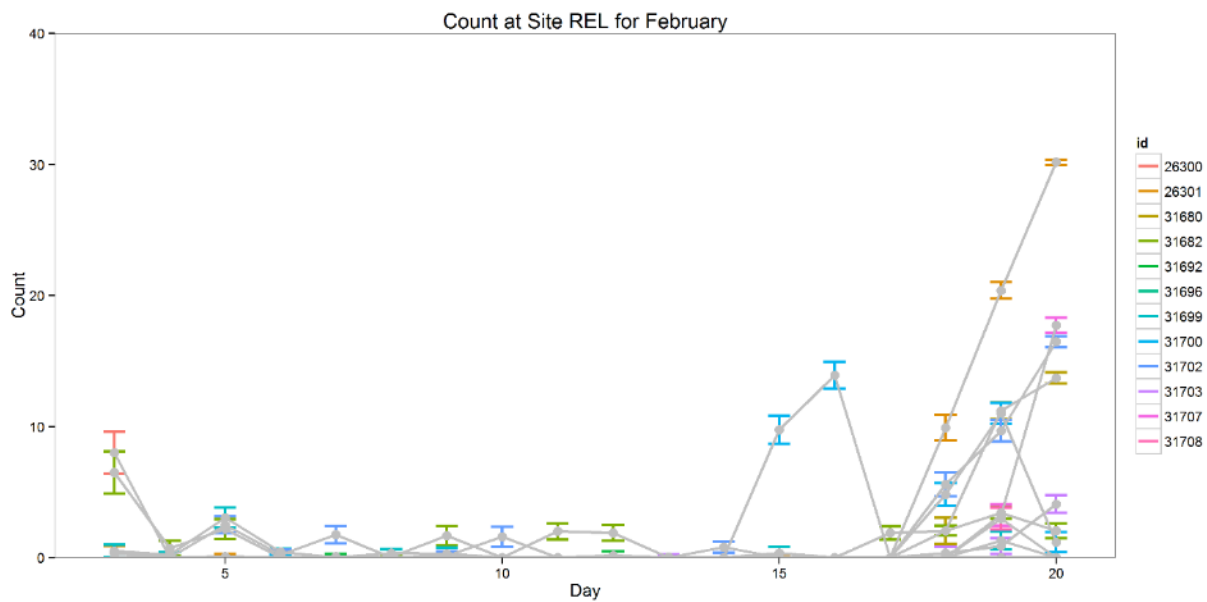
Figure 2.21. Daily mean detections at site REL for fish IDs that were consistently detected throughout the winter period (3 February 2014 – 21 February 2014). The gray point represents the mean for each fish-day and the error bars indicate standard error.
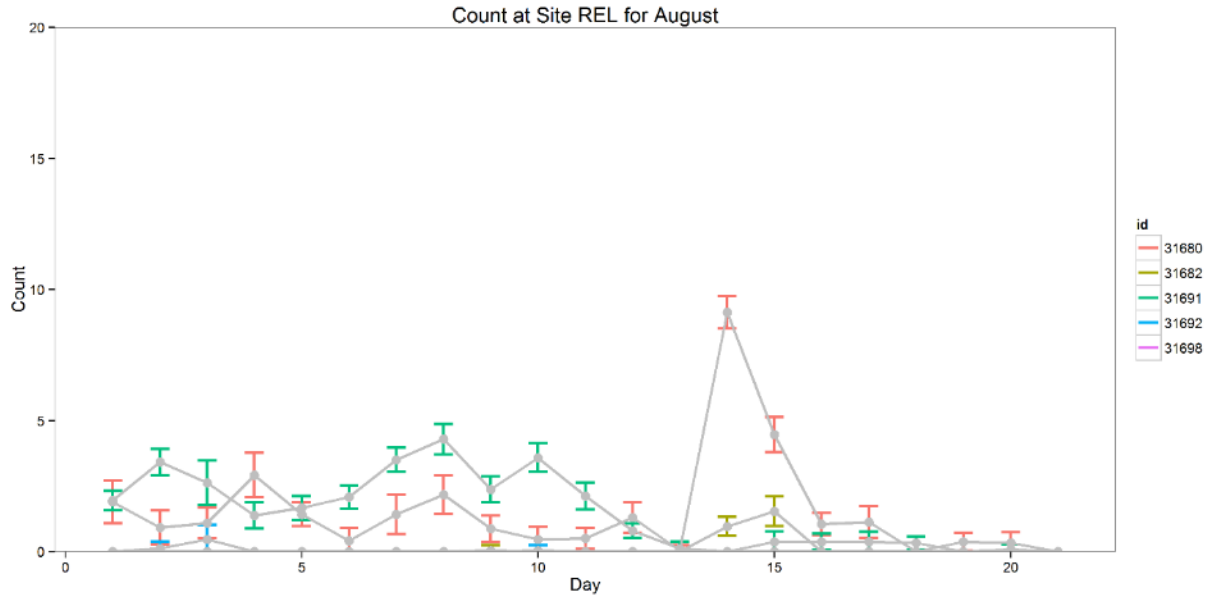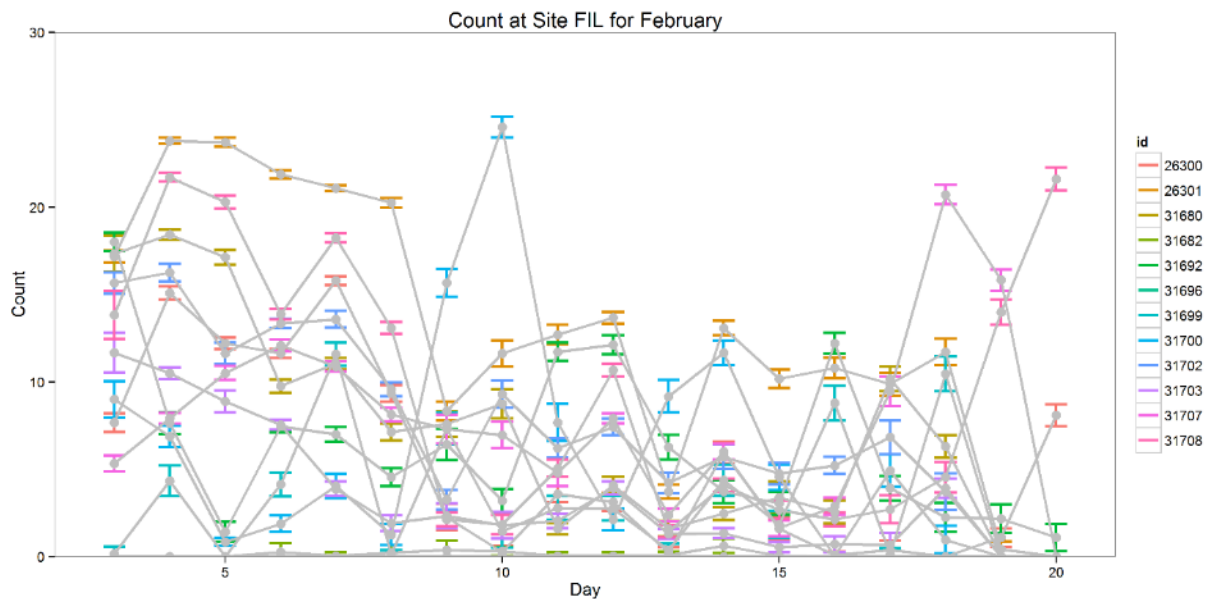

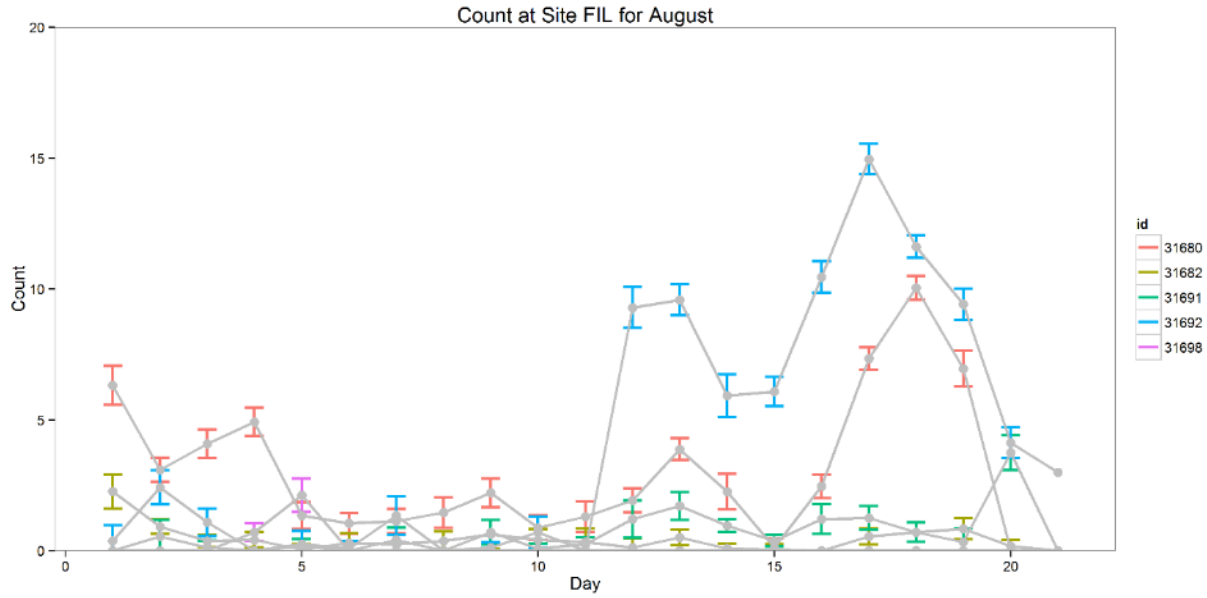Figure 2.22. Daily mean detections at site FIL for fish IDs that were consistently detected throughout the winter period (3 February 2014 – 21 February 2014). The gray point represents the mean for each fish-day and the error bars indicate standard error.
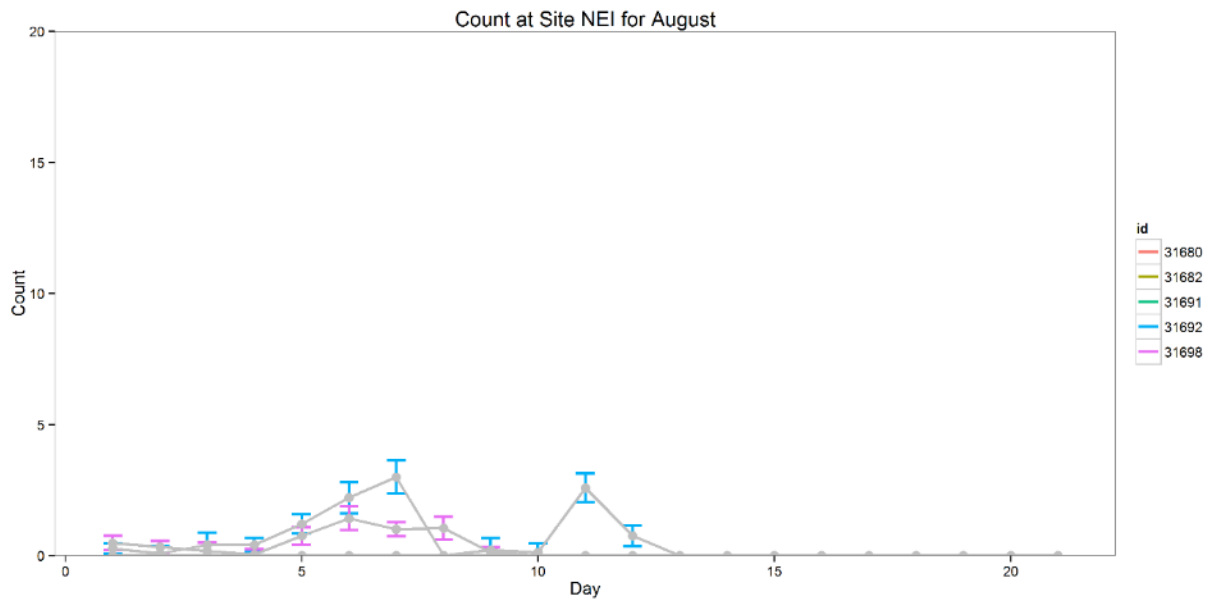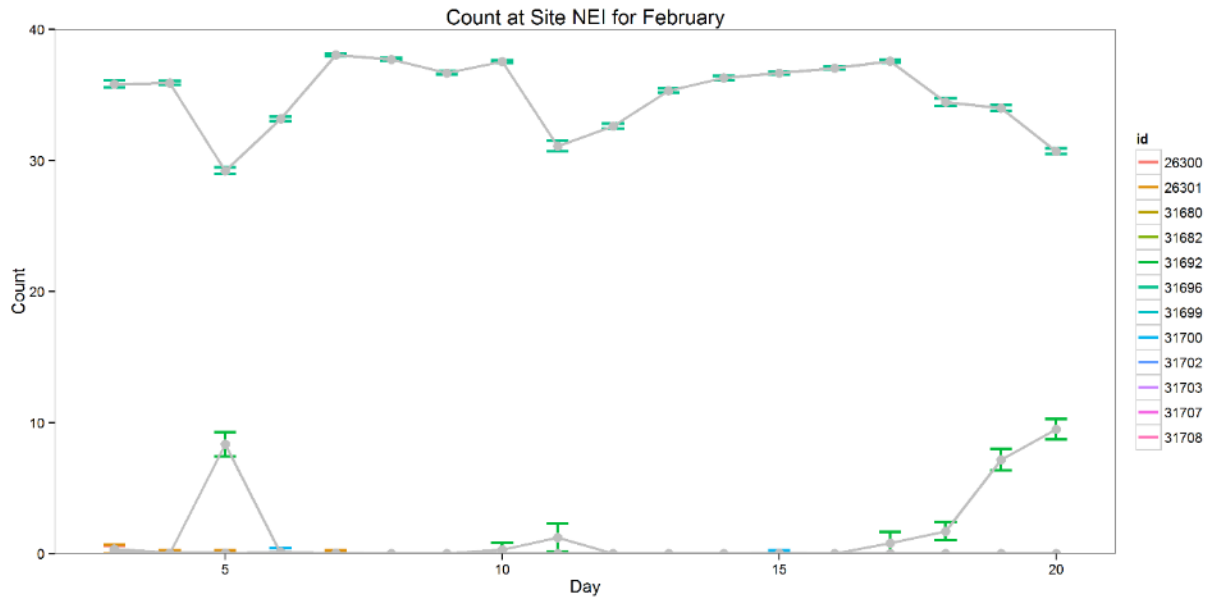
Figure 2.23. Daily mean detections at site NEI for fish IDs that were consistently detected throughout the winter period (3 February 2014 – 21 February 2014). The gray point represents the mean for each fish-day and the error bars indicate standard error.
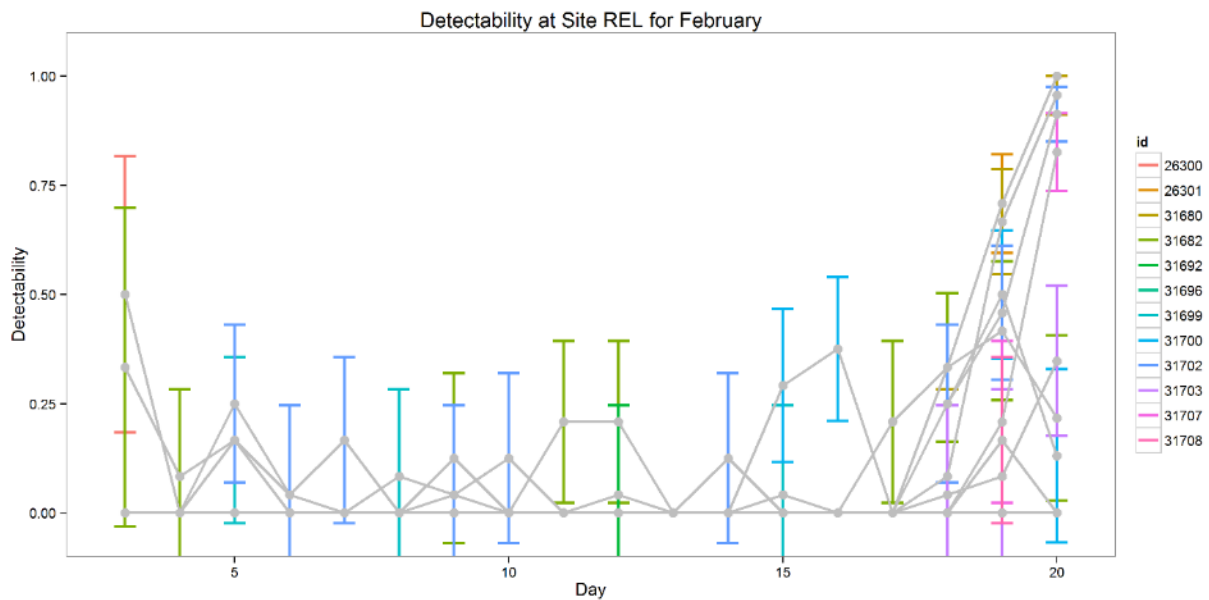
Figure 2.24. Daily mean Detectability at site REL for fish IDs that were consistently detected throughout the winter period (3 February 2014 – 21 February 2014). The gray point represents the mean for each fish-day and the error bars indicate standard error.
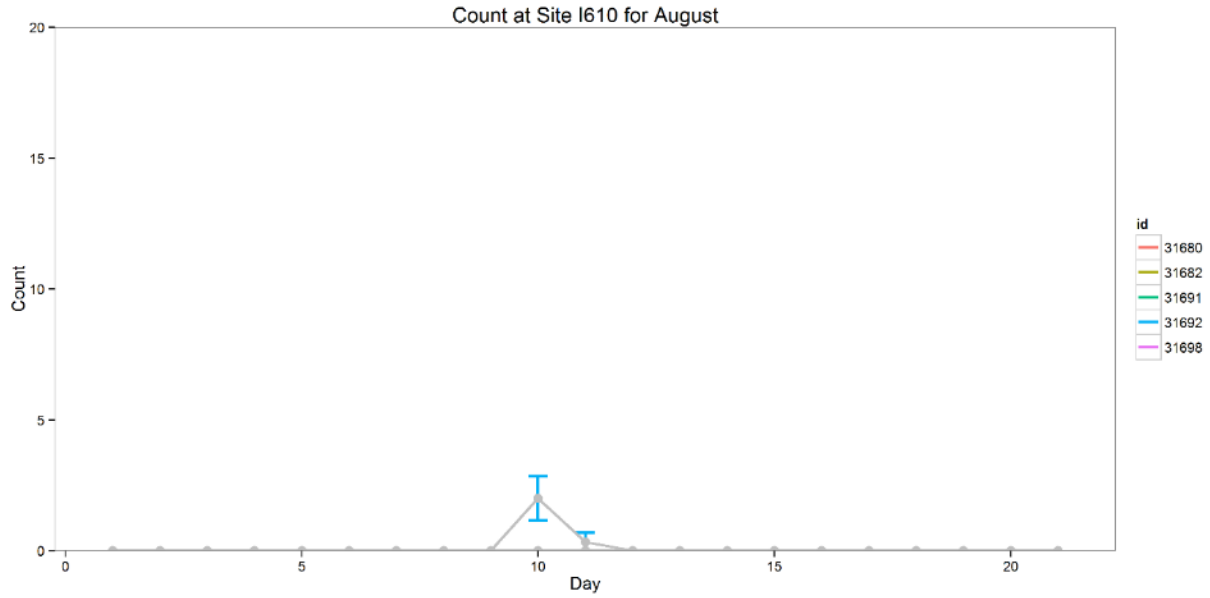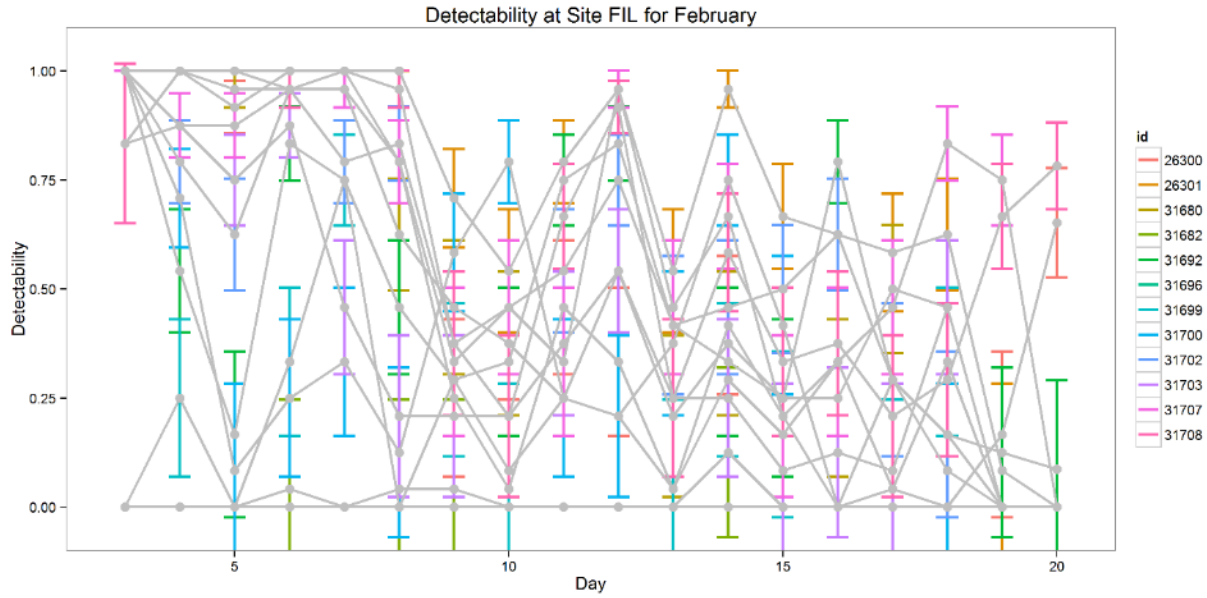
Figure 2.25. Daily mean Detectability at site FIL for fish IDs that were consistently detected throughout the winter period (3 February 2014 – 21 February 2014). The gray point represents the mean for each fish-day and the error bars indicate standard error.
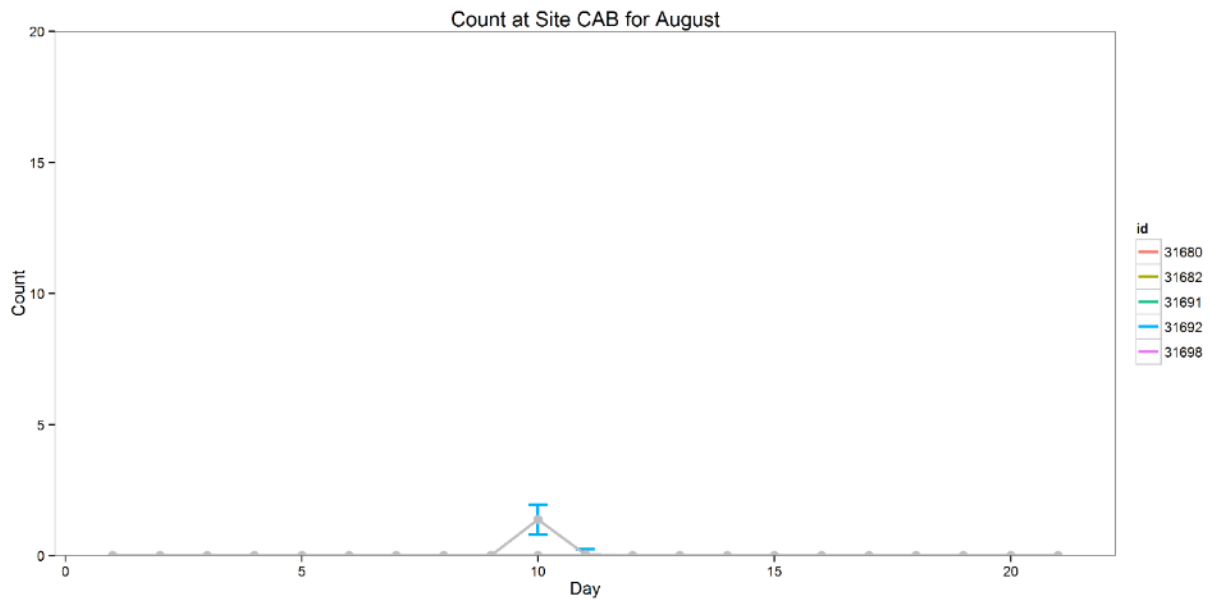

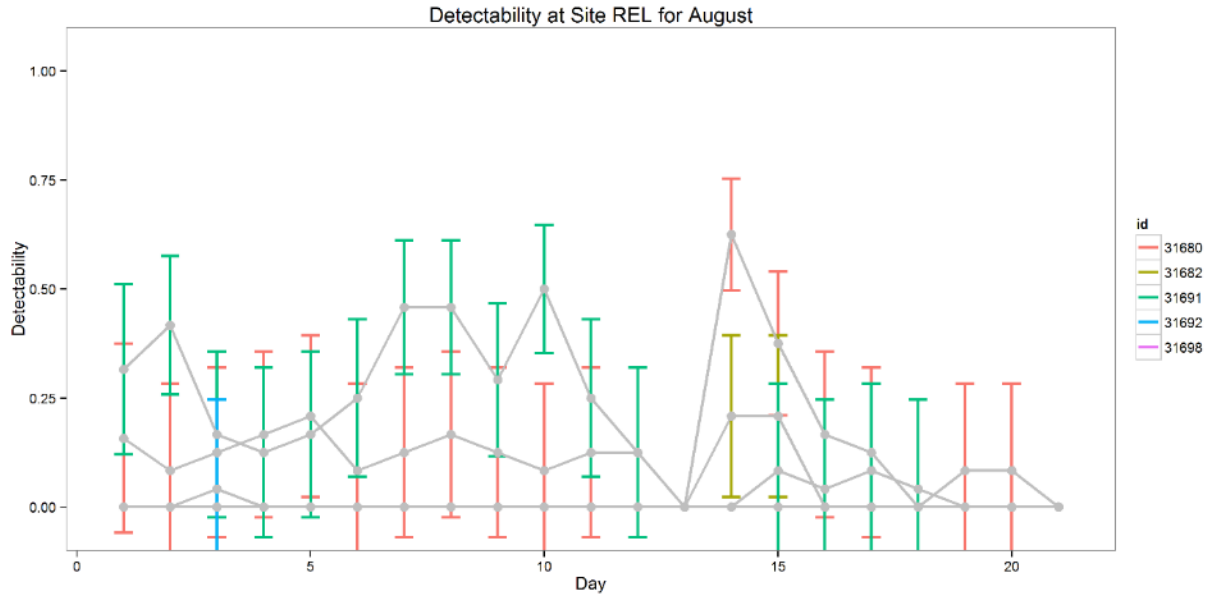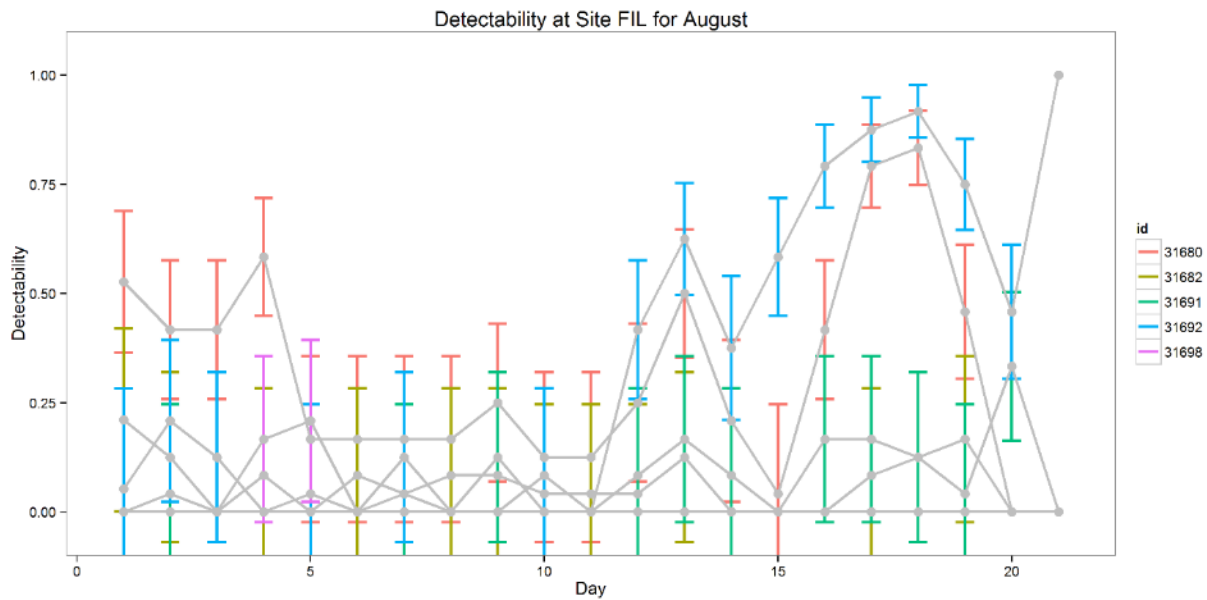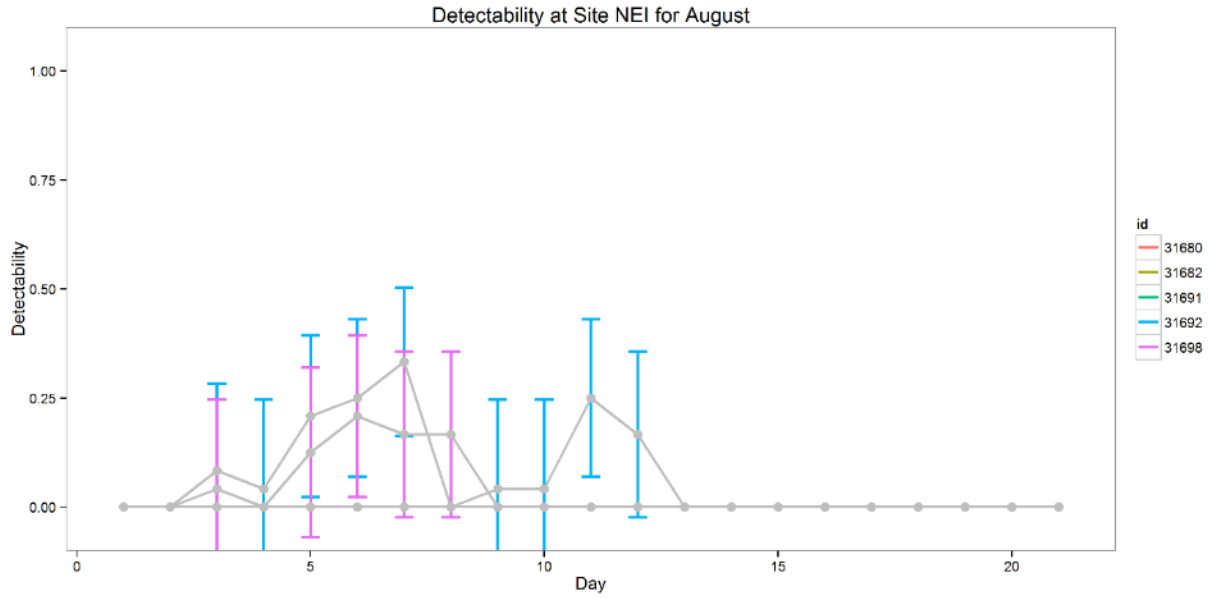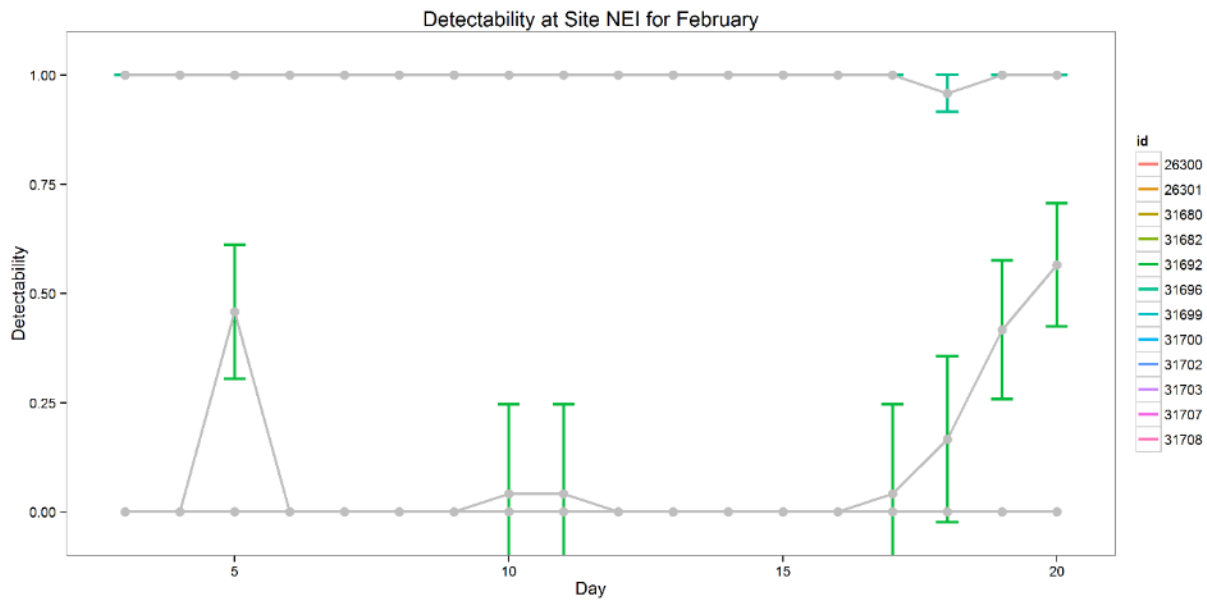
Figure 2.26. Daily mean Detectability at site NEI for fish IDs that were consistently detected throughout the winter period (3 February 2014 – 21 February 2014). The gray point represents the mean for each fish-day and the error bars indicate standard error.

A regression between velocity and cross stream gradient indicate high correlation for

during the winter period for both sites, REL ($R^2 = 0.976$) and FIL ($R^2 = 0.977$) where fish were

consistently detected (Table 2.5). Plots of 21 point weighted moving averages for both flow

variables across time further demonstrate the similarity of their patterns across all five sites

(Figs. 2.27 and 2.28). Weights are decreasing arithmetically from the center, where a weight of

10 was used. For GEE analyses, only velocity was used as a predictor variable, but any effects

noticed were treated as representative of both velocity and cross stream gradient metrics.+
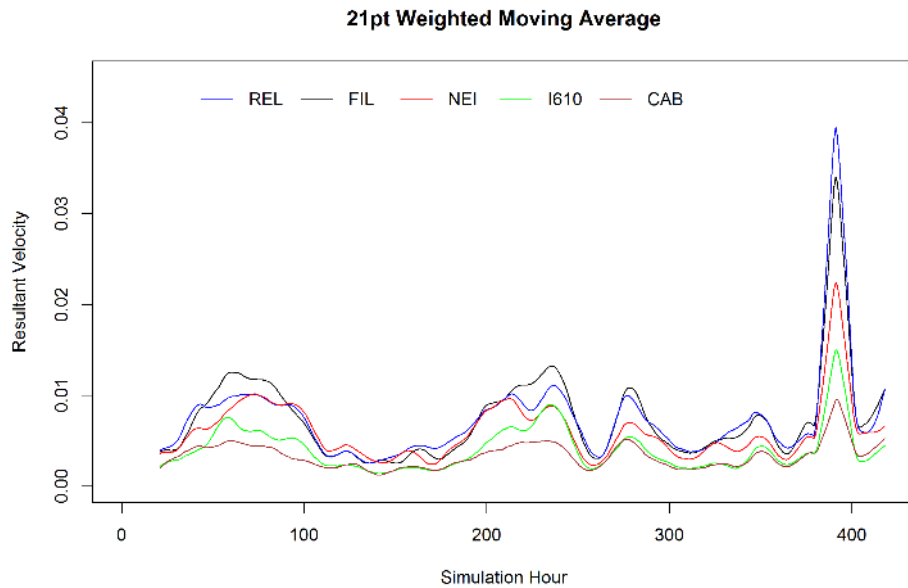
Figure 2.27. Twenty one-point weighted moving average for resultant magnitude of velocity m/s (referred to as velocity in the text) for each site during the winter simulation period. Weights decreased arithmetically from the center, where a weight of 10 was used.
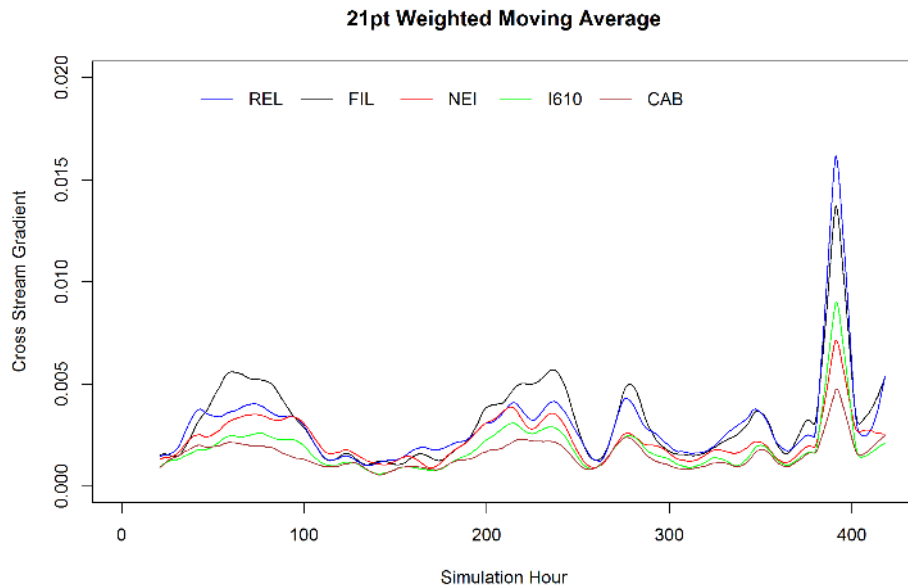
Figure 2.28. Twenty one-point weighted moving average with linear weighting for the horizontal derivative of velocity with respect to space m/s (referred to as cross stream gradient in the text) for each site during the winter simulation period. Weights decreased arithmetically from the center, where a weight of 10 was used.

During the winter period, GEEs were performed for two different sites (REL and FIL). Again the AR-1 correlation structure performed best for both models (Table 2.8). Temperature and day/night were the only variables remaining in the most parsimonious model for site REL (QICc=977.9; Table 2.9). Temperature had a positive correlation with Detectability at this site. Velocity and day/night were the only two variables in the most parsimonious GEE for site FIL (QICc=5,626; Table 2.10). Temperature had a negative correlation with Detectability at FIL. Mean detectability was higher at night for both sites for the winter period.

Table 2.8. Correlation structure results from the winter generalized estimating equations (GEEs). One GEE per site (REL and FIL) was analyzed. Each shared a similar structure with velocity, temperature, day/night period, and all one-way interactions were treated as predictor variables, and Detectability as a response variable. An AR-1 correlation structure performed best for both models.

Correlation Structure for the Winter Period

REL		FIL	
Structure	CIC	Structure	CIC
AR-1	***8.3***	AR-1	***20.3***
Exchangeable	18.2	Exchangeable	153.5
Independence	31.6	Independence	88.7

Table 2.9. Results of the most parsimonious model (QICc=977.91) from the pre-opening winter period generalized estimating equation (GEE) for site REL with an AR-1 correlation structure. Detectability was used as a response variable. Velocity, temperature, day/night period, and all one-way interactions were initially considered as predictor variables.

GEE Results Winter REL

	Estimate	SE
Intercept	-10.34	1.35
Temperature	0.52	0.10
Day/Night	0.84	0.24

Table 2.10. Results of the most parsimonious model (QICc=5,626.2) from the pre-opening winter period generalized estimating equation (GEE) for site FIL with an AR-1 correlation structure. Velocity, temperature, day/night period, and all one-way interactions were initially considered as predictor variables.

GEE Results Winter FIL

	Estimate	SE
Intercept	-0.42	0.30
Velocity	0.38	0.18
Day/Night	0.06	0.07

Response to Sector Gate Openings

For the summer period, the same four fish were used here as the *Fine Scale Detectability* section. The AR-1 correlation structure was determined best for the summer period by CIC (16.8 vs independence = 104, exchangeable = 20.3). The most parsimonious model included site, before/after sector gate opening, and an interaction between the two as predictor variables for Detectability (QICc=3046.4; Table 2.11). Mean Detectability was lower at site REL than site FIL for the summer period (Fig. 2.14 vs. Fig. 2.15; Table 2.11).

Table 2.11. Results from of the most parsimonious model (QICc=3,046.4) of the summer period sector gate opening generalized estimating equation (GEE). This model used Detectability as a response variable and before/after sector gate opening, day/night, site, and all one way interactions were treated as predictor variables.

GEE Results Summer Opening

	Estimate	SE
Intercept	-1.36	0.47
Site	-2.14	0.67
Open	-0.05	0.34
Site:Open	0.56	0.33

During the winter, the same 11 fish were used here as the *Fine Scale Detectability* section. There was some discrepancy when selecting the correlation structure. As with other information criterion, lower CIC scores suggests a better fit when choosing a proper correlation structure (Hin and Wang, 2009). However, a positive CIC value was obtained for exchangeable (52.5) and independence (121) and a negative CIC was obtained for AR-1 (-29.3). To aid in model selection, another information criterion value, quasi-log-likelihood under the independence model information criteria (QIC), a measure of fit for clustered, non-independent data that can select for best working correlation structures for GEEs was used (Pan, 2001). It may not be the most appropriate criterion for selecting among correlation structures, but it is still

commonly used (Hin and Wang, 2009). All QIC values for these GEEs were positive. The QIC

for AR-1 was more than an order of magnitude higher for these models, suggesting a much

poorer fit (AR-1 = 207,697; independence = 7,956; exchangeable = 7,849). To further aid in

model selection, a GLMM with a binomial error structure and logit link with a similar design

were created and compared to all GEEs in this section. Detectability was the response, site,

before/after opening, day/night, and all one-way interactions were treated as fixed effects, while

id and day were treated as random effects. Parameter estimates were similar among the winter

sector gate response GEE with an exchangeable correlation structure, the GEE with an

independence correlation structure and the GLMM (Table 2.12). All parameter estimations from

the GEE with an exchangeable correlation structure, the GEE with an independence correlation

structure, and the GLMM were all within one standard error. However, there was an order of

magnitude difference in parameter estimation between the winter GEE with an AR-1correlation

structure, the GLMM, and both of the other GEEs (Table 2.12). The GEE with an exchangeable

correlation structure was used here because of the negative CIC score associated with the AR-1

structured GEE, much lower QIC score, and similarities between it and the GLMM. Results

from this GEE indicate that no terms could be removed (QICc=7,849.3; Table 2.12). Higher

mean Detectability was observed at night, at site FIL, and before the sector gate opening (Table

2.12). Higher mean Detectability for REL at night and higher mean Detectability for REL after

the opening were also indicated by this model (Table 2.12).

Table 2.12. Results comparing all correlation structures for generalized estimating equations (GEEs) and a generalized linear mixed model (GLMM) for winter sector gate opening effects. Each GEE shared a similar design with Detectability treated as a response variable and before/after sector gate opening, day/night, site, and all one way interactions treated as predictor variables. Two different criteria (correlation information criterion, CIC, and quasi-log-likelihood under the independence model information criteria, QIC) were used to test for the best correlation structure among the GEEs. Ambiguous results for were found, so a GLMM was created to compare parameter estimates. The GLMM had Detectability as the response, site, before/after opening, day/night, and all one-way interactions as fixed effects, while fish id and day were treated as random effects. It can be seen here that parameter estimations for the Independence and exchangeable structured GEEs and the GLMM were similar, while the AR-1 structure was different by over an order of magnitude. The GEE with an exchangeable correlation structure was selected because it had the lowest QIC, the lowest positive CIC, and had similar parameter estimations to the GLMM and Independence GEE. The most parsimonious model (QICc = 7,849) included all parameters and corresponds to the upper left quadrant.

Winter Sector Gate Opening Comparison

GEE: Exchangeable (CIC= 52.5; QIC=7,849)					GEE: Independence (CIC=121; QIC=7,956)				
	Estimate	SE	Wald	*p*		Estimate	SE	Wald	*p*
Intercept	-2.02	0.61	10.84	*<0.001*	Intercept	-1.94	0.61	10.31	*0.001*
Site	1.11	0.74	2.24	0.134	Site	0.81	0.75	1.17	0.280
Open	1.66	0.60	7.73	*0.005*	Open	1.64	0.57	8.17	*0.004*
Day/Night	0.27	0.12	4.86	*0.027*	Day/Night	0.27	0.12	4.91	*0.027*
Site:Open	-4.25	0.77	30.24	*<0.001*	Site:Open	-4.49	0.76	34.63	*<0.001*
Site:Day/Night	0.62	0.16	15.52	*<0.001*	Site:Day/Night	0.75	0.17	20.56	*<0.001*
GEE: AR-1 (CIC=-29.3; QIC=207,697)					GLMM				
	Estimate	SE	Wald	*p*		Estimate	SE	Z-value	*p*
Intercept	2.37E+15	8.64E+14	7.5	*0.006*	Intercept	-2.62	0.40	-6.51	*<0.001*
Site	-1.12E+17	1.00E+15	1.23E+04	*<0.001*	Site	0.93	0.20	4.64	*<0.001*
Open	3.28E+14	3.61E+14	0.82	0.364	Open	2.34	0.27	8.74	*<0.001*
Day/Night	-5.02E+14	8.59E+13	34.1	*<0.001*	Day/Night	0.30	0.07	4.30	*<0.001*
Site:Open	2.64E+16	7.26E+14	1.32E+03	*<0.001*	Site:Open	-5.10	0.21	-23.99	*<0.001*
Site:Day/Night	1.06E+16	1.03E+14	1.06E+04	*<0.001*	Site:Day/Night	0.77	0.16	4.68	*<0.001*

Discussion

During the summer pre-opening period, Red Drum in BSJ exhibited a strong behavioral response to small wind driven subtidal current velocities. The largest effect sizes for any parameter/model combination were observed at sites REL and FIL for the summer pre-opening period. In unimpounded natural systems, tidal periodicities and salinity were found to be strong predictors of Red Drum behavior (Dresser and Kneib, 2007; Bacheler et al., 2009). One study found that individuals repeated the same movement behaviors during large daytime tidal shifts (>1 m per tidal shift; Dresser and Kneib, 2007). A possible explanation given was that high tides made foraging habitat available that is either subaerial or too shallow during lower tides. Across the 18 day summer pre-opening period, the range of elevations was 0.2 m and the total salinity change was 1.3. With these changes it is unlikely that any observed response to velocity was due to newly available habitat or a response to salinity. However, the effect size for velocity for both REL and FIL pre-opening models were an order of magnitude larger than the next best variable. This relatively strong positive response indicates a response to small current velocities without the effects of a change in salinity and solar-lunar tidal effects.

I did not observe as strong of a response to velocity during the winter pre-opening time period. A potential explanation of these results could be fish response to cold fonts. The velocity parameter was not included in the most parsimonious GEE at site REL, but temperature was included, albeit with a small effect size. Velocity was included in the most parsimonious model for site FIL, but the effect size was small. Temperature was not included for site FIL. Cold fronts cause temperatures to decrease and winds (including wind induced current velocities) to increase. Wind is the major factor determining the hydrodynamics within BSJ (see Chapter 1 for details). The relationships between temperature and velocity at both sites during the winter

110

could be due to cold front effects. Two cold fronts occurred during the winter period from simulation hours 22-85 and 166-240. Their effects increased both velocity and cross stream gradient (Figs. 2.27 and 2.28). In both cases, the highest velocities and cross stream gradients outside of sector gate openings occurred during these two events at FIL. A positive correlation between mean detectability at FIL and velocity was observed. For site REL, a positive correlation between mean detectability and temperature was observed. This could indicate a behavioral response to cold fronts. If true, then it could be inferred that fish prefer FIL over REL during these high energy events.

Mixed results from the sector gate opening models could be due to different biotic and abiotic conditions for each event. Unlike pre-opening conditions, higher velocities were observed at site REL during sector gate openings. Therefore, an increase in detectability at site REL following a sector gate opening could be a response to high flows associated with these events. Higher mean Detectability was observed for REL after the opening for the winter period, suggesting that fish were detected at this location more often after the event. A potential reason for this could be the flushing event attracted fish to this site. Attractant flows have been suggested as being important cues for many different fish species (Schmettering and McEvoy, 2000). In contrast, lower mean detectability was observed at REL after the sector gate opening during summer opening. Higher and longer flows during the winter opening may be why there was an increase in Detectability observed then, but not during summer. A short term increase of marine fish species richness was observed following both sector gate openings (Chapter 3). One of the fishes, Gulf Menhaden (*Brevoortia patronus*), was observed in high abundances immediately following the winter sector gate opening. Gulf Menhaden has been suggested as an important prey item that Red Drum have selected for in the wild (Scharf and Schlight, 2000).

In a previous study, Red Drum movement patterns and detections were not associated with available prey in BSJ (Smith, 2012). Of nine total Red Drum captured in BSJ, only one fish stomach contained actual prey items and these were Blue Crabs (*Callinectes sapidus*; Brogan 2010; Smith, 2012; Smith, unpublished data). Blue Crabs are somewhat rare in the Bayou as they only were collected via seine and baited minnow traps (modified to target crabs) twice in five years (Smith, 2012; Smith, unpublished data). It has been postulated that these results may indicate a lack of adequate foraging opportunities in BSJ under normal conditions. It could be that high energy, long openings corresponding with times when potential prey items are in high abundance are necessary for fish to respond and potentially orient to the flow. These conditions and increased detectability near the sector gate were observed only for the winter opening.

The summer sector gate opening introduced low salinity water into BSJ and this could have deterred a shift in habitat preference similar to that observed in winter. Red Drum spawn in the late summer and fall near tidal passes. Due to the buoyancy of newly broadcast eggs, salinities above 20 PSU could greatly increase spawning success for Red Drum (Peters and McMichael Jr 1987, Brown et al., 2004). Low salinities in BSJ may prevent successful spawning in BSJ. Based on total length measurements and previous studies relating size to age and maturity, many, if not most or all, of the tagged fish in BSJ could have been at or near spawning size/age during the summer sector gate opening (Boothby and Avault Jr, 1971). A sector gate opening releasing fresher water into the Bayou may have deterred spawning capable fish from the attractant flow. It would be interesting to compare the behavior observed here to a sector gate opening during spawning season when salinities were higher in Lake Pontchartrain than BSJ.

One of the concerns was that Red Drum would escape from the Bayou during sector gate openings. Prior to any sector gate opening, four fish that were transplanted into BSJ were observed outside of the Bayou. Three fitted with external dart tags were recaptured outside of BSJ. Two of these fish were recaptured within the same area of Rigolets Pass, approximately 50 km through water from the mouth of BSJ. One was recaptured near Seabrook Inlet in Lake Pontchartrain, approximately 6 km through water from the mouth of BSJ. Additionally, a telemetry tagged fish, ID 31693, was detected as a part of another VEMCO receiver array maintained by the Louisiana Department of Wildlife and Fisheries (LDWF) approximately 35 km from BSJ in the eastern part of Lake Pontchartrain. With the sector gate closed, a 91.44 cm sluice valve is the largest opening available for fish to escape. A head differential is typically maintained with higher water surface elevations in Lake Pontchartrain than in BSJ. It is also typical for sluice valves to not be opened completely nor for long periods of time. Observed escapement under normal conditions caused concern for potential escapement during a sector gate opening. However, no evidence of escapement was observed. All fish that were detected before openings were subsequently detected in BSJ afterwards and none were detected as a part of LDWF's extensive VEMCO receiver array in Lake Pontchartrain.

The high site fidelity and decreased actively at night quantified here corroborate previous findings (Adams and Tremain, 2000; Dresser and Kneib, 2007). Mean sedentariness was high, above 50% for all fish x month-year combinations except one, suggesting that most of the time fish stayed within one receiver's range and were inactive. This could be indicative of Red Drum's small home range and high site fidelity (Matlock, 1987; Adams and Tremain, 2000; Dresser and Kneib, 2007). Other studies, based on mark-recapture data, have suggested high levels of site fidelity for this species (Adams and Tremain, 2000; Dresser and Kneib, 2007).

However, this study represents the first ever quantification of inactivity at the behavioral level. Sedentariness was lower during the day, suggesting fish were more active during the day, which is similar to previous findings (Dresser and Kneib, 2007).

A non-linear pattern of Detectability and Sedentariness across time was observed graphically with both a potential a seasonal pattern (Figs. 2.3-2.7). Month-year was also found to be an important fixed effect for both Detectability and Sedentariness. No attempts were made here to determine the nature of this relationship, because of a lack of data across years (i.e, 18 months instead of multiple years). If a larger dataset were available, then estimating potential non-linear and/or seasonal trends may be possible. Higher mean detectability and lower sedentariness was observed in the fall months. These metrics, especially a lower mean Sedentariness, could be indicative of increased activity. They also coincide with spawning times, which peak in the late summer through the fall (Matlock, 1987; Wilson and Nieland, 1994). These potential increases in activity could be related to some type of spawning behavior. The exact nature of this behavior is difficult to interpret as none of the site locations represent what could be considered adequate spawning habitat for Red Drum, but may be an important consideration for future studies. This is especially important if a gate opening in the fall when salinities are higher in Lake Pontchartrain than BSJ is considered.

This study demonstrates that Red Drum, a mid-trophic level estuarine dependent fish, exhibited high site fidelity, distinct patterns of activity across a large temporal scale, and their response to subtidal flow. These findings are absent of large (or any) tidal periodicity, variation in distance from shore, and salinity fluctuation all of which have been shown to be influential abiotic factors determining their distribution and behavior (Dresser and Kneib 2007, Bacheler et al., 2009). The semi-natural state of BSJ essentially removed these effects, allowing for a more

controlled test of behavior across a large temporal scale, response to changes in flow and

temperature on a fine scale, and diurnal/nocturnal behaviors.

References Cited

Adams, DH, and DM Tremain. 2000. Association of large juvenile Red Drum, *Sciaenops ocellatus*, with an estuarine creek on the Atlantic coast of Florida. *Environmental Biology of Fishes* 58: 183-94.

Andrews, KS, GD Williams, and PS Levin. 2010. Seasonal and ontogenetic changes in movement patterns of Sixgill Sharks. *PLoS ONE* 5(9): e12549. doi:10.1371/journal.pone.0012549.

Bacheler, NM, LM Paramore, JA Buckel, and JE Hightower. 2009. Abiotic and biotic factors influence the habitat use of an estuarine fish. *Marine Ecology Progress Series* 377: 263-77.

Bass, RJ, and JW Avault, Jr. 1975. Food habits, length-weight relationship, condition factor, and growth of juvenile ed Drum, *Sciaenops ocellatus*, in Louisiana. *Transactions of the American Fishery Society* 104.1: 35-45.

Beckman, DW, CA Wilson, and AL Stanley. 1988(b). Age and growth of Red Drum, *Sciaenops ocellatus*, from offshore waters of the northern Gulf of Mexico. *Fishery Bulletin* 81: 17-28.

Boothby, RN, and JW Avault, Jr. 1971. Food habits, length-weight relationship, and condition factor of the Red Drum (*Sciaenops ocellata*) in southeastern Louisiana. *Transactions of the American Fisheries Society* 100.2: 290-95.

Brogan, SJ. 2010. Red Drum (*Sciaenops ocellatus*) Habitat use in an urban system; behavior of reintroduced fish in Bayou St. John, New Orleans. Thesis. University of New Orleans.

Brown, C. A., S. A. Holt, G. A. Jackson, D. A. Brooks, and G. J. Holt. "Simulating Larval Supply to Estuarine Nursery Areas: How Important Are Physical Processes to the Supply of Larvae to the Aransas Pass Inlet?" *Fisheries Oceanography* 13.3 (2004): 181-96. Print.

Coastal Protection and Restoration Authority (CPRA). 2012. Louisiana's Comprehensive Master Plan for a Sustainable Coast (Final): 2012 Coastal Master Plan. http://www.coastalmasterplan.louisiana.gov/.

Dresser, BK, and RT Kneib. 2007. Site fidelity and movement patterns of wild subadult Red Drum, *Sciaenops ocellatus* (Linnaeus) within a salt marsh-dominated estuarine landscape. *Fisheries Management and Ecology* 14: 183-190.

Højsgaard, S, U Halekoh, and J Yan. 2006. The R Package geepack for generalized estimating equations. *Journal of Statistical Software* 15.2: 1-11.

Kuznetsova, A, PB Brockhoff and RHB Christensen (2014). lmerTest: Tests in Linear Mixed Effects Models. R package version 2.0-20. http://CRAN.R-project.org/package=lmerTest.

Layman, CA, DA Arrington, RB Langerhans, and BR Silliman. 2004. Degree of fragmentation affects fish assemblage structure in Andros Island (Bahamas) estuaries. *Caribbean Journal of Science* 40.2: 232-244.

Lellis-Dibble, KA, KE McGlynn, and TE Bigford. 2008. Estuarine Fish and Shellfish Species in U.S. Commercial and Recreational Fisheries: Economic Value as an Incentive to Protect and Restore Estuarine Habitat. U.S. Dep. Commerce, NOAA Tech. Memo. NMFSF/SPO-90, 94 pp.

Lowe, CG, DT Topping, DP Cartamil, and YP Papastamatiou. 2003. Movement patterns, home range, and habitat utilization of adult Kelp Bass *Paralabraz clathratus* in a temperate no-take marine reserve. *Marine Ecology Progress Series* 256: 205-16.

Matlock, GC, 1987. The life history of the Red Drum, pp. 1-47 in Manual of Red Drum Aquaculture, edited by G.W. Chamberlain, R.J. Miget and M.G. Haby. Texas Agricultural Extension Service and Sear Grant College Program, Texas A&M University, College Station, Texas.

McEachron, LW, RL Colura, and BW Bumguardner. 1998. Survival of Stocked Red Drum in Texas. *Bulletin of Marine Science* 62.2: 359-68.

Muthukumarana, S, CJ Schwarz, and TB Swartz. 2008. Bayesian analysis of mark-recapture data with travel time-dependent survival probabilities. *The Canadian Journal of Statistics* 36.1: 5-28.

Pearson, JC 1928. Natural history and Conservation of Redfish and other Commercial Sciaenids on the Texas Coast. *Bulletin of U.S. Bureau of Fisheries* 44:129-214.

Peters, KM, and RH McMichael, Jr. 1987. Early life history of the Red Drum, *Sciaenops ocellatus* (Pisces: Sciaenidae), in Tampa Bay, Florida. *Estuaries* 10.2: 92-107.

R Core Team (2015). R: A language and environment for statistical computing. R Foundation for Statistical Computing, Vienna, Austria. URL http://www.R-project.org/.

Scharf, FS, and KK Schlight. 2000. Feeding habits of Red Drum (Sciaenops ocellatus) in Galveston Bay, Texas: seasonal diet variation and predator-prey size relationships. *Estuaries* 23.1: 128-39.

Schmetterling, DA, and DH McEvoy. 2000. Abundance and diversity of fishes migrating to a Hydroelectric Dam in Montana. *North American Journal of Fisheries Management* 20: 711-719.

Schwarz, GE. 1978. Estimating the dimension of a model. *The Annals of Statistics* 6.2: 461-464.

Smith, PW. 2012. Fish assemblage dynamics and Red Drum habitat selection in Bayou St. John and associated urban waterways located within the city of New Orleans, Louisiana. Thesis. University of New Orleans.

Thomas, RG. 1991. Environmental factors and production characteristics affecting the culture of red drum, *Sciaenops ocellatus*. Dissertation. Louisiana State University.

Valentine-Rose, L, JA Cherry, JJ Culp, KE Perez, JB Pollock, DA Arrington, and CA Layman. 2007. Floral and faunal differences between fragmented and unfragmented Bahamian tidal creeks. *Wetlands* 27.3: 702-718.

Wetherbee, BM, SH Gruber, and RS Rosa. 2007. Movement patterns of juvenile Lemon Sharks *Negaprion brevirostris* within Atoll Das Rocas, Brazil: a nursery characterized by tidal extremes. *Marine Ecology Progress Series* 343: 283-93.

Wilson, CA and DL Nieland. 1994. Reproductive biology of Red Drum, *Sciaenops ocellatus*, from the neritic waters of the northern Gulf of Mexico. *Fishery Bulletin* 92(4): 841-850.

Zeller, DC. 1999. Ultrasonic Telemetry: its application to coral reef fisheries research. *Fishery Bulletin* 97.4: 1058-1065.

Chapter 3

Response of Fishes to Two Restoration Projects in Bayou St. John and City Park Lagoons, Estuarine Urban Waterways in New Orleans, Louisiana

Introduction

Estuaries include essential habitat for many fish and shellfish species (Lellis-Dibble et al., 2008). Many of these species are economically important, with approximately 68% of commercial fishery landings in the United States by value being estuarine species (Lellis-Dibble et al., 2008). Reducing connectivity through impoundment or fragmentation (or both) can negatively affect estuarine ecosystem functioning and related fisheries (Llanso *et al*., 1998; Layman et al., 2004; Valentine-Rose et al., 2007). Fragmentation restricts tidal flow, which can be a primary determinant of estuarine community structure (Warren et al., 2002). Fragmented estuaries often contain more freshwater plant and animal assemblages and can lack estuarine dependent fishes common in nearby, unfragmented waterways (Layman et al., 2004; Valentine-Rose et al., 2007). However, restoring waterway connectivity properly can increase diversity and partially restore ecosystem function (Llanso et al., 1998; Warren et al., 2002; Layman et al., 2005).

Many anthropogenic impacts have affected Bayou St. John (BSJ) and City Park Lagoons (CPL) over the past 300 years, since the founding of New Orleans (Ward, 1982). These waterways have been dredged, dammed, pumped, cemented, channelized, shortened, lengthened, widened, narrowed, and disconnected from and reconnected to various natural and artificial waterways (Ward, 1982; Brogan, 2010). Currently, there is a series of pumps, culverts, sluice valves, butterfly valves, storm water drains, and diversions that control water flow in, out, and throughout this aquatic system. Recent initiatives have been put in place to help improve these

severely altered fragmented estuarine waterways (Brogan, 2010; BKI, 2011; Schroeder, 2011; Smith, 2012; Chapter 1).

A previous study on fish assemblages in BSJ and CPL suggested that some significant decreases in taxonomic diversity occurred following Hurricanes Katrina and Rita (Smith, 2012). I (Smith, 2012) found that the shoreline fish assemblages in CPL had lower than expected taxonomic diversity for two years following the Hurricanes in 2005. These assemblages rebounded and remained stable from 2008 – 2010. Shoreline fish assemblages in BSJ remained stable, with lower than expected taxonomic diversity across sampling methods and years. Only data since 2008 was used here because of the changes observed in a previous study (Smith, 2012).

Broadly, the goals of this study were to determine the response of shoreline fish assemblages in BSJ and CPL to management activities associated with the adaptive water management plan for this aquatic system. I wanted to determine if shoreline fish assemblages were affected by the removal of an outdated flood control structure and if there was a response in the diversity of fish guilds as a result of experimental flood gate openings. More specifically, I asked:

1. Did fish assemblages change after the removal of an outdated waterfall structure that impeded exchange between Bayou St. John and Lake Pontchartrain? If so, which species contributed most to the difference and was there a correlation between different assemblages and water quality parameters? Also, were there differences in assemblages across sampling sites?

2. How did flood gate openings affect fish guild species richness? Was there a change in species richness of freshwater, estuarine, or marine fishes? Were the changes

similar across all sampling sites? Were these changes associated with the amount of time passed since the last flood gate opening?

Materials and Methods

Study Area

Bayou St. John is an urban waterway located in the north-central portion of the City of New Orleans, Louisiana (Fig. 3.1). Much of its banks have been stabilized by concrete and it is surrounded by houses and roadways with 16 bridges crossing it. It is approximately 6.5 km long and for most of its length has a north-south orientation. The width of the Bayou varies from 45 m to 200 m. Average depth is approximately 2.5 m, with the northern section (north of I610) being significantly deeper and wider than the southern section (Martinez et al., 2008; Brogan, 2010). The northern extremity is partially connected to Lake Pontchartrain via a sector gate (30 1' 27.32" N, -90 4' 58.33" E). The most southern point ends at the corner of Jefferson Davis Parkway and Lafitte Street (29 58' 23.9" N, -90 5' 28.53" E). Its connection with Lake Pontchartrain provides BSJ with brackish water (salinity range ~ 1.5 to 8).
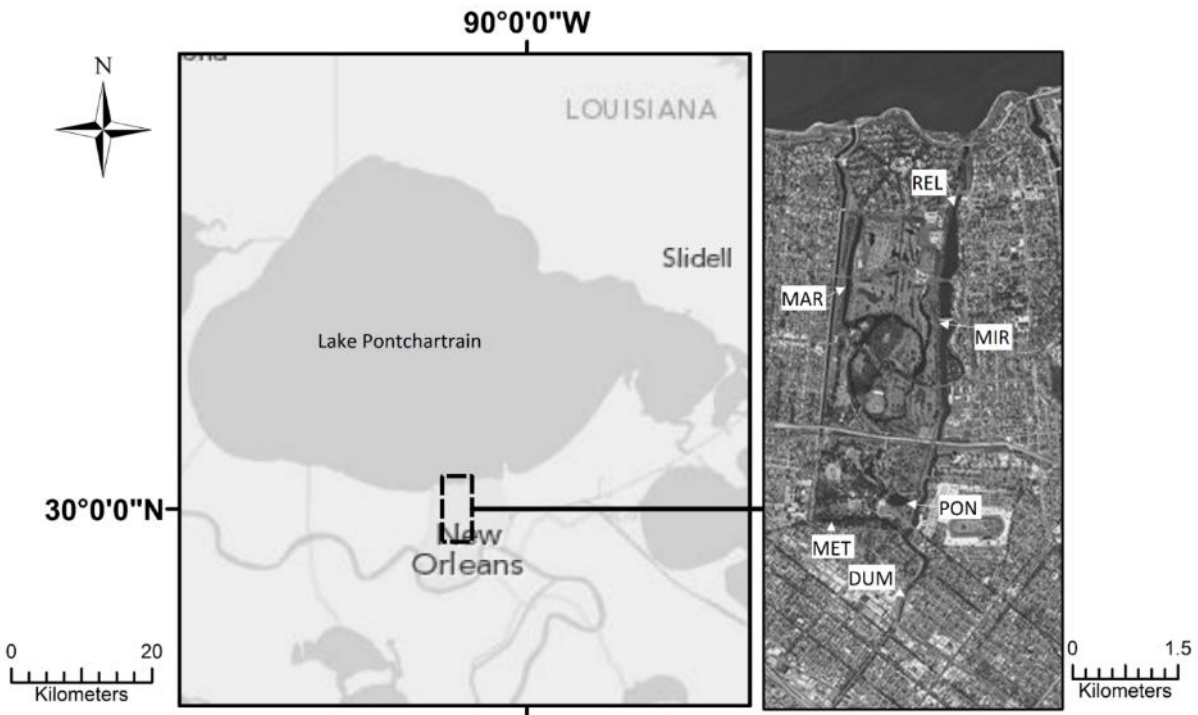
Figure 3.1. Map showing the study area, its location in Southeastern Louisiana, and seining site locations. As can be seen in the larger map, both Bayou St. John and City Park Lakes and Lagoons are located within the New Orleans, LA City Limits. The six seine sites are designated with a three letter label. Three seining sites are located in Bayou St. John (REL, MIR, DUM) and three are located in the City Park Lagoons (MAR, PON, MET). Note the amount of urbanization along the waterways on the aerial photograph on the right. Also, note Bayou St. John's connection with Lake Pontchartrain to the north and its abrupt ending to the south. This figure was created using ArcMap 10.1.

Field Methods

From January 2008 through July 2014, UNO Nekton Research Laboratory personnel from UNO sampled six sites within BSJ and CPL monthly using a 4.57 x 1.83 m beach seine with 0.95 cm mesh (Fig 3.1). Three sites were located in BSJ (Robert E. Lee [REL], Mirabeau [MIR], and Dumaine [DUM]), and three in CPL (Marconi [MAR], Metairie Bayou [MET], and Pontchartrain Lagoon [PON]). These samples were geared towards assemblage analyses by using three standardized seine hauls per site each month with data recorded for each haul. Salinity, conductivity, specific conductivity, and temperature were recorded for each haul using an YSI 30 handheld conductivity meter. A total of 1,373 samples were collected. All fishes

were counted and identified to species in the field. A sub-sample of fishes was euthanized in an ice water bath as part of a separate study, per UNO-IACUC protocol (UNO – IACUC # 09-015). All other fishes were released.

Data Analysis

To determine any changes in fish assemblages after the removal of the waterfall structure, I conducted analysis of similarity (ANOSIM) using PRIMER v6 Software (Clarke, 1993; Clarkeand Gorley, 2006). To minimize seasonal effects, which are common in estuarine fish assemblages (O'Connell *et al.*, 2014), I only compared collections within each season. I determined seasons by using agglomerative hierarchical clustering with group-average linking (Kaufman and Rousseeuw, 1990; Clark and Warwick, 2001). This method clustered like month groups based upon similar fish assemblages. After this, collections made from January 2008 – April 2013 were compared to collections from May 2013 – July 2014 to test if there were any assemblage changes after removal of the outdated flood control structure. All species count data were square root transformed to minimize the effects of rare species and Bray-Curtis similarity indices were generated. For each season, a two-factor crossed ANOSIM was performed, before and after flood control structure removal and site to test for significant differences ($\alpha = 0.05$). Samples that included less than two species were removed for all analyses. This created unequal sampling size, but two-factor crossed ANOSIM designs are robust to minor amounts of missing data (Clarke and Warwick, 2001). For any significant differences in before and after waterfall removal, a two-dimensional non-metric multidimensional scaling (MDS) plot was created to visualize the separation, similarity percentages routines (SIMPER), and biota – environmental stepwise routines (BEST) were performed. SIMPER tests determine which species from the

assemblages are driving differences. I used a backward eliminating BEST procedure to correlate environmental parameters (temperature and salinity) with assemblage data.

Changes in species richness were analyzed during the time period from the initial sector gate opening (19 August 2013) until the end of the study (31 July 2014) to test for any differences in fish guilds. Fishes were assigned to one of three possible guilds *a priori* (Freshwater, Estuarine, Marine; Table 3.1). Nordlie (2003) and Able and Fahay (2010) were the primary sources used for guild assignment. Both of these sources and many others use more classifications than in the present study (e.g., Nordlie, 2003 uses seven guilds). Here, I use three guilds for two reasons: 1. The spatial scale of the current study is smaller and has lower diversity and 2. The objective of this study is not to describe the ecological function of fishes in BSJ across time; it is to determine if changes in species richness for any guild is associated with sector gate openings. Fishes that primarily complete their entire lifecycle in freshwater habitats were classified as Freshwater; fishes that have been shown to complete their entire lifecycle in estuaries were classified as Estuarine; and fishes that require marine habitats to complete their lifecycle were classified as Marine. Estuarine dependent fishes (e.g., Red Drum, *Sciaenops ocellatus*) were categorized as Marine. Fishes that opportunistically use estuaries (e.g., Leatherjack, *Oligoplites saurus*), but often complete their entire lifecycle in marine environments were categorized as Marine. Only fishes that have been shown to complete their entire life cycle in estuarine environments were categorized as Estuarine. For all but one species, Atlantic Needlefish (*Strongylura marina*), there was little ambiguity using these criteria. Its classification differed between the two primary sources. Fahay and Able (2010) described it as an estuarine resident, while Nordie (2003) admitted controversy, but categorized them as Marine Transient.

For this study *S. marina* was categorized as Estuarine because of the strict requirement that Marine fishes require marine habitats.

One Generalized Linear Mixed Model (GLMM) per guild was used to compare species richness with sector gate openings. They were designed to test for significant differences in the number of fish species among sites and time since the last sector gate opening. Statistical tests for Freshwater and Estuarine guilds shared a similar design. The number of fish species per guild was the response variable, site location was treated as a fixed predictor variable, and season and time since last opening were treated as random predictor variables. A similar design was considered for the Marine guild, but Marine species were only collected at one site (REL) during this time period. For the Marine GLMM, the number of Marine species at REL was used as a response variable. Time since last opening and season were treated as random predictor variables. Likelihood ratio chi-square tests were performed comparing models with and without the random time since last opening effect ($\alpha = 0.05$). For each GLMM, a Poisson error distribution with logit link was used. Laplace approximations were used to approximate each parameter (Bolker et al., 2008). All GLMMs were performed in R ver. 3.1.1, the lme4 package, and the glmer() function (Bates et al., 2014; R Core Team, 2014).

Results

Samples were categorized into two different seasons. January, February, March, September, October, November, and December clustered together and are hereto referred to as the "Cool Season". April, May, June, July, and August clustered together and are hereto referred to as the "Warm Season". Six hundred and sixty-one samples were analyzed from the Cool Season and 564 samples were analyzed from the Warm Season. A total of 29 species were collected, 19 of which were collected during both seasons. Gulf Menhaden (*Brevoortia*

patronus), Yellow Bass (*Morone mississippiensis*), Hybrid Striped Bass (*Morone saxatalis x chrysops*), Black crappie (*Pomoxis nigromaculatus*), Pinfish (*Lagodon rhomboides*), and Spot (*Leiostomus xanthurus*) were only collected in the Cool Season, while Atlantic Needlefish, Redspotted Sunfish (*Lepomis miniatus*), Leatherjack, and Spotted Seatrout (*Cynoscion nebulosus*) were only collected during the Warm Season (Table 3.1).

Table 3.1. List of species sampled monthly using a seine net January 2008 through July 2014. The Cool Season is January – March and September – December, and the Warm Season is April – August. Each fish was divided into one of three guilds (Freshwater, Estuarine, or Marine) based upon life history traits from a literature review.

Species	Cool Season	Warm Season	Guild
Lepisosteus oculatus	X	X	Freshwater
Anchoa mitchilli	X	X	Estuarine
Brevoortia patronus	X		Marine
Dorosoma petenense	X	X	Freshwater
Menidia beryllina	X	X	Estuarine
Strongylura marina		X	Estuarine
Fundulus chrysotus	X	X	Freshwater
Fundulus grandis	X	X	Estuarine
Lucania parva	X	X	Freshwater
Gambusia affinis	X	X	Freshwater
Heterandria formosa	X	X	Freshwater
Poecilia latipinna	X	X	Estuarine
Cyprinodon variegatus	X	X	Estuarine
Syngnathus scovelli	X	X	Estuarine
Morone mississippiensis	X		Freshwater
Morone saxatalis x chrysops	X		Freshwater
Lepomis gulosus	X	X	Freshwater
Lepomis macrochirus	X	X	Freshwater
Lepomis microlophus	X	X	Freshwater
Lepomis miniatus		X	Freshwater
Micropterus salmoides	X	X	Freshwater
Pomoxis nigromaculatus	X		Freshwater
Oligoplites saurus		X	Marine
Lagodon rhomboides	X		Marine
Cynoscion nebulosus		X	Marine
Leiostomus xanthurus	X		Marine
Gobiosoma bosc	X	X	Estuarine
Microgobius gulosus	X	X	Estuarine
Herichthys cyanoguttatus	X	X	Freshwater
Total	**25**	**23**	

For the Cool Season, there were significant differences among site groups (Global R = 0.191, p = 0.001). Each pairwise test between site groups were also significantly different (ANOSIM, Global R > 0.071, p = 0.001). There was also a significant difference between fish assemblages before and after removal of the outdated flood control structure (ANOSIM, Global R = 0.044, p = 0.039). In an MDS plot, clear separation between groups is not apparent (Fig. 3.2). SIMPER analysis suggests that ten fish species were found to be driving the difference between these groups, with Rainwater Killifish (*Lucania parva*), Bluegill (*Lepomis macrochirus*), Rio Grande Cichlid (*Herichthys cyanoguttatus*), and Least Killifish (*Heterandria formosa*) having a higher average abundance after the removal of the structure. Inland Silverside (*Menidia beryllina*), Naked Goby (*Gobiosoma bosc*), Western Mosquitofish (*Gambusia affinis*), Largemouth Bass (*Micropterus salmoides*), and Gulf Pipefish (*Syngnathus scovelli*) all were drivers and had lower average abundances after removal (Table 3.2). BEST analysis found the strongest relationship between fish assemblages and salinity only ($\rho = 0.08$, p = 0.001). The mean salinity during the Cool Season across sites before removal was 2.6 and after removal was 1.9.
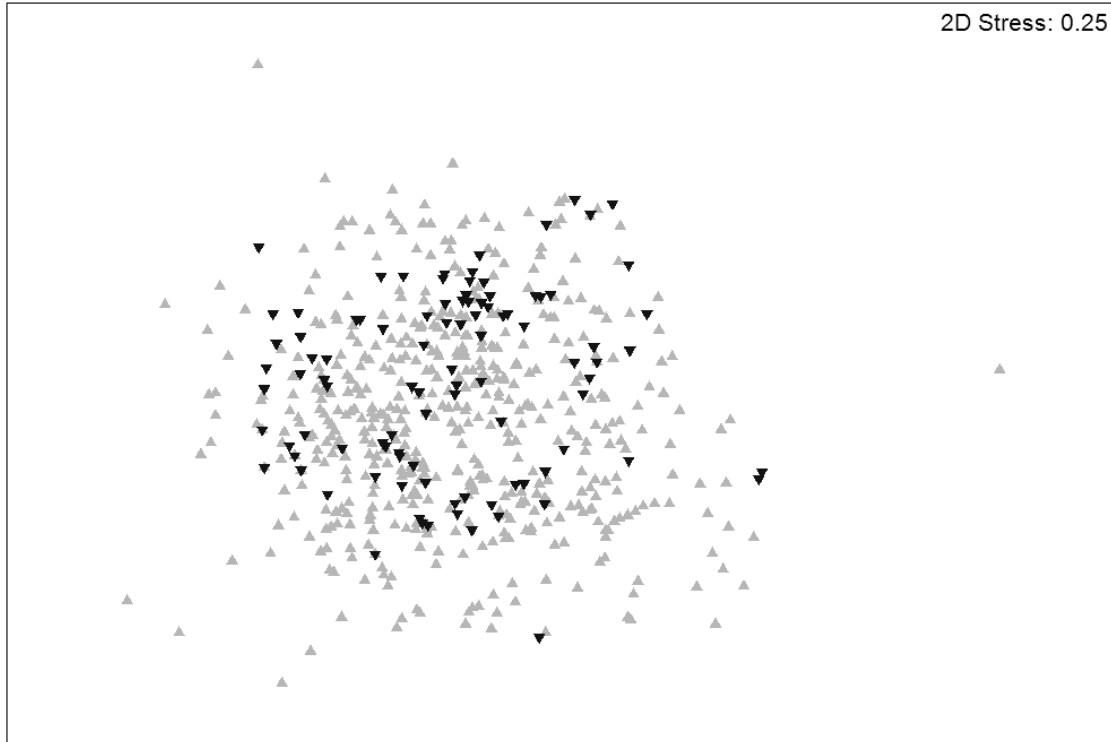
Figure 3.2. Non-metric multidimensional (MDS) plot showing samples before (gray up-arrow) and after (black down-arrow) the removal of an outdated flood control structure. Samples closer together are more similar. Clear separation would be indicated by clustering of samples. There is no apparent clustering of samples before or after the removal of the flood control structure.

Table 3.2. Before and after flood control structure removal average abundances, percent contribution to assemblage change, and cumulative percent contribution to assemblage change are shown. Note that both average abundance columns are based on the square root transformed dataset. These results are based on SIMPER analysis for the Cool Season. Note that all values were rounded to the nearest 0.01, this results in some cumulative percent contributions to not appear to be additive, when they are.

Species	Before removal average abundance	After removal average abundance	Percent contribution to assemblage change	Cumulative percent contribution to assemblage change
Lucania parva	2.16	3.80	22.22	22.22
Lepomis macrochirus	2.56	3.10	18.53	40.74
Menidia beryllina	1.10	0.25	12.26	53.00
Gobiosoma bosc	0.55	0.40	10.31	63.31
Gambusia affinis	0.35	0.10	8.77	72.08
Herichthys cyanoguttatus	0.08	0.24	5.80	77.88
Micropterus salmoides	0.13	0.01	4.17	82.05
Heterandria formosa	0.03	0.17	3.90	85.95
Cyprinodon variegatus	0.02	0.01	3.39	89.35
Syngnathus scovelli	0.04	0.01	3.33	92.68

For the Warm Season, there were significant differences among site groups (Global R = 0.154, p = 0.001). Each pairwise test between site groups were also significantly different (ANOSIM, Global R > 0.008, p = 0.001). There was not a significant difference between fish assemblages before and after removal of the outdated flood control structure during the Warm Season (ANOSIM, Global R = 0.027, p = 0.081).

Time since last opening was not found to be a significant predictor for either Freshwater or Estuarine species richness ($X^2 = 0.055$, df = 1, $p = 0.814$; $X^2 = 0.001$, df = 1, $p = 0.972$; respectively). No obvious trend in Freshwater or Estuarine guild species richness can be seen in a plot of means and standard error across time (Fig. 3.3, Fig. 3.4; respectively). This suggests there was no trend observed for Freshwater or Estuarine species richness for any site after sector gate openings. Time since last opening was a significant predictor for Marine richness at site REL ($X^2 = 19.517$, df = 1, $p < 0.001$). A negative correlation for the mean number of Marine species collected with respect to time since last sector gate opening was observed (Fig. 3.5). No Marine species were collected for any sites, except REL. Within site REL, no Marine species were collected longer than one month after a sector gate opening.
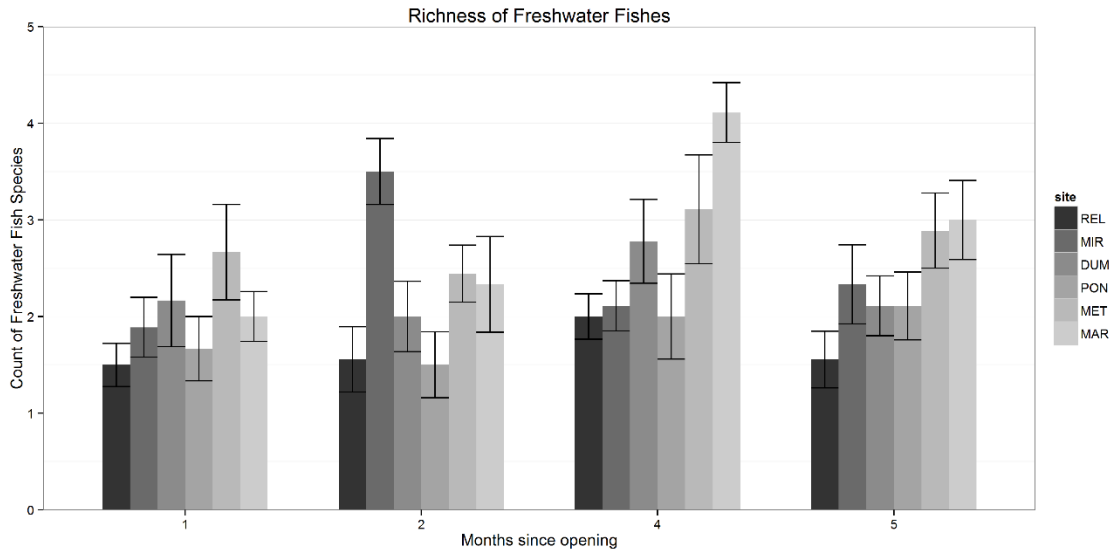
Figure 3.3. Mean count of Freshwater fish species per month with standard error bars for each site from 19 August 2013 until 31 July 2014. This shows how the richness of Freshwater fishes changes with respect to time since last sector gate opening. Note the lack of pattern shown in this graph.
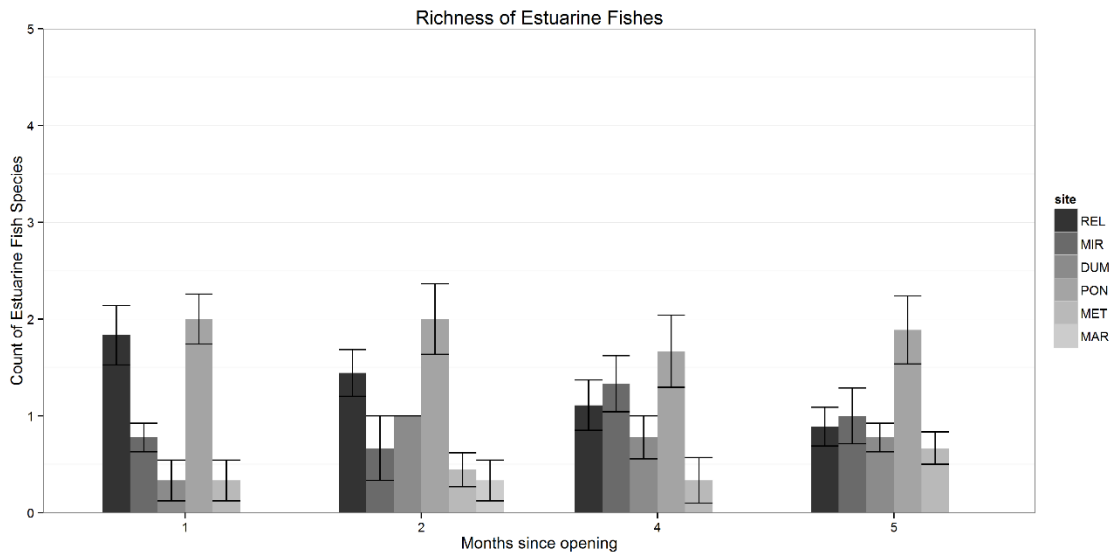
Figure 3.4. Mean count of Estuarine fish species per month with standard error bars for each site from 19 August 2013 until 31 July 2014. This shows how the richness of Estuarine fishes changes with respect to time since last sector gate opening. Note the lack of pattern shown in this graph.
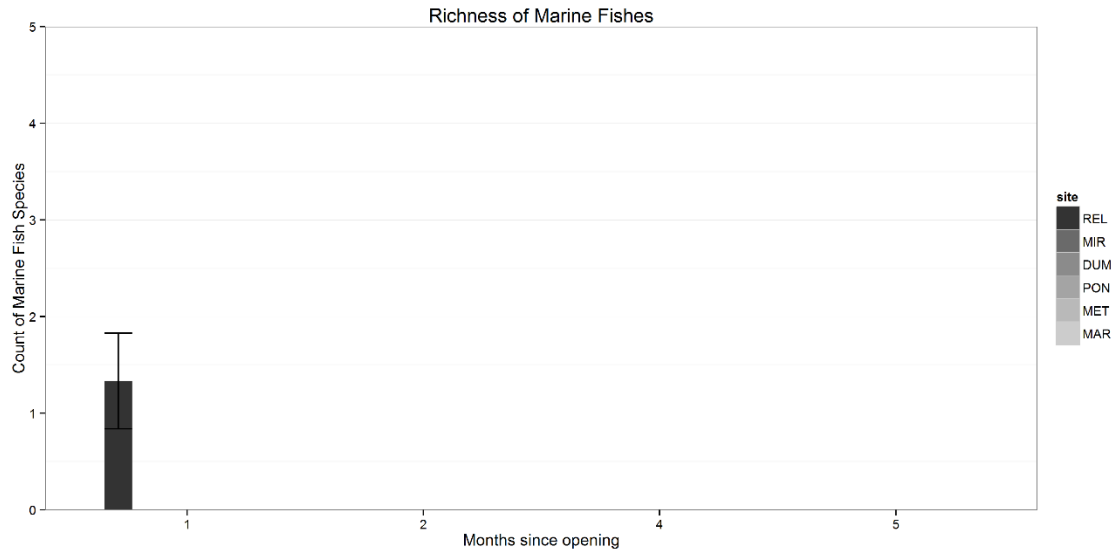
Figure 3.5. Mean count of Marine fish species per month with standard error bars for each site from 19 August 2013 until 31 July 2014. This shows how the richness of Marine fishes changes with respect to time since last sector gate opening. All collections produced no Marine fishes, except if the opening was less than 2 months after a sector gate opening at site REL.

Discussion

The lack of consistent significant differences in fish assemblages before and after the removal of an outdated flood control structure suggests that the removal effort alone had limited impacts. A low Global R value was associated with the differences in fish assemblages during the Cool Season. This suggests minor compositional changes (O'Connell et al., 2014). The lack of clear separation in the MDS plot further suggests the difference between assemblages is minor. While salinity was found to be significantly correlated with fish assemblages, the low ρ indicates little of the overall variation was explained. During the Cool Season, a lower mean salinity was observed after removal of the outdated flood control structure. Model simulations from a previous study indicate that removal of this structure should increase connectivity with Lake Pontchartrain (Schroeder, 2011). It could be assumed that an increase in connectivity would be associated with an increased salinity in BSJ and CPL. However, it was not observed.

131

The observed salinity decrease could be due to other processes such as local and regional weather patterns or stochastic events. Local precipitation and evaporation rates within the BSJ and CPL watershed could result in decreased salinities, but can be difficult to measure. River discharges, which are associated with local and regional rainfall, were found to be the most important driver of Lake Pontchartrain salinity (Sikora and Kjerfve, 1985). Stochastic events also greatly influence local salinities, such as tropical systems or Bonnet Carre Spillway openings. Two tropical systems (Tropical Strom Lee during September 2011, and Hurricane Isaac during August 2012) and a large Bonnet Carre Spillway opening (May 2011) occurred during the study period before dam removal. Additionally, the Mississippi River Gulf Outlet (MRGO), which was an open channel from Breton Sound that connects to Lake Pontchartrain approximately 5 km east of BSJ via the Inner Harbor Navigation Canal, was closed (July 2009). The MRGO has been shown to increase salinity in Lake Pontchartrain (Sikora and Kjerfve, 1985; Carillo et al., 2001; Li et al., 2008) thus the closing of this structure could have resulted in decreased salinities in Lake Pontchartrain. These events or local and regional rainfall could be driving the decrease in salinity observed after dam removal. Fish assemblages in Lake Pontchartrain are thought to be resilient but vary with respect to stochastic events, yearly regional weather patterns, and seasonality (O'Connell et al., 2004; O'Connell et al., 2014). Shoreline assemblages in CPL were also found to have significant decreases in biodiversity immediately following a large stochastic event, but recovered after 2 years (Smith, 2012). SIMPER analysis indicated all fishes that contributed to assemblage differences with an increase in abundance were Freshwater and three of five fishes that decreased in abundance were Estuarine. Two Freshwater fishes, Largemouth Bass and Western Mosquitofish, also declined. Results from the SIMPER and BEST analyses along with overall salinity trends suggest that the

minor assemblage differences observed in the Cool Season are probably a response to environmental changes, not removal of the waterfall structure. However, it should be noted that Inland Silverside average abundances decreased which has been observed in other estuarine waterways following tidal restoration (Raposa, 2002; Warren et al., 2002).

The observed increase in Marine fish richness following sector gate openings suggests that the combination of removal of the outdated structure followed by timely sector gate openings provides a pulse of young marine organisms. Many of these organisms (Spot, Pinfish, Leatherjack, and Gulf Menhaden) have never been collected in shoreline habitats of BSJ or CPL in the previous seven and a half years of sampling (Smith, 2012; current study). During experimental flood gate openings, Marine fishes were only collected within one month following an opening and at the site closest to the flood gate. The lack of Marine species in consecutive months may be because the initial pulse of organisms dissipates throughout shoreline habitats in the Bayou. If this were true, some Marine species should have been collected at other sites during this study period, however, no Marine species were collected elsewhere. They were not. Three possible explanations for this are that: 1. newly settled Marine fishes are at low densities and therefore difficult to detect; 2. Marine fishes emigrate out of the Bayou, possibly through sluice gates; or 3. Marine fishes shift from using shoreline habitats to using other habitats. All marine species collected were young of the year (YOY), with Leatherjack representing the most marine oriented fish collected in the Bayou in over forty years of sampling (Smith, 2012; current study). The one specimen was an early juvenile and while there is little information on their habitat use, larval abundances were found to be in the highest concentration between the 20 m isobar and shore along the Louisiana coast (Ditty et al., 2004). Adults and juveniles have been collected in the Pontchartrain Estuary but are typically collected farther down estuary or during

times of higher salinities (O'Connell et al., 2009). Their tendencies for being more common in higher salinities, along with their rarity in other samples suggest that more openings may not greatly affect Leatherjack densities. However, the observation of the most marine oriented fish species directly following a sector gate opening does provide evidence that openings may transport rare, young marine fishes into BSJ. Large numbers of other Marine fishes, such as Spot (n = 154), and Gulf Menhaden (n = 256), were collected at site REL following an opening. Previously, larger individuals of both species were commonly found in BSJ, but only in open water habitats (Smith, 2012). It could be that Spot and Gulf Menhaden shift from the shoreline to deeper habitats in BSJ. Spot are a benthically oriented fish found in shallow water habitats in the Lake Pontchartrain and other NGOM estuaries (O'Connell et al., 2009). The degraded shoreline habitats may not suitable for them and they may seek other habitats. Gulf Menhaden undergo morphometric changes as they shift from larvae to juveniles (Suttkus, 1956). This change is apparent in external meristic traits like body depth to length ratio. Internally, larvae have a straight gut tube, teeth, and no functional gill rakers, while juveniles have a pyloric caeca, gizzard, and more prominent gill rakers (Suttkus, 1956; Deegan, 1986). The changes in internal anatomy coincide with a shift in feeding strategies and habitat use. Larvae actively prey on planktonic organisms in inshore habitats, while juveniles and adults filter feed in open water (Deegan, 1986). The majority of Gulf Menhaden collected were larvae, with few (< 5%) being early juveniles. This along with their standard length (< 35 mm) suggests they were transitioning from larvae to juveniles. All Gulf Menhaden from a previous study found in open water habitats were juveniles or adults (Smith, 2012). The combined results from both studies suggests the lack of Gulf Menhaden in later samples may be due to a shift from shoreline habitats to pelagic habitats. This shift could be to increase foraging efficiency and may coincide

with the transition from larvae to early juveniles. Five YOY Pinfish were collected following the late February sector gate opening. The timing of this likely coincides with their up estuary migration that occurs after spawning in marine waters (Hansen, 1969). They are closely associated with grass flats (Stoner and Livingston, 1984). The lack of subsequent collections containing Pinfish could be because BSJ lacks suitable habitat. These early findings suggest that dam removal followed by timely sector gate openings transport Marine fishes into the Bayou and that some of these fishes settle into nearby shoreline habitats. Future openings could increase the densities of fishes in BSJ that occur near the sector gates in Lake Pontchartrain.

Increased monitoring with additional openings would yield further insight into flood gate opening effects. With more data, the inclusion of more elegant statistical methods (e.g., assemblage analyses) that include more detailed compositional and within species abundance could be applied. This would be a better analytical tool for understanding how the flood gate openings affect the fishes in BSJ and CPL in the long term. Several studies have noted a fast response in fish assemblages to tidal restoration with noticeable changes occurring within months in a Bahamian island (Layman et al., 2005) to near complete restoration occurring around eight years in some northeastern US marshes (Warren et al., 2002). Analyzing short term effects using GLMMs does offer some advantages. They provided useful information by testing specific hypotheses. For example, do openings increase the density of young marine organisms in the Bayou (BKI, 2011)? The inclusion of a reference site(s) is common for monitoring as part of a before-after-control-impact (BACI) design is desirable when available (Neckles et al., 2002; Raposa, 2002). Many studies use down estuary locations as reference or control sites (citation). Lake Pontchartrain is immediately down estuary from BSJ and is not an appropriate reference because it lacks nearby gently sloping shoreline habitat common in BSJ and CPL. CPL could be

considered an up estuary pseudo-reference site. No direct changes in connectivity were made

and similar across year assemblage effects were seen. Additionally, no changes in fish guild

species richness were observed for any of the three CPL sites adding confidence that the effects

observed in BSJ were a result of sector gate openings.

This study provides important preliminary information that can be applied to other

coastal restoration and flood protection projects in Louisiana. Flood protection and coastal

restoration are inter-related and major concerns for the state of Louisiana. Many hard structures

that include sector gates are under construction and in development in southern Louisiana

(CPRA, 2012). Several of these remain open except when the risk of floods from stochastic

meteorological events, such as tropical storms is high. Many sector gates remain closed year

round and primarily serve as drainage reservoirs for excess water (i.e., from rainwater runoff) to

be pumped out of inhabited areas. BSJ represents the only fragmented brackish water way in

coastal Louisiana undergoing an adaptive management program to increase connectivity down

estuary through intermittent sector gate openings. Recovery rates of salt marsh habitats have

been associated with increased connectivity and tidal exchange (Warren et al., 2002; Thrush et

al., 2008), with more diversity being negatively associated with fragmentation and isolation

(Layman et al., 2004; Valentine-Rose, 2007). While restoration efforts increased tidal exchange

and connectivity, complete defragmentation allowing for unimpeded tidal exchange is not

feasible for BSJ without local flooding during normal daily high water levels (BKI, 2011). This

scenario may become more common as more coastal land is loss, sea level rises, and more

coastal protection projects begin (CPRA, 2012). The results of this study indicate that timely

openings could restore important low to mid trophic level estuarine dependent fishes common in

oligohaline habitats (e.g., Gulf Menhaden and Spot) and this practice should considered in other parts of coastal Louisiana if a continuously open connection cannot be maintained.

References Cited

Able, KW, Fahay, MP. 2010. *Ecology of Estuarine Fishes, Temperate Waters of the Western North Atlantic.* The Johns Hopkins University Press.

Bates, D, M Maechler, B Bolker, and S Walker. 2014. _lme4: Linear mixed-effects models using Eigen and S4_. R package version 1.1-7, <URL: http://CRAN.R-project.org/package=lme4>.

Bolker, BM, ME Brooks, CJ Clark, SW Geange, JR Poulssen, MHH Stevens, and JS White. 2008. Generalized linear mixed models: a practical guide for ecology and evolution. *Trends in Ecology and Evolution* 24.3: 127-135.

Burk-Kleinpeter Incorporated (BKI) 2011. Bayou St. John Water Management Study Phase 1. Prepared for the Orleans Levee District. 56 pp.

Carillo, AR, CR Berger, MS Sarruff, and BJ Thibodeaux. 2001. Salinity changes in the Pontchartrain Basin Estuary, resulting from Mississippi river gulf outlet partial closure plans, 2001, U.S. Army Corps of Engineers - ERDC/CHL TR-01-14.

Clarke, KR. 1993. Non-parametric multivariate analyses of changes in community structure. *Australian Journal of* Ecology 18: 117-143.

Clarke, KR and WM Warwick. 2001. Change in marine communities: an approach to statistical analysis and interpretation, 2nd ed. Plymouth: PRIMER-E.

Clarke, KR and RN Gorley. 2006. PRIMER v6: User Manual/Tutorial. PRIMER-E, Plymouth.

Coastal Protection and Restoration Authority (CPRA). 2012. Louisiana's Comprehensive Master Plan for a Sustainable Coast (Final): 2012 Coastal Master Plan. http://www.coastalmasterplan.louisiana.gov/.

Deegan, LA. 1986. Changes in body composition and morphology of young-of-the-year gulf menhaden *Brevoortia patronus* Goode, in Fourleague Bay, Louisiana. *J. Fish Biol.* 29: 403-415.

Hansen, DJ. 1969. Food, growth, migration, reproduction, and abundance of Pinfish, *Lagodon rhomboides*, and Atlantic Croaker, *Micropogon undulatus*, near Pensacola, Florida. Fish Bull 68: 135-156.

Kaufamn, JB, and PJ Rousseeuw. 1990. *Finding groups in data: an introduction to cluster analysis.* New York: Wiley.

Layman, CA, DA Arrington, RB Langerhans, BR and Silliman. 2004. Degree of fragmentation affects fish assemblage structure in Andros Island (Bahamas) estuaries. *Caribbean Journal of Science* 40.2: 232-244.

Layman, CA, DA Arrington, and MA Blackwell. 2005. Community-Based Collaboration Restores Tidal Flow to an Island Estuary (Bahamas). *Ecological Restoration* 23.1: 58-59.

Lellis-Dibble, KA, KE McGlynn, TE and Bigford. 2008. Estuarine Fish and Shellfish Species in U.S. Commercial and Recreational Fisheries: Economic Value as an Incentive to Protect and Restore Estuarine Habitat. U.S. Dep. Commerce, NOAA Tech. Memo. NMFSF/SPO-90, 94 pp.

Li, C, N Walker, A Hou, I Georgiou, H Roberts, E Law, JA McCorquodale, E Weeks, X Li, and J Crochet. 2008. Circular plumes in Lake Pontchartrain estuary under wind straining. *Estuarine, Coastal and Shelf Science* 80: 161-172.

Llanso, RJ, SS Bell, and FE Vose. 1998. Food Habits of Red Drum and Spotted Seatrout in a Restored Mangrove Impoundment." *Estuaries* 21.2: 294-306.

Martinez, L, S O'Brien, and S Brogan. 2008. Bathymetric survey of Bayou St. John. Internal Report. University of New Orleans. New Orleans, LA. 5 pp.

Neckles, HA, M Dionne, DM Burdick, CT Roman, R Buchsbaum, and E Hutchins. 2002. A monitoring protocol to assess tidal restoration of salt marshes on local and regional scales. *Ecological Restoration* 10.3: 556-563.

Nordlie, FG. 2003. Fish communities of estuarine salt marshes of eastern North America, and comparisons with temperate estuaries of other continents. *Reviews in Fish Biology and Fisheries* 13: 281-325.

O'Connell, MT, RW Hastings, and CS Schieble. 2004. Fish assemblage stability over fifty years in the Lake Pontchartrain Estuary; comparisons among habitats using canonical correspondence analysis. *Estuaries* 27: 807-817.

O'Connell, MT, AMU O'Connell, and RW Hastings. 2009. A Meta-analytical comparison of assemblages from multiple estuarine regions of southeastern Louisiana using a taxonomic-based method. *Journal of Coastal Research* 54: 101-112.

O'Connell, MT, AMU O'Connell, CS Schieble. 2014. Response of Lake Pontchartrain Fish Assemblages to Hurricanes Katrina and Rita. *Estuaries and Coasts* 37: 461-475.

R Core Team (2014). R: A language and environment for statistical computing. R Foundation for Statistical Computing, Vienna, Austria. URL http://www.R-project.org/.

Raposa, K. 2002. Early responses of fishes and crustaceans to restoration of a tidally restricted New England salt marsh. *Restoration Ecology* 10.4: 665-676.

Schroeder, RL. 2011. Exchange flows in an urban water body Bayou St. John response to the removal of flood control structures, future water elevation control and water quality. Thesis. University of New Orleans.

Sikora, WB, and B Kjerfve. 1985. Factors influencing the salinity regime of Lake Pontchartrain, Louisiana, a shallow coastal lagoon: analysis of a long-term data set. *Estuaries* 8.2: 170-80.

Smith, PW. 2012. Fish assemblage dynamics and Red Drum habitat selection in Bayou St. John and associated urban waterways located within the city of New Orleans, Louisiana. Thesis. University of New Orleans.

Stoner, AW, and RJ Livingston. Ontogenetic patterns in diet and feeding morphology in sympatric Sparid fishes from seagrass meadows. *Copeia* 1984.1: 174-187.

Suttkus RD. 1956. Early life history of the Gulf Menhaden, *Brevoortia patronus* in Louisiana. *Transactions of the North American Wildlife and Natural Resources Conference* 390-407.

Thrush, SF, J Halliday JE Hewitt, and AM Lohrer. 2008. The effects of habitat loss, fragmentation, and community homogenization on resilience in estuaries. *Ecological Applications* 18.1: 12-21.

Valentine-Rose, L, JA Cherry, JJ Culp, KE Perez, JB Pollock, DA Arrington, and CA Layman. 2007. Floral and faunal differences between fragmented and unfragmented Bahamian tidal creeks. *Wetlands* 27.3: 702-718.

Ward, KA. 1982. Ecology of Bayou St. John. Thesis. University of New Orleans.

Warren, RS, PE Fell, R Rozsa, AH Brawley, AC Orsted, ET Olson, V Swamy, WA Niering. 2002. Salt marsh restoration in Connecticut: 20 years of science and management. *Restoration Ecology* 10.3: 437-513.

Appendix I – IACUC Documentation

Institutional **A**nimal **C**are and **U**se **C**ommittee
University of New Orleans, 2000 Lakeshore Drive, New Orleans, LA 70148: 504-280-6303

IACUC

PROTOCOL for the Use of Live Vertebrates in Field Research

INSTRUCTIONS: Complete all items on the application form or mark not applicable. **Please email this form and supporting documents to iacuc@uno.edu. Sign and send the signature page along with supporting documents not available in electronic format to the IACUC Office, College of Sciences, Room 1100.** *A protocol can be reviewed only after all questions have been answered completely. Answers to the questions must be given in the spaces provided. Do not refer to or attach passages from grants. All required signatures must be obtained before the application will be reviewed.* **SUBMISSION DEADLINE:** The IACUC meets in the first week of every month. An application must be received by the 15th day of the previous month in ordered to be considered.

IACUC Use Only	
Assigned IACUC Protocol Number _____ 09-009 ____	Approval Date __ Aug. 13, 2009 ___

Submission Date: 24jul09   ☒ Initial Review   ☐ Renewal of IACUC #09-009

Principal Investigator: Martin O'Connell	Degrees: B.Sc., M.Sc., Ph.D.
Position/Title: Assistant Professor	Department: EES
Address: 1008 GP	E-mail: moconnel@uno.edu
Phone: 3-4032 (GP 1008)	Emergency Contact & Phone: 3-4037 (GP 1007)

Part I. Introduction

a. Title of Project (If project relates to a grant application, give that title): Establishing a unified tagging program to assess post-hurricane fisheries in the Pontchartrain Basin.

b. Duration of Project: two years

c. Source of Funds: ☐ Departmental   ☐ LA Board of Regents   ☐ NIH   ☐ NSF
☒ Other, specify: NOAA funds through the Pontchartrain Restoration Act

d. Location(s) of Field Research: State Louisiana , County Various Parishes , Country USA

e. Type of property where field research will take place: ☐ Private Property   ☐ NWR
☐ National Park   ☐ State Park   ☐ National Forest
☒ Other, specify: public fresh, estuarine, and marine waters

Is permission required to perform research at this location? ☐ Yes ☒ No

If yes, provide support that there was permission to access the site.

UNO IACUC Protocol Form Version 09/08

Part II. Lay Person Project Summary

Briefly explain in language understandable to a layperson the objectives of your study. The abstract must describe the species and use of animals. Briefly describe the scientific purpose, the specific aims, and how the animals will be used to achieve your goals. How will this research advance knowledge? Do not exceed 400 words (1 page). Do not provide summaries of past accomplishments or references to published work in this section or other sections of this application

Our main goal is to use a standardized tagging approach to address multiple fishery issues in multiple areas of the Pontchartrain Basin. We have combined four separate tagging projects that will benefit from sharing personnel and equipment in accomplishing each of their goals. The four projects are:
1. the development of a marine sport fish tag and recapture program for the Pontchartrain Basin;
2. assessing site fidelity and habitat use by recreational fishes at artificial reefs in Lake Pontchartrain;
3. determining bycatch impacts and trophic responses of Lake Borgne catfish species; and
4. testing possible nursery and pupping habitats of lemon sharks at the Chandeleur Islands.
The goal of the marine sport fish tag project is to build on the success of the Coastal Conservation Association (CCA) in developing a tagging program in the Barataria Basin and begin a similar program in the Pontchartrain Basin. The CCA will establish a marine sport fish tag and recapture program utilizing a diverse partnership, but designed specifically to employ and educate anglers, through their participation in the program, about the importance and need for management and conservation. This program will gather data through the use of Pontchartrain Basin anglers to improve understanding of marine sport fish movements and patterns of habitat use, age structure, growth and mortality rates, estimates of population size, and rates of immigration and emigration. The goal of the artificial reef project is to tag recreational fishes at the reefs and, through recapture, determine how much these fishes use and rely on these habitats. Data generated by this project can be used as evidence of the relative ecological value of these structures. Tagging Gafftopsail catfish (Bagre marinus) in Lake Borgne and analyzing recapture data will elucidate trophic connections that may explain how bycatch disposal is affecting the local fisheries. Recent analysis of fishery-independent data collected over seven years by the NRL revealed that these catfishes represent a larger-than-expected proportion of estuarine biomass. The Chandeleur Islands may be lost if another Katrina-like storm hits them. We would like to use a tagging project to confirm that this area is one of the few places in the Gulf of Mexico used as nursery and pupping habitats by lemon sharks. NOTE: CCA individuals will only be conducting floy tagging. UNO personnel will be conducting both floy tagging and satellite tagging.

Part III. Environmental and Bio-safety Issues

A. Please check YES or NO for each of the following questions.

☐ Yes ☒ No Will humans be exposed to biohazards, chemical hazards, or radioactive compounds during the course of animal experimentation?

☒ Yes ☐ No Will personnel be at risk of potential health hazards (zoonoses, toxins, bites) associated with the handling of wild animal?

☐ Yes ☒ No Are the study species known to harbor rabies?

B. If any of the questions above is answered yes, you must list the agents and doses (as appropriate), and the precautions taken to protect research and animal technicians. In the case of species known to harbor rabies, indicate whether personnel have been immunized.

Although we will be briefly handling lemon sharks as part of our research, we are focusing our tagging efforts on small, young animals (less than 1 m). To avoid bites from these animals, we take typical fish-handling precautions such as using protective gloves and clothing. All of the personnel working on this aspect of the project have years of experience with handling all sizes of sharks and each person has a stellar field record of safety.

Part IV. Procedures on Wild Animals

Wild animal subjects are those animals not specifically bred and sold for research, teaching, or agricultural purposes. Investigators conducting observation, photography, audio or video recording only are not required to complete this form.

IV.a. Provide a complete description of the proposed use of animals. **This is the most important section of the protocol.** Please describe exactly the procedures done on all live animals in a sequential time frame. Describe and justify the invasiveness of the technique (Ex: collection of urine or feces vs. drawing blood). Provide enough detail so IACUC can evaluate the appropriateness of all procedures.

The project has two main areas involving the handling of live wild fishes: 1. the capturing and tagging of multiple species with floy tags in Lake Pontchartrain by our researchers and CCA-trained anglers and 2. the capturing and tagging of six lemon sharks at the Chandeleur Islands using satellite tags. Floy tagging (conducted by both UNO and CCA personnel) involves inserting a small (1 mm X 100 mm) flexible plastic tag in the dorsal musculature of a live captured fish. For all of these activities, we emphasize the quick handling, tagging, and release of the fishes because the goal is to have these animals live in the wild so that they can be recaptured alive at a later date. A stressed, injured, or exhausted animal serves no purpose for the project goals. Fishes are typically taken with hook-and-line because this method causes less stress to the animal compared with typical fishery gear such as gillnets, trawls, and seines. In some situations, we (UNO personnel only) will use a gillnet to capture and tag fishes, but all precautions are taken to remain near the net and fish it on a regular basis. More specifically, our gillnetting procedure involves using the LDWF 'strike method' for capturing fishes which minimizes the time fishes are actually in the net. The gillnet is deployed from the back of the boat and held in the water column by weights and floats. Once deployed, the boat quickly circles the gillnet three times. This drives the fishes into the net. After the circling is completed, the net is retrieved and live fishes removed. The whole procedure rarely lasts more than 15 minutes. This lets us capture the fishes alive and minimizes the handling and tagging time. A typical floy tagging procedure begins with the capture of the animal. Fishes are brought on board immediately and secured either on the deck or in a shallow container of local water with dilute FinQuel (MS-222). Depending on which species is being tagged, the hook is quickly removed from the animal using either fingers or a needlenose pliers. While the fish is secured, a floy tag is inserted just under the dorsal fin using a large gauge needle designed for tagging. The tagger then lightly pulls on the tag to confirm that it is secured and rubs an antibiotic gel on the fish at the point of attachment. The fish is immediately released back into the water and the whole tagging process takes less than a minute to complete. The justification for this type of tagging is that we want the brightly colored tag to be easily noticed when the animal is recaptured. The size and shape of the tag makes it comparable to typical external parasites which may occur on many of these species. Maumus Claverie, Chairman of the CCA-LA Tagging Program, has 22 years of experience with this tagging technique and he provides evidence that tagged fishes, "…exhibit no signs of pain or distress when properly tagged," (see attached letter of support).

Attaching satellite tags to six juvenile lemon sharks is slightly more complicated but many of the techniques are the same as the floy tagging. Note that only UNO personnel will be conducting satellite tagging. During multiple trips to the Chandeleur Islands six lemon sharks between 1.2 and 1.8 m will be collected alive using rod and reel. The sample size was limited to six due to budget constraints, however, with a reasonably large difference between the groups a significant difference would still be seen (effect size ≥ 2). Once each shark is captured and brought aboard it will be sexed, measured, weighed, and fitted

with a Wildlife Computer (Redmond, WA) SPOT5 fin mounted satellite tag. These satellite tags send real time data updates whenever the animal's fin breaks the surface and the wet/dry sensor becomes dry. At a rate of 250 transmissions a day and while collecting location, temperature, and haulout data, the battery life of the tag will be approximately six months. Using a leather punch tool, the SPOT5 tag will be secured to the first dorsal fin of the shark using four steel screws that will be attached to a plastic backing plate to keep the tag secured to the animal. Steel screws will be used in an effort to protect the animal, it is anticipated that within a year the steel will corrode and the tag will fall off. The animal will then be placed into an underwater pen to ensure that the tag does not result in a significant decrease in the swimming ability of the shark. The tag will be left in place for as long as possible until the battery nears the end of its power supply. Before the tags stop transmitting, a trip will be planned and efforts made to recapture the sharks and remove the tags from the animals.

IV.b. In the table below, list the species, numbers of animals, common names, and location of the study. *If the species cannot be exactly predicted, indicate range of species or families anticipated*

Species	Number of Animals	Common Name	Study Site
Negaprion brevirostris	6	lemon shark	Chandeleur Islands
Cynoscion nebulosus	20	spotted seatrout	Lake Pontchartrain
Ariopsis felis	40	hardhead catfish	Lake Pontchartrain
Bagre marinus	20	gafftopsail catfish	Lake Pontchartrain
Pogonias cromis	10	black drum	Lake Pontchartrain
Carcharhinus leucas	5	bull shark	Lake Pontchartrain

IV.c. Why was this particular population of animals chosen?

The lemon shark was chosen because we have shown that the Chandeleur Islands is the northernmost pupping ground of this species in the Western Hemisphere and the Chandeleur Islands are threatened by increased hurricane activity. The other fishes were chosen because there is a need to better understand the movements and population dynamics of all Lake Pontchartrain fishes.

IV.d. Briefly describe the following conditions of animal capture.

    1. Describe the method of capture/trapping technique. Is this method an accepted method for this species?
    Hook and line fishing is an acceptable method for catch and release collection of fishes. A baited hook is taken by the fish, the hook is then set in the jaw of the animal by a quick tug of the line, and the fish is brought to the boat by reeling in the line.

    2. How often will traps/nets be monitored?
    Gillnets will be fished within 15 minutes of being set (see description of strike method above).

UNO IACUC Protocol Form Version 09.08

3. How long will captured animals be held in captivity?
between 1 and 5 minutes.

4. Is capture of non-target species anticipated and if so how will such animals be dealt with?
No, for the lemon shark work and all fishes are targets for the floy tag work.

5. What are the expected injury and mortality rates resulting from capture? (The total number of animals requested must include an estimate of those injured/killed during capture)
We expect zero mortalities for the lemon shark work and about 1% mortality for floy tagged fishes.

6. What measures will be taken to prevent injury and alleviate stress during capture?
We will use MS-222 when fishes exhibit increased thrashing behavior that may cause them harm and preclude safe tagging methods. When the decision is made to anesthetize the fish, it will be immersed in the treated water and allowed to calm down before tagging procedes. After tagging, the fish will allowed to recover (i.e., self orient) and returned to the water.

7. Do cages, traps or other devices used in capturing wild animals provide protection from predators and other environmental hazards? ☒Yes   ☐No

8. What will be the impact of capture on subsequent behavior and survival of those animals released back into the wild after the study?
As described by Mr. Claverie, there appears to be little or no impact on tagged fishes.

IV.e.   Will captured animals be artificially marked? ☒Yes   ☐No

If yes, answer the following questions.

1.   Describe the method of marking. Is this method an accepted method for this species?
Both tagging methods are described above and they are widely accepted methods.

2.   Describe the potential consequences of the marking procedure on animal behavior and survival, if any. (e.g. impaired locomotion, increased visibility to predators).
There may be slightly impaired locomotion for the lemon sharks for six months while the floy tags offer little problems.

IV.f.   Will captured animals be released into the field? ☒Yes   ☐No
If yes, answer the following questions.

1.   Where will the animals be released after the study?
At the site of capture.

2.   Describe the condition of release in terms of how the released animals will be able to avoid predators, seek shelter, and avoid inclement weather.
Lemon sharks will be held in underwater pens until they recover while flot tagged fishes (if they don't swim away) will be held under water until they can swim under their own power.

UNO IACUC Protocol Form Version 09.08

3. If animals are anesthetized, will they be held until anesthesia leaves their system before release?
Yes.

4. Will there be a potential for human or animal consumption of released contaminated animals?
None of these fishes will be contaminated.

IV.g. Answer the following questions about the effects of the study on the physical or biotic characteristics of the field site.

1. Will any structure be erected to contain or capture study species? ☐Yes ☒No
If yes, how will this structure impact other species in the area?

2. Will non-native species be released at the site? ☐Yes ☒No
If yes, provide proper permits to the IACUC and describe the impact on other species.

IV.h. Will animals be transported to or from the field during this study? ☐Yes ☒No
If yes, complete parts a and b below:

a) Species	Method of Transport	Duration of Transport

b) Briefly describe transport procedures and precautions taken to protect animals from undue stress.

IV.i. Do any of the species require state or federal permits/licenses for use and capture?
☒Yes ☐No

If yes, which documents are required and have you obtained these permits/licenses? Please furnish IACUC with copies of these documents as soon as you receive them.

We have a state scientific collecting permit (see attached).

Part V. Justification of animal usage

V.a.   Method used to determine number of animals needed for this study:

☒ Citation of previous research, with sufficient information to indicate that previous research is similar enough in concept and methodology to use similar samples sizes in the proposed research.
☐ Power Analysis indicates that the proposed number of experiments is the lowest required for statistically valid test of the hypothesis – Describe below
☐ Specific experimental needs – Describe below
☐ This is a pilot study to obtain preliminary data to determine if a larger study is needed.
☐ These experiments are technically difficult and multiple attempts will be needed to obtain satisfactory data from each experiment. Describe below.
☐ Other – explain in detail below

V.b.   Why must animals be used in this research and what non-animal alternatives were considered and deemed unacceptable *(e.g., mathematical models, in vitro biological systems, computer simulations)*?

We cannot use models for either of these tagging projects because the point is to discover what the actual animals are doing. The data we will collect are what future scientists can use to model fish behavior in the region.

V.c. Sources for alternatives to animal use.

Describe the sources used to determine that alternatives to the use of live animals are not available. Please retain a copy of your searches in the event of an audit. Search help is available at NIH Alternatives Search Tips: http://nihlibrary.ors.nih.gov/training/AlternativesSearchTipSheet5-24-04.pdf

Search Engines used [e.g., Medline, AGRICOLA, PubMed. Google is not acceptable]:

AGRICOLA, BIOSIS, Zoological Record, Biological Abstracts

Keyword used: "lemon sharks" "Negaprion brevirostris" tagging MS-222 tracking alternatives ()

Inclusive years of search: 1969 to present

Date search was conducted: 24 July 2009 and 12 August 2009 - Zero matched for all three search engines.

As requested, on 12 August 2009 I have conducted more web searches to determine if there are any alternatives to tagging live lemon sharks. None of the various combinations of the terms above produced results. When the word "alternatives" is removed, though, I found 47 articles in Biological Abstracts on lemon sharks. I am familiar with many of these articles and their tagging methods are the basis of the method we are using.

Part VI. Pain, Anesthesia, Analgesia, and Euthanasia

VI.a. Number of Animals in USDA Pain Categories

Enter the number of animals of each species under the appropriate USDA pain category. Count the animal only once and if an animal is used in multiple categories, count the animal in the highest pain category

USDA Category C: *[USDA AWA, 2.36(b)(5)]* **No pain, distress or use of pain-relieving drugs** *(e.g. studies, experiments, tests or procedures where animals do not experience pain or distress but may have only transitory discomfort such as venipuncture, injection, toe-clipping and/or tattooing)*

USDA Category D: *[USDA AWA, 2.36(b)(6)]* **Painful or Distressful with use of Analgesia/Anesthesia/Sedative/Tranquilizers** *(e.g. painful or stressful experiment, tests or procedures that are conducted with the use of appropriate anesthetics, analgesics, and/or sedative drugs that will prevent pain or distress: also includes procedures performed on anesthetized animals that are not allowed to regain consciousness).*

USDA Category E: *[USDA AWA, 2.36(b)(7)]* **Painful or Distressful without Pain or Stress Relieving Measures** *(e.g. painful or stressful procedures that are conducted without the use of appropriate anesthetics, analgesics, and sedative drugs or other measures to prevent or relieve pain or distress; painful and stressful procedures not amenable to relief by therapeutic means.*

Species	Category C	Category D	Category E	Total # of Animals
lemon sharks		6		6
multiple species	catch dependent			catch dependent

Justify any procedures falling into USDA Category E (Pain without analgesia, anesthesia, or sedation):

VI.b. Will any un-anesthetized animals be restrained for longer than 10 minutes?

☒ No ☐ Yes, provide information in table below

Species	Method of Restraint	Duration of Restraint

VI.c. Will sedative/anesthetic(s) be used?

☐ No ☒ Yes, provide information in table below

UNO IACUC Protocol Form Version 09.08

Species	Drug	Dose (mg/kg)	Route of Administration
lemon sharks	MS-222	100 mg/ml	gill exposure
multiple species	MS-222	100 mg/ml	gill exposure

Provide the method of monitoring depth of anesthesia:

☐ Not applicable   ☐ Toe Pinch Reflex   ☐ Corneal Reflex   ☐ Tail Pinch Reflex

☐ Web Pinch Reflex   ☐ Blood Pressure   ☐ Heart and Respiratory Rate

☒ Other, explain Observation of fish self orientation

VI.d. Will analgesic(s) be used?

☒ No   ☐ Yes, provide information in table below

Species	Drug	Dose (mg/kg)	Route

VI.e. Euthanasia

1. Describe the method of euthanasia for each species; provide choice of drug, dosage and route of administration: NA

Specify the method to confirm death (*e.g. opening the chest of all animals or removal of head*).

2. Is this method of euthanasia an acceptable method for this species?

☐ Yes   ☐ No, provide scientific justification:

VII. Personnel Qualifications and Training

Complete all columns in the table below to provide specific information regarding the qualifications of the principal investigator(s) and anyone else participating in this research including technicians and students. Personnel added to the project must be submitted through a protocol amendment.

Name/Title/Role	Years of experience with animal research	Experience with species used in this protocol	Experience with techniques used in this protocol	Completed UNO Animal Training Program
Martin O'Connell/Assistant Professor/PI	25 years	☒ Yes ☐ No	☒ Yes ☐ No	☒ Yes ☐ No
Christopher Schieble/Research Associate/Field Researcher	17 years	☒ Yes ☐ No	☒ Yes ☐ No	☒ Yes ☐ No
Jonathan McKenzie/Graduate Student/Researcher	4 years	☒ Yes ☐ No	☒ Yes ☐ No	☒ Yes ☐ No
Christopher Davis/Graduate Student/Researcher	3 years	☒ Yes ☐ No	☒ Yes ☐ No	☒ Yes ☐ No
		☐ Yes ☐ No	☐ Yes ☐ No	☐ Yes ☐ No
		☐ Yes ☐ No	☐ Yes ☐ No	☐ Yes ☐ No
		☐ Yes ☐ No	☐ Yes ☐ No	☐ Yes ☐ No

If any of the people do not have experience with either the species or techniques, please outline the steps to provide training:

UNO IACUC Protocol Form Version 09/08

151

Institutional Animal Care and Use Committee (IACUC)

Field Research Protocol Application Signature Page

This page must be signed and delivered to UNO IACUC office prior to review

A) Title of Project: Establishing a unified tagging program to assess post-hurricane fisheries in the Pontchartrain Basin.

B) PRINCIPAL INVESTIGATOR CERTIFICATIONS

- I certify that the animal care and use described in this protocol is exactly as described in the funding application (if applicable) for this protocol.
- I certify that I have determined that the research proposed herein is not unnecessarily duplicative of previously reported research.
- I assure that all personnel listed on this project are qualified to conduct this study in a humane and scientific manner consistent with the Guide for the Care and Use of Laboratory Animals (http://grant.nih.gov/grants/olaw/references/phspol.htm) and the provisions of the Animal Welfare Act (http://www.nal.usda.gov/awic/legislat/usdaleg1.htm).
- I certify that I am familiar with and will comply with all pertinent institutional, state, and federal rules and policies.

I have read the assurances and I understand that failure to comply with these assurances may result in suspension or termination of this animal activity and the filing of a report of non-compliance with the UNO Institutional Official and appropriate governing agencies.

_____   Date_____
Principal Investigator
(Per signature not acceptable)

As Department Chair of the PI, I have reviewed the protocol and endorse its submission and that the science is significant and appropriate.

_____   Date _____
Department Chair
(Per signature not acceptable)

UNO IACUC Protocol Form Version 09.08

**Institutional Animal Care and Use Committee
(IACUC)
Protocol Amendment Form**

Submission Date: 29 June 2011

1. Principal Investigator: Martin O'Connell

2. Department: EES

    Phone: 4032 Email: moconnel@uno.edu

3. IACUC Protocol # 09-009

4. Title: Establishing a unified tagging program to assess post-hurricane fisheries in the Pontchartrain Basin.

5. Amendment(s) Requested: *(Check all that apply, separate amendments may be required in some cases).*

    ☒ To change status, add or delete personnel, complete only Item 6.

    ☐ Change in funding; if adding or changing NIH funding, include a copy of NIH notification of change and/or new Vertebrate Animal Section "f".

    ☐ Add a new title with no changes to the experimental techniques and/or design.

    ☐ Add a new title with changes and/or additions as indicated by the checked boxes below.

    If any of the boxes below are checked, please fill out sections 7 and 8 below.

    ☐ Change (add/delete) in the number of animals approved for use by this protocol.

    ☐ Change (add/delete) in the strain(s) approved for use by this protocol.

    ☐ Change (add/delete) in the specie(s) approved for use by this protocol. *(Request for the addition of cats, dogs, or primates to a protocol for which initial approval did not include that species will not be considered under an amendment. A new IACUC Research Application must be submitted to use these species.)*

    ☐ Change in the dosing of a previously approved drug or agent. State the new dose, route of administration and frequency.

    ☐ Change (add/delete) in drug(s)/agent(s) approved for this protocol. List dose, route of administration and frequency.

    ☐ Change in the schedule of sample collection. List new schedule.

☐ Modify a previously approved procedure in this protocol. Provide detail and indicate whether additional animals will be required.

☐ Add a procedure. Provide a sequential description; if surgical procedure, clarify length of surgery and post-op monitoring. For sample collections, provide amount, mode, and frequency. Indicate whether additional animals will be required. Indicate if the USDA pain category changes. If applicable, provide additional alternative search keywords and date of search.

☐ Other (specify):

6. Personnel Information:

Name/Title/Role	Years of experience with animal research	Experience with species used in this protocol	Experience with techniques used in this protocol	Completed UNO Laboratory Animal Training Program*
Martin O'Connell/Assistant Professor/PI	27	☒ Yes ☐ No	☒ Yes ☐ No	☒ Yes ☐ No
Christopher Schieble/Research Associate/Field Researche	19	☒ Yes ☐ No	☒ Yes ☐ No	☒ Yes ☐ No
Jonathan McKenzie/Graduate Student/Researcher	6	☒ Yes ☐ No	☒ Yes ☐ No	☒ Yes ☐ No
Patrick Smith/Graduate Student Researcher	4	☒ Yes ☐ No	☒ Yes ☐ No	☒ Yes ☐ No
Will Stein/Graduate Student Researcher	2	☒ Yes ☐ No	☒ Yes ☐ No	☒ Yes ☐ No

*New personnel must complete UNO Laboratory Animal Training Program prior to participation.

7. Description of Change(s): *[Describe in detail how the proposed amendment changes the original protocol. Provide listings requested on first page. Use appropriate species names and origin or strain if applicable. For procedural changes, please indicate species and number of animals that will be affected by the proposed change(s).]*

The following person is no longer an NRL employee:

Tables:

Christopher Davis/Graduate Student/Researcher

8. Justification for each proposed change:

154

9. By submission of this amendment, I, as principal investigator, understand that protocols must be renewed every three years to remain active. All amendments approved within a three-year period are bound to the approval date of the protocol, which they amend. After three years, all procedures and aspects approved via amendment(s) that are anticipated to remain as a component of the study must be included in the renewal protocol

Principal Investigator Signature:

155

Vita

Patrick William Smith was born on 6 February 1985 in Newnan, Georgia and grew up in Augusta, GA. He received his Bachelor's of Science degree in Biology from Georgia Regents University in May 2008 and his Master's of Science degree in Earth and Environmental Sciences from University of New Orleans (UNO) in May 2012. He continued working with Dr. Martin O'Connell's Nekton Research Laboratory at UNO on restoration impacts of fishes in urbanized waterways. During his time working under Dr. O'Connell, he worked on a variety of projects ranging from fisheries gear comparisons to invasive fish behavior. Patrick is currently employed as a Coastal Scientist with the Lake Pontchartrain Basin Foundation.